UNIVERSIDAD AUTÓNOMA DE SAN LUIS POTOSÍ

FACULTAD DE CIENCIAS QUÍMICAS

Posgrado en Ciencias Farmacobiológicas

Significancia diagnóstica del perfil de lípidos y sus razones (colesterol/c-HDL, triglicéridos/c-HDL, c-LDL/c-HDL, WBC/c-HDL y FBG/c-HDL) para predecir síndrome metabólico

Tesis que para obtener el grado de:

Maestría en Ciencias Farmacobiológicas

Presenta:

Cárdenas Juárez Abraham

Director de Tesis: **Dra. en C. Diana Patricia Portales Pérez**

Codirectora: **Dra. en C. Mariana Haydee García Hernández**

San Luis Potosí, S.L.P. FECHA: enero de 2026

Significancia diagnóstica del perfil de lípidos y sus razones (colesterol/c-HDL, triglicéridos/c-HDL, c-LDL/c-HDL, WBC/c-HDL y FBG/c-HDL) para predecir síndrome metabólico

Este proyecto se realizó en la Unidad de Investigación Biomédica Delegación Zacatecas del Instituto Mexicano del Seguro Social (IMSS), en el periodo comprendido entre agosto del 2023 y mayo del 2025, bajo la dirección de la Dra. Diana Patricia Portales y Pérez y la Dra. Mariana Haydee García Hernández.

El programa de Maestría en Ciencias Farmacobiológicas de la Universidad Autónoma de San Luis Potosí pertenece al Sistema Nacional de Posgrados de Calidad (SNP) del CONAHCYT, registro 003382. Número de la beca otorgada por CONAHCYT: 4000215. Número de CVU: 1317126.

Los datos del trabajo titulado: Significancia diagnóstica del perfil de lípidos y sus razones (colesterol/c-HDL, triglicéridos/c-HDL, c-LDL/c-HDL, WBC/c-HDL y FBG/c-HDL) para predecir síndrome metabólico. Se encuentran bajo el resguardo de la Facultad de Ciencias Químicas y pertenecen a la Universidad Autónoma de San Luis Potosí.

UNIVERSIDAD AUTÓNOMA DE SAN LUIS POTOSÍ
Facultad de Ciencias Químicas
Centro de Investigación y Estudios de Posgrado
Posgrado en Ciencias Farmacobiológicas
Programa de Maestría
Formato M15

Solicitud de Registro de Tesis Maestría

San Luis Potosí SLP a 11/ 25/ 2023

Comité Académico
En atención a: Dra. Claudia Escudero Lourdes

Por este conducto solicito a Usted se lleve a cabo el registro de tema de tesis de Maestría, el cual quedo definido de la siguiente manera: Significancia diagnóstica del perfil de lípidos y sus razones (colesterol/c-HDL, triglicéridos/c-HDL, c-LDL/c-HDL, WBC/c-HDL y FBG/c-HDL) para predecir síndrome metabólico
que desarrollará el/la estudiante: Abraham Cárdenas Juárez
bajo la dirección y/o Co-dirección de: Dra. Diana Patricia Portales Pérez y Dra. Mariana Haydee García Hernández.

Asimismo, le comunico que el proyecto en el cual trabajará el alumno involucrará el manejo de animales de experimentación, estudios con seres humanos o muestras derivadas de los mismos, el manejo y/o generación de organismos genéticamente modificados y requiere de aval de Comité de Ética e investigación de la FCQ.

(Complete la opción que aplique en su caso):

(X) Sí debido a que: Se trabajará con muestras sanguíneas de humanos para determinaciones bioquímicas.

( ) No

( ) No Aplica

Sin otro particular, quedo de Usted.

A T E N T A M E N T E

Abraham Cárdenas Juárez	Dra. Diana Patricia Portales Pérez
Nombre y firma del estudiante	Nombre y firma del/la Director/a de Tesis

INSTITUTO MEXICANO DEL SEGURO SOCIAL
SEGURIDAD Y SOLIDARIDAD SOCIAL

Dirección de Prestaciones Médicas
Unidad de Educación e Investigación
Coordinación de Investigación en Salud

Dictamen de Aprobado

Comité Local de Investigación en Salud **3301**.
HOSP GRAL ZONA/MF 1 ZACATECAS

Registro COFEPRIS **17 CI 32 056 012**
Registro CONBIOÉTICA **CONBIOETICA 32 CEI 001 2017082**

FECHA **Viernes, 29 de noviembre de 2024**

Doctor (a) Mariana Haydee García Hernández

P R E S E N T E

Tengo el agrado de notificarle, que el protocolo de investigación con título **Marcadores derivados del perfil de lípidos (índice TyG y las razones TC/HDL-c, TG/HDL-c, LDL-c/HDL-c, FBG/HDL-c y WBC/HDL-c) para identificar a individuos con síndrome metabólico en población mexicana** que sometió a consideración para evaluación de este Comité, de acuerdo con las recomendaciones de sus integrantes y de los revisores, cumple con la calidad metodológica y los requerimientos de ética y de investigación, por lo que el dictamen es **A P R O B A D O**:

Número de Registro Institucional
R-2024-3301-034

De acuerdo a la normativa vigente, deberá presentar en junio de cada año un informe de seguimiento técnico acerca del desarrollo del protocolo a su cargo. Este dictamen tiene vigencia de un año, por lo que en caso de ser necesario, requerirá solicitar la reaprobación del Comité de Ética en Investigación, al término de la vigencia del mismo.

UNIVERSIDAD AUTÓNOMA DE SAN LUIS POTOSÍ

FACULTAD DE CIENCIAS QUÍMICAS

Posgrado en Ciencias Farmacobiológicas

Significancia diagnóstica del perfil de lípidos y sus razones (colesterol/c-HDL, triglicéridos/c-HDL, c-LDL/c-HDL, WBC/c-HDL y FBG/c-HDL) para predecir síndrome metabólico

Tesis que para obtener el grado de: **Maestría en Ciencias Farmacobiológicas**

Presenta: **Cárdenas Juárez Abraham**

SINODALES:

Presidente: **Dr. Juan Manuel Vargas Morales**

Secretario: **Dra. Edith Elena Uresti Rivera**

Vocal: **Dra. Diana Patricia Portales Pérez**

Vocal: **Dra. Mariana Haydee García Hernández**

Vocal: **Dr. Juan Diego Cortés García**

San Luis Potosí, S.L.P. FECHA: enero de 2026

INTEGRANTES DEL COMITÉ ACADÉMICO

Dra. Diana Patricia Portales Pérez. Director de tesis. Adscrita al Posgrado de Ciencias Farmacobiológicas de la Facultad de Ciencias Químicas de la Universidad Autónoma de San Luis Potosí, S.L.P.

Dra. Mariana Haydee García Hernández. Codirectora de tesis. Adscrita a la Unidad de Investigación Biomédica Delegación Zacatecas del Instituto Mexicano del Seguro Social, IMSS.

Dra. Edith Elena Uresti Rivera. Tutora de tesis. Adscrita al Posgrado de Ciencias Farmacobiológicas de la Facultad de Ciencias Químicas de la Universidad Autónoma de San Luis Potosí, S.L.P.

Dr. Juan Manuel Vargas Morales. Tutor de tesis. Adscrito al Posgrado de Ciencias Farmacobiológicas de la Facultad de Ciencias Químicas de la Universidad Autónoma de San Luis Potosí, S.L.P.

Carta Cesión de Derechos

San Luis Potosí SLP a 01/ 09/ 2026

En la ciudad de San Luis Potosí el día 09 del mes de enero del año 2026. El que suscribe Abraham Cárdenas Juárez. Alumno(a) del programa de posgrado en Ciencias Farmacobiológicas adscrito a la Facultad de Ciencias Químicas manifiesta que es autor(a) intelectual del presente trabajo terminal, realizado bajo la dirección de: la Dra. Diana Patricia Portales Pérez y la Dra. Mariana Haydee García Hernández cede los derechos del trabajo titulado: Significancia diagnóstica del perfil de lípidos y sus razones (colesterol/c-HDL, triglicéridos/c-HDL, c-LDL/c-HDL, WBC/c-HDL y FBG/c-HDL) para predecir síndrome metabólico a la **Universidad Autónoma de San Luis Potosí**, para su difusión con fines académicos y de investigación.

Los usuarios de la información no deben reproducir de forma total o parcial texto, gráficas, imágenes o cualquier contenido del trabajo si el permiso expreso del o los autores. Éste, puede ser obtenido directamente con el autor o autores escribiendo a la siguiente dirección dportale@uaslp.mx; mariana.haydee.gh@gmail.com. Si el permiso se otorga, el usuario deberá dar el agradecimiento correspondiente y citar la fuente del mismo.

Abraham Cárdenas Juárez

Nombre y firma del alumno

UNIVERSIDAD AUTÓNOMA DE SAN LUIS POTOSÍ
Facultad de Ciencias Químicas
Centro de Investigación y Estudios de Posgrado
Posgrado en Ciencias Farmacobiológicas
Programa de Maestría

Formato M28

Carta de Análisis de Similitud

San Luis Potosí SLP a 01/ 12/ 2026

L.B. Reyna Nayeli Ortiz Quintero
Biblioteca de Posgrado FCQ

Asunto: Reporte de porcentaje de similitud de tesis de grado

Por este medio me permito informarle el porcentaje de similitud obtenido mediante Ithenticate para la tesis titulada Significancia diagnóstica del perfil de lípidos y sus razones (colesterol/c-HDL, triglicéridos/c-HDL, c-LDL/c-HDL, WBC/c-HDL y FBG/c-HDL) para predecir síndrome metabólico presentada por el autor Abraham Cárdenas Juárez. La tesis es requisito para obtener el grado de Maestría en el Posgrado en Ciencias Farmacobiológicas. El análisis reveló un porcentaje de similitud de 45% Es importante aclarar que un porcentaje de similitud significativo se debió a la existencia de artículos publicados por el alumno en revistas indexadas, y que se anexan al final del documento de tesis.

Agradezco sinceramente su valioso tiempo y dedicación para llevar a cabo una exhaustiva revisión de la tesis. Quedo a su disposición para cualquier consulta o inquietud que pueda surgir en el proceso.

Sin más por el momento, le envío un cordial saludo.

A T E N T A M E N T E

Dra. Claudia Escudero Lourdes

Coordinador Académico del Posgrado en Ciencias Farmacobiológicas

Resumen

Introducción. El síndrome metabólico (SMet) es una condición fisiopatológica compleja que se caracteriza por hipertrigliceridemia, hiperglucemia, hipertensión, niveles bajos de HDL-c y obesidad visceral. Su presencia identifica a individuos con un mayor riesgo de desarrollar enfermedades cardiovasculares y diabetes tipo 2. Sin embargo, la falta de métodos prácticos y confiables para su diagnóstico limita su aplicación en la determinación temprana de personas en riesgo. **Objetivo**. Analizar la utilidad diagnóstica de marcadores derivados del perfil de lípidos (índice TyG y las razones TC/HDL-c, TG/HDL-c, LDL-c/HDL-c, FBG/HDL-c y WBC/HDL-c) en la detección del SMet en población mexicana. **Métodos**. Se diseñó un estudio retrospectivo y analítico que incluyó 619 individuos. Se desarrolló un modelo de regresión logística para evaluar las asociaciones de los distintos marcadores como factores de riesgo con la presencia de SMet, se determinaron los puntos de corte de los marcadores mediante un análisis de curvas ROC y el índice de Youden. **Resultados**. Se observó una asociación positiva y significativa entre todos los marcadores con la presencia del SMet. Los valores de corte para los marcadores que mejor predijeron el SMet fueron TyG ≥4.8 (sensibilidad = 91.4%, especificidad = 74.3%), TC/HDL-c ≥3.7 (sensibilidad = 74.3%, especificidad = 75.7%), TG/HDL-c ≥3.3 (sensibilidad = 82.5%, especificidad = 84.0%), y FBG/HDL-c ≥2.0 (sensibilidad = 85.1%, especificidad = 79.7%). **Conclusión**. Nuestro estudio demostró la capacidad diagnóstica de los distintos marcadores en detectar el SMet, lo que sugiere que estos marcadores pueden ser útiles en la práctica clínica para el diagnóstico oportuno y preciso del SMet.

Palabras clave: síndrome metabólico; perfil de lípidos; índice TyG; razón TC/HDL-c, razón TG/HDL-c, razón FBG/HDL-c.

Abstract

Introduction. Metabolic syndrome (MetS) is a complex pathophysiological condition characterized by hypertriglyceridemia, hyperglycemia, hypertension, low HDL-c levels, and visceral obesity. Its presence identifies individuals at increased risk of developing cardiovascular disease and type 2 diabetes. However, the lack of practical, cost-effective and reliable diagnostic methods limits its utility in identifying at-risk individuals. **Objective**. To evaluate the diagnostic utility of lipid profile-derived markers (TyG index, and the TC/HDL-C, TG/HDL-C, LDL-C/HDL-C, FBG/HDL-C, and WBC/HDL-C ratios) for the detection of MetS in Mexican population. **Methods**. A retrospective, analytical study was conducted involving 619 individuals. A logistic regression model was used to evaluate the associations of different markers as risk factors for the presence of MetS. Cut-off points for the markers were determined using ROC curve analysis and the Youden index. **Results**. A positive and significant association was observed between all markers and the presence of MetS. The cut-off values for the markers that best predicted MetS were: TyG ≥4.8 (sensitivity = 91.4%, specificity = 74.3%), TC/HDL-C ≥3.7 (sensitivity = 74.3%, specificity = 75.7%), TG/HDL-C ≥3.3 (sensitivity = 82.5%, specificity = 84.0%), and FBG/HDL-C ≥2.0 (sensitivity = 85.1%, specificity = 79.7%). **Conclusion**. This study demonstrated the diagnostic relevance of these markers in detecting MetS, supporting their potential application in clinical practice for the timely and accurate diagnosis of the condition.

Keywords: metabolic syndrome; lipid profile; TyG index; TC/HDL-c ratio, TG/HDL-c ratio, FBG/HDL-c ratio.

Index

Introduction

Metabolic syndrome (MetS) is considered a silent epidemic that represents a global public health concern. Over time, it has been described under various names in scientific literature, such as syndrome X, deadly quartet, or insulin resistance syndrome, among others (Sherling et al., 2017). MetS is not a single disease, but rather a set of metabolic alterations that, according to the clinical definition of "syndrome," coexist in the same individual with a frequency greater than expected by chance. These alterations include glucose intolerance, insulin resistance (IR), central obesity, dyslipidemia, and arterial hypertension (Bovolini et al., 2021; Eckel et al., n.d.).

The first description of this constellation of disorders is attributed to Dr. Eskil Kylin in 1923, who identified the coexistence of hypertension, hyperglycemia, and gout. Later, in 1956, Dr. Jean Vague observed an association between central adiposity (android obesity), atherosclerosis, diabetes, gout, and nephrolithiasis (Eckel et al., n.d.). However, it was Dr. Gerald Reaven who, in 1988, proposed the central role of IR in the pathophysiology of MetS and highlighted its significance as a risk factor for the development of type 2 diabetes (T2D) and cardiovascular disease (CVD) (Reaven, 1988).

Several studies have shown that MetS substantially increases the risk of developing multiple chronic conditions. Compared to individuals without MetS, those with the syndrome have an estimated 5-fold increased risk of developing T2D, a 2-fold increased risk of developing CVD over a 5- to 10-year period, a 2- to 4-fold increased risk of stroke, a 3- to 4-fold increased risk of acute myocardial infarction, and a 2-fold increased risk of mortality associated with these events (Lopez-Candales et al., 2017).

To address this concern, several organizations have developed diagnostic guidelines for MetS to help clinicians identify individuals at risk. Despite sharing common components (IR, obesity, dyslipidemia, and hypertension) these guidelines differ in their diagnostic emphasis and criteria (Huang, 2009).

The World Health Organization (WHO) first defined MetS in 1988, making IR mandatory for diagnosis. Patients must exhibit IR (measured through: fasting plasma glucose >100 mg/dL, plasma glucose >140 mg/dL at 120 minutes after a 75-grams glucose load, or the presence of T2D) plus at least two additional factors: obesity (BMI ≥30 kg/m² or waist-to-hip ratio >0.90 men and >0.85 in women), dyslipidemia (TG ≥150 mg/dL or HDL-c <35 mg/dL in men and <39 mg/dL in women); hypertension (≥140/90 mmHg); and presence or microalbuminuria. However, because it requires specialized biochemicals test, the WHO definition is rarely used in large-scale or routine clinical settings (Huang, 2009).

The European Group for the study of Insulin Resistance (EGIR) revised the definition in 1999, maintaining IR as a required feature but simplifying its assessment to fasting insulin levels above the 75th percentile. EGIR also required at least two of the following: central obesity (WC ≥94 cm in men and ≥80 cm in women), hypertension, or dyslipidemia. It removed microalbuminuria and excluded individuals with T2D, increasing practicality but limiting applicability (Huang, 2009).

In 2005, the International Diabetes Federation (IDF) proposed new criteria, shifting focus from IR to central obesity as the mandatory feature, using WC cut-offs tailored to different ethnic groups. This adjustment recognizes varying fat distribution and cardiometabolic risk across different populations. However, the IDF has been criticized for overemphasizing obesity at the expenses of IR, which remains central component of MetS pathophysiology (Reaven, 2006).

The National Cholesterol Education Program Adult Treatment Panel III (NCEP-ATP III), also in 2005, introduced the most widely adopted definition. It does not require a specific mandatory component; instead, MetS is diagnosed when three or more of five criteria are met: elevated blood pressure (>130/85 mmHg), high WC (>40 inches in men and >35 inches in women), elevated FBG (≥100 mg/dL), high TG (≥150 mg/dL), and low HDL-c (<40 mg/dL in men and <50 mg/dL in women) (Huang, 2009).

Over the past two decades, the global prevalence of MetS has increased substantially, closely linked to the rising epidemics of obesity and diabetes. The NCEP-ATP in the United States estimates that more than 20% of the adult population in Western countries has MetS. However, prevalence varies considerably depending on the diagnostic criteria used and among different ethnic groups. Factors such as sex, age, ethnic origin, and environmental and sociocultural aspects can significantly influence these estimates (Balkau et al., 2003). Mexico has some of the highest rates of MetS, with a prevalence ranging from 41% to 54% among adults over 40 years of age (Gutiérrez-Solis et al., 2018).

The diagnosis of MetS is traditionally based on clinical guidelines that consider variables such as triglycerides (TG), high-density lipoprotein cholesterol (HDL-c), fasting blood glucose (FBG), waist circumference (WC), body mass index (BMI), and blood pressure. However, these guidelines have several limitations, including variability between definitions and a lack of adaptation to different populations. Moreover, they do not consider the distribution of adipose tissue, and their applicability may be limited in resource-poor settings. To address these challenges, alternative markers derived from lipid profiles have emerged and shown promise for the timely and accurate detection of metabolic alterations associated with MetS. These include the triglyceride-glucose (TyG) index, as well as the total cholesterol (TC)/HDL-c, TG/HDL-c, low-density lipoprotein cholesterol (LDL-c)/HDL-c, FBG/HDL-c, and white blood cell count (WBC)/HDL-c ratios (Bovolini et al., 2021; Cardenas-Juarez et al., 2024; Grundy et al., 2004)

Given the close association between MetS and chronic non-communicable diseases, prevention and control strategies should focus on modifiable risk factors, such as unhealthy diets, sedentary lifestyles, and poor health habits. In this context, early diagnosis serves as a fundamental tool for reducing the morbidity and mortality associated with MetS. Accordingly, this study assesses the diagnostic value of alternative lipid-based indices as practical markers for early MetS detection in the Mexican adult population, where prevalence remains alarmingly high.

Background Information

Pathophysiology of metabolic syndrome

Its pathophysiology is multifaceted, resulting from the complex interaction among various components, including visceral adipose tissue (VAT) and its endocrine activity, IR, dyslipidemia, and hypertension.

The accumulation of VAT is associated with an increased risk of developing IR, T2D), and CVD compared to the accumulation of subcutaneous adipose tissue. Furthermore, visceral adiposity is the primary source of free fatty acids (FFAs) due to its high rate of catabolic activity (lipolysis), which leads to an increased flow and ectopic accumulation of FFAs, resulting in lipotoxicity. Chronic exposure to elevated circulating levels of FFAs plays a crucial role in cellular dysfunction in the liver, pancreas, and skeletal muscle (Bovolini et al., 2021).

The liver plays a central role in lipid metabolism through the uptake of serum FFAs and the synthesis, storage, and transport of lipid metabolites. Typically, the liver's response to chronically elevated levels of FFAs and other dietary lipids results in hepatic IR, which increases gluconeogenesis and contributes to hyperglycemia. FFAs released into the portal circulation are transported to the liver, where they are stored as triglycerides and stimulate the production of very low-density lipoproteins (vLDL). In the bloodstream, triglycerides in vLDL are transferred to high-density lipoproteins (HDL) by the action of cholesterol ester transfer protein, resulting in triglyceride-enriched HDL particles. These modified HDL particles become better substrates for hepatic lipase, leading to their rapid removal from circulation, which decreases HDL bioavailability and causes dyslipidemia, characterized by low plasma HDL-c and high triglycerides levels (Huang, 2009; Samuel & Shulman, 2016).

Regarding the pancreas, elevated levels of circulating FFAs are associated with structural and functional damage, including oxidative stress in the endoplasmic reticulum and apoptosis of pancreatic β-cell, which impairs insulin synthesis and secretion (Sharma & Alonso, 2014). Furthermore, since VAT accumulation is typically

linked to overweight and obesity, the increased insulin demand in these states induces overload, resulting in pancreatic β-cell dysfunction and contributing to IR (Bovolini et al., 2021).

Increased FFAs flux into the muscle tissue also inhibit insulin signaling. Although the exact mechanisms remain unclear, lipid accumulation within myocytes is the most likely cause of muscle IR, as impaired fatty acid β-oxidation and reduced glycogen synthesis have been observed in association with this accumulation (Samuel et al., 2010)

The harmful effects of VAT in overweight and obesity are largely due to its endocrine and immunological modulation. As adipocytes enlarge and adipose tissue expands because of lipid accumulation, the secretion of adipokines (including hormones, proinflammatory cytokines, and peptides) is altered (Fahed et al., 2022). Key proinflammatory cytokines include tumor necrosis factor alpha (TNF-α) and interleukins (IL) 6, 18, and 1β. These factors contribute both to local and systemic inflammation and directly induce IR. IR develops through multiple mechanisms, such as decreased expression of the insulin receptor and glucose transporter-4 (GLUT-4), as well as activation of Ser/Thr kinases that inhibit the insulin signaling pathway by phosphorylating insulin receptor substrate-1 (IRS-1) on Ser residues. This phosphorylation inhibits the phosphatidylinositol 3-kinase (PI3K) pathway, preventing GLUT-4 translocation to the cell membrane of adipocytes, myocytes, and cardiomyocytes (Boucher et al., 2014; Kwon & Pessin, 2013a)

Another important factor in obesity-associated inflammation is the activation of toll-like receptors (TLRs), particularly TLR-2 and TLR-4. Although TLRs are ubiquitously expressed, increased expression of TLR-4 has been observed in muscle and adipose tissue under obese conditions. Activation of these receptors by FFAs promotes Ser/Thr phosphorylation of IRS-1 via the activation of c-Jun N-terminal kinase (JNK), a kinase that inhibits nuclear factor kappa B (NF-κB). Additionally, FFAs induce the activation of the TLR-4/NF-κB pathway in resident macrophages within visceral adipose tissue stimulates the synthesis and secretion of proinflammatory cytokines such as IL-6, TNF-

α, IL-1β, and IL-18, all of which contribute to the chronic inflammatory state of adipose tissue in obesity (Kwon & Pessin, 2013b)

Another essential component of MetS is hypertension, defined as a transient or sustained elevation of systemic blood pressure that can lead to cardiovascular damage. It is characterized by resting blood pressure values greater than 130/85 mmHg and is associated with several anthropometric and metabolic abnormalities. The development of hypertension in MetS is multifactorial. It is partially mediated by endothelial dysfunction caused by the generation of reactive oxygen species, which is promoted by FFAs; activation of the sympathetic nervous system induced by hyperinsulinemia; and inhibition of the enzyme nitric oxide synthase. Additionally, cytokines derived from adipose tissue, such as TNF-α and IL-6, contribute to this dysfunction. Hyperactivity of the renin-angiotensin-aldosterone system, commonly observed in obesity, also plays a significant role in the development of hypertension (Samson & Garber, 2014)

Lipid profile-derived markers as diagnostic tools in metabolic pathologies

Several studies have proposed lipid profile-derived markers as alternative diagnostic tools for the early and accurate detection of various metabolic pathologies. Among these, TyG index has been evaluated as a marker of IR in the Mexican population (TyG ≥4.65; sensitivity: 84.0%, specificity: 45.0%) (Simental-Mendía et al., 2008), as a diagnostic marker for MetS in Brazil (TyG ≥4.52; sensitivity: 84.3%, specificity: 75.75%) (Ferreira et al., 2021), and as a predictor of coronary events in patients with T2D in China (TyG ≥9.32; sensitivity: 46.0%, specificity: 63.6%) (Wang et al., 2020)

For their part, the TG/HDL-c ratio has been evaluated as a marker of IR in Argentina (TG/HDL-c ≥3.50; sensitivity: 43.0%, specificity: 81.0%) (Salazar et al., 2013) and Taiwan (TG/HDL-c ≥2.19; sensitivity: 72.4%, specificity: 65.1%) (Yeh et al., 2019), as well as a diagnostic marker of MetS in Mexico (TG/HDL-c ≥3.46; sensitivity: 79.6%, specificity: 76.4%) (Baez-Duarte et al., 2022), China (TG/HDL-c ≥1.49; sensitivity: 72.4%, specificity: 80.8%) (Nie et al., 2021), and Germany, with sex-specific cut-off

points (men: TG/HDL-c ≥2.80; sensitivity: 80.0%, specificity: 71.0%; women: TG/HDL-c ≥1.90; sensitivity: 80.0%, specificity: 75.0%) (von Bibra et al., 2017). It has also been proposed as a marker of non-alcoholic fatty liver disease (NAFLD) in the Italian population (TG/HDL-c ≥1.64; sensitivity: 60.4%, specificity: 74.6%) (Catanzaro et al., 2022).

Regarding other markers, the TC/HDL-c ratio has been evaluated as a risk factor for CVD in the U.S. population, with a hazard ratio (HR) of 1.39 (95% CI: 1.22–1.58) in men and 1.39 (95% CI: 1.17–1.66) in women (Ingelsson et al., 2007). Similarly, the LDL-c/HDL-c ratio has been associated with cardiovascular risk in the same population (men: HR = 1.35; 95% CI: 1.18–1.54; women: HR = 1.36; 95% CI: 1.14–1.63) (Ingelsson et al., 2007). In addition, the LDL-c/HDL-c ratio has been analyzed as a marker of NAFLD in China (LDL-c/HDL-c ≥1.66; sensitivity: 54.22%, specificity: 71.43%) (Zou et al., 2021), and as a predictor of coronary artery disease following acute myocardial infarction, also in China (LDL-c/HDL-c ≥2.15; sensitivity: 84.5%, specificity: 20.2%) (Gao et al., 2022).

Finally, other indicators have been proposed, such as the FBG/HDL-c ratio, which has been associated with cardiovascular risk in China (HR = 1.284; 95% CI: 1.010–1.631) (Guo et al., 2020), and the WBC/HDL-c ratio, evaluated as a predictor of mortality due to coronary artery disease (HR = 2.036; 95% CI: 1.258–3.296) (Wu et al., 2021).

Justification

Metabolic syndrome is a complex pathophysiological condition characterized by four main features: insulin resistance, central obesity, atherogenic dyslipidemia, and endothelial dysfunction. Its diagnosis is important for several reasons. First, it allows discrimination between a specific group of patients with a shared pathophysiology, those with an increased risk of developing type 2 diabetes and cardiovascular diseases. Second, analyzing the interrelationships among the components of metabolic syndrome provides deeper insight into the underlying mechanisms and their association with an elevated risk of fatal complications. Third, it supports epidemiological and clinical research on different approaches to pharmacological treatments, lifestyle interventions, and preventive strategies. In response to this need, multiple clinical guidelines have been developed to establish diagnostic criteria for metabolic syndrome. However, due to the heterogeneity of its clinical manifestations and interindividual variability, significant limitations remain in the application and standardization of these guidelines. Therefore, the development and validation of complementary diagnostic tools is essential to enhance early detection and enable timely intervention on modifiable risk factors, such as unhealthy dietary habits and physical inactivity. Timely diagnosis is critical to reducing the morbidity and mortality associated with this condition. In this context, various lipid profile-derived markers have been proposed as tools for the early and accurate identification of metabolic syndrome-related pathologies. However, studies have shown that the optimal cutoff points for identifying individuals at risk may vary by ethnic background. Consequently, it is particularly relevant to evaluate their diagnostic utility markers for detecting metabolic syndrome in the Mexican population.

Hypothesis

H_0: The different markers derived from the lipid profile (TyG index and the ratios: TC/HDL-c, TG/HDL-c, LDL-c/HDL-c, FBG/HDL-c and WBC/HDL-c) will not have diagnostic utility in the identification of metabolic syndrome in the Mexican population.

H_1: The different markers derived from the lipid profile (TyG index and the ratios: TC/HDL-c, TG/HDL-c, LDL-c/HDL-c, FBG/HDL-c and WBC/HDL-c) will indeed have diagnostic utility in the identification of metabolic syndrome in the Mexican population.

Objectives

General objective

To determine and compare the diagnostic accuracy of various lipid profile-derived markers (TyG index and the ratios: TC/HDL-c, TG/HDL-c, LDL-c/HDL-c, FBG/HDL-c, and WBC/HDL-c) for the identification of metabolic syndrome in the adult Mexican population.

Specific objectives

1. To recruit a representative sample of approximately 800 adults participants to perform conventional laboratory tests and collect their anthropometric data.
2. To classify participants according to the presence or absence of metabolic syndrome based on the NCEP-ATP III guidelines, and to perform descriptive and inferential statistical analysis to characterize both study groups (presence or absence of metabolic syndrome).
3. To design a multivariate binary logistic regression model to determine the associations between different markers derived from the lipid profile and the presence of metabolic syndrome.
4. To determine the cut-off point for each lipid profile-derived marker in which greater joint sensitivity and specificity are obtained through an analysis of ROC curves and the Youden index.

Clinical significance of the lipid profile ratios TC/HDL-c, TG/HDL-c, FBG/HDL-c and TyG index, in the diagnosis of metabolic syndrome

Cardenas-Juarez A[a], Portales-Pérez DP[bc], Rivas-Santiago B[a], García-Hernández MH[a*]

[a]Unidad de Investigación Biomédica, Delegación Zacatecas, México. Instituto Mexicano del Seguro Social, IMSS.

[b]Facultad de Ciencias Químicas, Universidad Autónoma de San Luis Potosí, Manuel Nava 6, Zona Universitaria, 78210, San Luis Potosí, SLP, México.

[c]Centro de Investigación en Ciencias de la Salud y Biomedicina, Universidad Autónoma de San Luis Potosí, Sierra Leona 550, Lomas de San Luis, 78210, San Luis Potosí, SLP, México.

*Corresponding author: Mariana Haydee García-Hernández, PhD.

Unidad de Investigación Biomédica, Delegación Zacatecas.

Instituto Mexicano del Seguro Social, IMSS.

Interior Alameda No. 45. 98000 Zacatecas, Zac, México.

Phone: (52-492) 92 260 19 Fax. 01 492 922 18 81

Email: mariana.haydee.gh@gmail.com

ORCID: 0000-0002-9244-5706

Abstract

Introduction. Metabolic syndrome (MetS) is a pathophysiological condition defined by a set of metabolic alterations such as hypertriglyceridemia, hyperglycemia, hypertension, low HDL-c levels, and visceral obesity. Its presence identifies people with an increased risk of developing cardiovascular diseases and type 2 diabetes; however, the lack of practical and reliable methods for its diagnosis limits the identification of people with this condition. **Objective**. Analyze the diagnostic utility of markers derived from the lipid profile (TyG index and the ratios TC/HDL-c, TG/HDL-c, LDL-c/HDL-c, FBG/HDL-c and WBC/HDL-c) in the determination of MetS. Methods. A retrospective study was designed which included 619 individuals. A logistic regression model was used to evaluate the associations of the different markers with MetS, and the cut-off points of the markers were determined through an analysis of ROC curves and the Youden index. **Results**. A positive and significant association was observed between all markers and the presence of MetS. The cut-off values for the markers that best predicted MetS were TyG ≥4.8 (sensitivity = 91.4%, specificity = 74.3%), TC/HDL-c ≥3.7 (sensitivity = 74.3%, specificity = 75.7%), TG/HDL-c ≥3.3 (sensitivity = 82.5%, specificity = 84.0%), and FBG/HDL-c ≥2.0 (sensitivity = 85.1%, specificity = 79.7%). **Conclusion**. Our study demonstrated the diagnostic relevance of the different markers in detecting MetS, suggesting that these ratios may be useful in clinical practice for the opportune and accurate diagnosis of MetS.

Keywords: metabolic syndrome; lipid profile; TyG index; TC/HDL-c ratio, TG/HDL-c ratio, FBG/HDL-c ratio.

Introduction

Metabolic syndrome (MetS) is a pathophysiological condition in which four main characteristics are distinguished: insulin resistance (IR), central obesity, atherogenic dyslipidemia, and endothelial dysfunction (Huang, 2009). The MetS is defined by a set of metabolic alterations, according to the third report of the National Cholesterol Education Program Adult Treatment Panel (NCEP ATP-III), the diagnosis of this condition is granted if three or more of the following five criteria are met: blood pressure greater than 130/85 mmHg, waist circumference (WC) ≥40 inches in men and ≥35 inches in women, fasting blood glucose (FBG) levels ≥100 mg/dL, fasting triglyceride (TG) levels ≥150 mg/dL and fasting high-density lipoprotein cholesterol (HDL-c) levels <40 mg/dL in men and <50 mg/dL in women (Alberti et al., 2009). Its presence discriminates between a specific group of patients with a shared pathophysiology, those with an increased risk of developing cardiovascular disease (CVD), and type 2 diabetes (TD2). However, the lack of practical methods for its diagnostic implementation limits its application in the field of preventive medicine. In this context, different markers derived from the lipid profile have been proposed for the opportune and accurate diagnosis of different metabolic pathologies, for example, the following have been evaluated: the triglyceride-glucose index (TyG) as a marker of IR (Simental-Mendía et al., 2022), MetS (Ferreira et al., 2021) and coronary events in patients with T2D and in patients with acute coronary syndrome ; TG/HDL-c ratio as a marker of IR (von Bibra et al., 2017; Yang et al., 2021; Young et al., 2019), MetS (Baez-Duarte et al., 2022; Nie et al., 2021), diabetes (Chen et al., 2020), development of CVD (Azarpazhooh et al., 2021; McLaughlin et al., 2005) and non-alcoholic fatty liver disease (NAFLD) (Catanzaro et al., 2022); total cholesterol (TC)/HDL-c ratio as a predictor of premature myocardial infarction and CVD (Ingelsson et al., 2007; Ridker et al., 2005); low-density lipoprotein cholesterol (LDL-c)/HDL-c ratio as a marker of NAFLD (Zou et al., 2021) and as a predictor of coronary artery disease subsequent to acute myocardial infarction (Gao et al., 2022); likewise, FBG/HDL-c and white blood cell count (WBC)/HDL-c ratios have been evaluated as predictors of mortality resulting from coronary artery disease (Guo et al., 2020; Wu et al., 2021). However, previous studies

have shown that the cut-off points for determining people at risk can vary depending on their ethnic origin (Li et al., 2008; Tejera et al., 2021), therefore, the objective of this study was to determine and compare the accuracy diagnosis of the different markers derived from the lipid profile (TyG, TC/HDL-c, TG/HDL-c, LDL-c/HDL-c, FBG/HDL-c and WBC/HDL-c) in the diagnosis of MetS in the adult population of Mexico.

Participants and Methods

Study population

This retrospective study included the participation of 619 subjects (228 men and 391 women) aged 44.0 ± 13.0 years, from the metropolitan area of the city of Zacatecas, Mexico. No one of the individuals had vascular complications, pregnancy, hypothyroidism, or clinical infections disease. In addition, the individuals were not regular smokers, and they did not ingest alcohol on regular basis. People under regular pharmacological treatment for metabolic disorders (e.g., statins, hypoglycemic agents, insulin, etc.) were included and people under hormonal treatment (e.g., corticosteroids and levothyroxine), chemotherapy, as well as lactating women were excluded. All participants were informed about the study and signed an informed consent. The protocol was approved by the bioethics committee of the Mexican Institute of Social Security (IMSS), with the registration number R-2018-785-072 and SALUD-2012-01-182554.

Anthropometric and biochemical characteristics

Anthropometric measurements were obtained by trained personnel. Body mass index (BMI, Kg/m^2) and waist-hip ratio (WHR, waist cm/hip cm) were determined; a BMI <25 was considered normal weight, a BMI ≥25 and <30 was considered overweight, and a BMI ≥30 was considered obese. After fasting for 10 to 12 hours, a blood sample was taken by venipuncture for the determination of white blood cell count (WBC) and levels

of fasting blood glucose (FBG), glycated hemoglobin (Hb1Ac), total cholesterol (TC), high-density lipoprotein cholesterol (HDL-c), low-density lipoprotein cholesterol (LDL-c) and triglycerides (TG), in accordance with the conventional protocols of the IMSS Zone 1 General Hospital. The TyG index was used as a surrogate marker for the determination of triglyceride-driven insulin resistance; a TyG index ≥4.6 indicates insulin resistance. This index was calculated as Ln [fasting triglycerides (mg/dL)*fasting glucose (mg/dL)]/2 (Simental-Mendía et al., 2022). For their part, the ratios TC/HDL-c, TG/HDL-c, LDL-c/HDL-c, FBG/HDL-c and WBC/HDL-c were calculated by dividing the levels of TC (mg/dL), TG (mg/dL), LDL-c (mg/dL), FBG (mg/dL) and WBC ($x10^7$/dL) between the levels of HDL-c (mg/dL), respectively. The diagnosis of MetS was established according to the NCEP ATP-III criteria (Alberti et al., 2009), with values adjusted to the Mexican population (Baez-Duarte et al., 2010).

Statistical analysis

Statistical analysis was performed using SPSS software (IBM Statistics version 20.0). The Shapiro-Wilk test was used to determine the distribution of quantitative variables; because all variables presented a non-normal distribution, quantitative variables were compared using the nonparametric Mann-Whitney U test, while the chi-square test (X^2) was used for qualitative variables. The Spearman rank test was used to analyze the correlations between the TyG index and the TC/HDL-c, TG/HDL-c, LDL-c/HDL-c, FBG/HDL-c and WBC/HDL-c ratios with the different quantitative variables established. The association between the TyG index and the TC/HDL-c, TG/HDL-c, LDL-c/HDL-c, FBG/HDL-c and WBC/HDL-c ratios with MetS was analyzed using a logistic regression analysis. To define the cut-off, point at which the greatest sensitivity and specificity of the index and the ratios evaluated is obtained, the ROC (receiver operating characteristic) curve analysis and the Youden index were performed, and an area under the curve (AUC) ≥0.7 was considered acceptable. A value of $p<0.05$ was considered significant.

Results

Anthropometric and biochemical characteristics

A total of 619 people participated in this study, of whom 36.8% were men and 63.2% were women, whose average age was 44 ± 13.0 years. The individuals consisted in Mexican-mestizo population which is defined as people born in the country having a Spanish-derived last name, with family antecedents of Mexican ancestors (Salazar-Flores et al., 2010). Participants were classified according to the presence of MetS (43.5%, 94 males; 175 females) or its absence (control group) (56.5%, 134 males; 216 females). Participants diagnosed with MetS presented values of the TyG index and ratios of TC/HDL-c, TG/HDL-c, LDL-c/HDL-c, FBG/HDL-c and WBC/HDL-c, significantly higher compared to the control group ($p<0.001$). Both groups differ in obesity indicators such as BMI, WC and WHR, whose values were higher in the group with MetS ($p<0.001$) compared to the control group. Likewise, blood levels of FBG, Hb1Ac, TC, LDL-c, and TG were found to be statistically higher in the MetS group compared to the control, however, HDL-c blood levels were higher in the control group compared to people diagnosed with MetS ($p<0.001$) (Table 1).

Bivariate correlation analysis

The results of the bivariate correlation analysis demonstrated a statistically significant relationship between the TyG index and the TC/HDL-c, TG/HDL-c, LDL-c/HDL-c, FBG/HDL-c and WBC/HDL-c ratios with the MetS components: WC (rho = 0.360, $p<0.001$; rho = 0.288, $p<0.001$; rho = 0.355, $p<0.001$; rho = 0.210, $p<0.001$; rho = 0.360, $p<0.001$; rho = 0.135, $p<0.01$, respectively), FBG (rho = 0.735, $p<0.001$; rho = 0.333, $p<0.001$; rho = 0.344, $p<0.001$; 0.264, $p<0.001$; rho = 0.834, $p<0.001$; rho = 0.059, $p = 0.144$, respectively), HDL-c (rho = -0.356, $p<0.001$; rho = -0.704, $p<0.001$; rho = -0.688, $p<0.001$; rho = -0.551, $p<0.001$; rho = -0.662, $p<0.001$; rho = -0.535, $p<0.001$, respectively) and TG (rho = 0.850, $p<0.001$; rho = 0.589, $p<0.001$; rho = 0.919, $p<0.001$; rho = 0.319, $p<0.001$; rho = 0.439, $p<0.001$;

rho = 0.227, p<0.001, respectively). Likewise, significant correlations with the other established variables were observed (Table 2).

Multivariable association analysis

After observing that the study variables were correlated with the MetS components and, to investigate their association as risk factors for the development of this condition, a logistic regression analysis was performed. It was found that the association between MetS and the study variables remained significant, even after adjustment for sex and age: TyG (OR = 2.504, CI = 1.131 - 5.544, p<0.05); TC/HDL-c (OR = 2.449, CI = 1.245 - 4.818, p<0.01); TG/HDL-c (OR = 7.383, CI = 3.428 - 15.90, p<0.001); LDL-c/HDL-c (OR = 2.164, CI = 1.024 - 4.573, p<0.05); FBG/HDL-c (OR = 23.53, CI = 10.02 - 55.24, p<0.001); WBC/HDL-c (OR = 1.867, CI = 1.109 - 3.144, p<0.05) (Table 3).

ROC (receiver operating characteristic) curve analysis

According to the Youden index of the ROC curves, the optimal cut-off values of the TyG index and the ratios of the lipid profile in which the greatest joint sensitivity and specificity are obtained were the following: TyG (≥4.823), TC/HDL-c (≥3.701), TG/HDL-c (≥3.311), LDL-c/HDL-c (≥2.007), FBG/HDL-c (≥2.001) and WBC/HDL-c (≥101.06). Furthermore, the area under the curve was significant for: TyG (0.904), TC/HDL-c (0.812), TG/HDL-c (0.903), LDL-c/HDL-c (0.713), FBG/HDL-c (0.885) and WBC/HDL-c (0.660), with a significant value of p<0.001 in all cases. The TyG index (sensitivity = 91.40%, specificity = 74.30%) and the TC/HDL-c (sensitivity = 74.3%, specificity = 75.7%), TG/HDL-c (sensitivity = 82.50%, specificity = 84.00%) and FBG/HDL-c (sensitivity = 85.10%, specificity = 79.70%) ratios, were the markers that demonstrated the highest diagnostic accuracy (Table 4, Figure 1).

Discussion

In this study we analyzed the association of different markers of the lipid profile with MetS, our results demonstrated the diagnostic accuracy of the TyG index and the TC/HDL-c, TG/HDL-c, and FBG/HDL-c ratios to identify individuals at high risk of developing MetS in the Mexican-mestizo population. The cut-off values for the markers that best predicted MetS were: TyG index ≥4.8, TC/HDL-c ratio ≥3.7, TG/HDL-c ratio ≥3.3, and FBG/HDL-c ratio ≥2.0. Previous studies have established different cut-off points for some of these markers for the diagnosis of MetS. For example, in a study carried out in an adult population between 18 and 59 years of age in Brazil, the cut-off value for the TyG index ≥4.52 (sensitivity = 84.3%, specificity = 75.7%) was proposed (Ferreira et al., 2021), compared to the cut-off point that we propose in our study (≥4.8), we obtained greater sensitivity and specificity. Likewise, cut-off values have been established for the TG/HDL-c ratio in the diagnosis of MetS; in a study carried out in Mexican-mestizo adults, a value of ≥3.0 was proposed (sensitivity = 86.9%, specificity = 66.8%) (Baez-Duarte et al., 2022), which was similar to that observed in our analyzes (≥3.3), however, we obtained greater specificity and similar sensitivity with the cut-off point that we propose, likewise, cut-off points have also been established for this same ratio in the population of Germany (von Bibra et al., 2017), Argentina (Salazar et al., 2013) and China (Nie et al., 2021), however, as mentioned, the cut-off points must be established for each specific population due to the impact generated by ethnic origin on the distribution of the variables (Li et al., 2008; Tejera et al., 2021). On the other hand, it is important to mention that our study is the first to consider the FBG/HDL-c ratio as a diagnostic marker for MetS; our results demonstrated its high diagnostic accuracy at the cut-off point ≥2.0 (sensitivity = 85.1%, specificity = 79.7%; OR = 23.53) in our study population. From a clinical point of view, physicians and patients can benefit from establishing practical diagnostic methods that accurately identify individuals with MetS, facilitating the approach to pharmacological treatment, and recommending preventive lifestyle changes.

The main strength of our study is the participation of people in a risk state who were overweight or obese, but did not have MetS, which allowed us to demonstrate the robustness of the different markers as diagnostic tests. On the other hand, our study proposes novel markers as diagnostic tests for MetS. Some of the limitations of our work is that our analysis model only adjusts for age, sex and presence of obesity and does not consider other variables that could influence such as physical activity, diet, and hereditary family history.

Conclusion

In conclusion, our study demonstrated that the relative ratios of lipid profile are positively associated with the high risk of presenting MetS in Mexican-mestizo adults. The cut-off values for the markers that best predict MetS and in which the highest diagnostic accuracy was presented were: TyG index ≥4.8, and TC/HDL-c ≥3.7, TG/HDL-c ≥3.3 and FBG/HDL-c ≥2.0 ratios, these values maintained their significant association even after adjustment for age, sex and presence of overweight or obesity, suggesting that these ratios may be useful in clinical practice for a timely, accurate, and reproducible diagnosis of MetS.

Authors contributions

The authors confirm contribution to the article as follows: Material preparation, data collection, and analysis were performed by Cardenas-Juarez A. The first draft of the manuscript was written by Cardenas-Juarez A and all authors commented on previous versions of the manuscript. Study conception and design Garcia-Hernandez M.H., and Cardenas-Juarez A. Draft manuscript preparation: Cardenas-Juarez A., Portales-Perez D.P., and Rivas-Santiago B., review article and approve the final version of the manuscript. All authors read and approved the final manuscript.

Acknowledgments

None.

Conflict of Interest Statement

None of the authors has any potential financial conflict of interest related to this manuscript.

Grants and Funding

Financial support: The research reported in this manuscript was not supported. Garcia-Hernandez MH. Conflict of interest: none.

References

Alberti, K. G. M. M., Eckel, R. H., Grundy, S. M., Zimmet, P. Z., Cleeman, J. I., Donato, K. A., Fruchart, J.-C., James, W. P. T., Loria, C. M., Smith, S. C., International Diabetes Federation Task Force on Epidemiology and Prevention, Hational Heart, L. and B. I., American Heart Association, World Heart Federation, International Atherosclerosis Society, & International Association for the Study of Obesity. (2009). Harmonizing the metabolic syndrome: a joint interim statement of the International Diabetes Federation Task Force on Epidemiology and Prevention; National Heart, Lung, and Blood Institute; American Heart Association; World Heart Federation; International Atherosclerosis Society; and International Association for the Study of Obesity. *Circulation*, *120*(16), 1640–1645. https://doi.org/10.1161/CIRCULATIONAHA.109.192644

Azarpazhooh, M. R., Najafi, F., Darbandi, M., Kiarasi, S., Oduyemi, T., & Spence, J. D. (2021). Triglyceride/High-Density Lipoprotein Cholesterol Ratio: A Clue to Metabolic Syndrome, Insulin Resistance, and Severe Atherosclerosis. *Lipids*, *56*(4), 405–412. https://doi.org/10.1002/lipd.12302

Baez-Duarte, B. G., Sánchez-Guillén, M. D. C., Pérez-Fuentes, R., Zamora-Ginez, I., Leon-Chavez, B. A., Revilla-Monsalve, C., & Islas-Andrade, S. (2010). β-cell

function is associated with metabolic syndrome in Mexican subjects. *Diabetes, Metabolic Syndrome and Obesity : Targets and Therapy*, *3*, 301–309. https://doi.org/10.2147/DMSOTT.S12375

Baez-Duarte, B. G., Zamora-Ginez, I., Rodríguez-Ramírez, S. O., Pesqueda-Cendejas, L. K., & García-Aragón, K. H. (2022). TG/HDL index to identify subjects with metabolic syndrome in the Mexican population. *Gaceta Medica de Mexico*, *158*(5), 259–264. https://doi.org/10.24875/GMM.M22000693

Balkau, B., Vernay, M., Mhamdi, L., Novak, M., Arondel, D., Vol, S., Tichet, J., Eschwège, E., & D.E.S.I.R. Study Group. (2003). The incidence and persistence of the NCEP (National Cholesterol Education Program) metabolic syndrome. The French D.E.S.I.R. study. *Diabetes & Metabolism*, *29*(5), 526–532. https://doi.org/10.1016/s1262-3636(07)70067-8

Boucher, J., Kleinridders, A., & Kahn, C. R. (2014). Insulin receptor signaling in normal and insulin-resistant states. *Cold Spring Harbor Perspectives in Biology*, *6*(1). https://doi.org/10.1101/cshperspect.a009191

Bovolini, A., Garcia, J., Andrade, M. A., & Duarte, J. A. (2021). Metabolic Syndrome Pathophysiology and Predisposing Factors. *International Journal of Sports Medicine*, *42*(3), 199–214. https://doi.org/10.1055/a-1263-0898

Cardenas-Juarez, A., Portales-Pérez, D. P., Rivas-Santiago, B., & García-Hernández, M. H. (2024). Clinical Significance of the Lipid Profile Ratios and Triglyceride Glucose Index in the Diagnosis of Metabolic Syndrome. *Metabolic Syndrome and Related Disorders*, *22*(7), 510–515. https://doi.org/10.1089/met.2024.0045

Catanzaro, R., Selvaggio, F., Sciuto, M., Zanoli, L., Yazdani, A., He, F., & Marotta, F. (2022). Triglycerides to high-density lipoprotein cholesterol ratio for diagnosing nonalcoholic fatty liver disease. *Minerva Gastroenterology*, *68*(3), 261–268. https://doi.org/10.23736/S2724-5985.21.02818-X

Chen, Z., Hu, H., Chen, M., Luo, X., Yao, W., Liang, Q., Yang, F., & Wang, X. (2020). Association of Triglyceride to high-density lipoprotein cholesterol ratio and incident of diabetes mellitus: a secondary retrospective analysis based on a Chinese cohort study. *Lipids in Health and Disease*, *19*(1), 33. https://doi.org/10.1186/s12944-020-01213-x

Eckel, R. H., Grundy, S. M., & Zimmet, P. Z. (n.d.). The metabolic syndrome. *Lancet (London, England)*, *365*(9468), 1415–1428. https://doi.org/10.1016/S0140-6736(05)66378-7

Fahed, G., Aoun, L., Bou Zerdan, M., Allam, S., Bou Zerdan, M., Bouferraa, Y., & Assi, H. I. (2022). Metabolic Syndrome: Updates on Pathophysiology and Management in 2021. *International Journal of Molecular Sciences*, *23*(2). https://doi.org/10.3390/ijms23020786

Ferreira, J. R. S., Zandonade, E., de Paula Alves Bezerra, O. M., & Salaroli, L. B. (2021). Cutoff point of TyG index for metabolic syndrome in Brazilian farmers. *Archives of Endocrinology and Metabolism*, *65*(6), 704–712. https://doi.org/10.20945/2359-3997000000401

Gao, P., Wen, X., Ou, Q., & Zhang, J. (2022). Which one of LDL-C /HDL-C ratio and non-HDL-C can better predict the severity of coronary artery disease in STEMI patients. *BMC Cardiovascular Disorders*, *22*(1), 318. https://doi.org/10.1186/s12872-022-02760-0

Grundy, S. M., Hansen, B., Smith, S. C., Cleeman, J. I., Kahn, R. A., American Heart Association, National Heart, L. and B. I., & American Diabetes Association. (2004). Clinical management of metabolic syndrome: report of the American Heart Association/National Heart, Lung, and Blood Institute/American Diabetes Association conference on scientific issues related to management. *Circulation*, *109*(4), 551–556. https://doi.org/10.1161/01.CIR.0000112379.88385.67

Guo, Q.-Q., Zheng, Y.-Y., Tang, J.-N., Wu, T.-T., Yang, X.-M., Zhang, Z.-L., Zhang, J.-C., Yang, Y., Hou, X.-G., Cheng, M.-D., Song, F.-H., Liu, Z.-Y., Wang, K., Jiang, L.-Z., Fan, L., Yue, X.-T., Bai, Y., Dai, X.-Y., Zheng, R.-J., … Zhang, J.-Y. (2020). Fasting blood glucose to HDL-C ratio as a novel predictor of clinical outcomes in non-diabetic patients after PCI. *Bioscience Reports*, *40*(12). https://doi.org/10.1042/BSR20202797

Gutiérrez-Solis, A. L., Datta Banik, S., & Méndez-González, R. M. (2018). Prevalence of Metabolic Syndrome in Mexico: A Systematic Review and Meta-Analysis. *Metabolic Syndrome and Related Disorders*, *16*(8), 395–405. https://doi.org/10.1089/met.2017.0157

Huang, P. L. (2009). A comprehensive definition for metabolic syndrome. *Disease Models & Mechanisms*, *2*(5–6), 231–237. https://doi.org/10.1242/dmm.001180

Ingelsson, E., Schaefer, E. J., Contois, J. H., McNamara, J. R., Sullivan, L., Keyes, M. J., Pencina, M. J., Schoonmaker, C., Wilson, P. W. F., D'Agostino, R. B., & Vasan, R. S. (2007). Clinical utility of different lipid measures for prediction of coronary heart disease in men and women. *JAMA*, *298*(7), 776–785. https://doi.org/10.1001/jama.298.7.776

Kwon, H., & Pessin, J. E. (2013a). Adipokines mediate inflammation and insulin resistance. *Frontiers in Endocrinology*, *4*, 71. https://doi.org/10.3389/fendo.2013.00071

Kwon, H., & Pessin, J. E. (2013b). Adipokines mediate inflammation and insulin resistance. *Frontiers in Endocrinology*, *4*, 71. https://doi.org/10.3389/fendo.2013.00071

Li, C., Ford, E. S., Meng, Y.-X., Mokdad, A. H., & Reaven, G. M. (2008). Does the association of the triglyceride to high-density lipoprotein cholesterol ratio with fasting serum insulin differ by race/ethnicity? *Cardiovascular Diabetology*, *7*, 4. https://doi.org/10.1186/1475-2840-7-4

Lopez-Candales, A., Hernández Burgos, P. M., Hernandez-Suarez, D. F., & Harris, D. (2017). Linking Chronic Inflammation with Cardiovascular Disease: From Normal Aging to the Metabolic Syndrome. *Journal of Nature and Science*, *3*(4).

McLaughlin, T., Reaven, G., Abbasi, F., Lamendola, C., Saad, M., Waters, D., Simon, J., & Krauss, R. M. (2005). Is there a simple way to identify insulin-resistant individuals at increased risk of cardiovascular disease? *The American Journal of Cardiology*, *96*(3), 399–404. https://doi.org/10.1016/j.amjcard.2005.03.085

Nie, G., Hou, S., Zhang, M., & Peng, W. (2021). High TG/HDL ratio suggests a higher risk of metabolic syndrome among an elderly Chinese population: a cross-sectional study. *BMJ Open*, *11*(3), e041519. https://doi.org/10.1136/bmjopen-2020-041519

Reaven, G. M. (1988). Banting lecture 1988. Role of insulin resistance in human disease. *Diabetes*, *37*(12), 1595–1607. https://doi.org/10.2337/diab.37.12.1595

Reaven, G. M. (2006). The metabolic syndrome: is this diagnosis necessary? *The American Journal of Clinical Nutrition*, *83*(6), 1237–1247. https://doi.org/10.1093/ajcn/83.6.1237

Ridker, P. M., Rifai, N., Cook, N. R., Bradwin, G., & Buring, J. E. (2005). Non-HDL cholesterol, apolipoproteins A-I and B100, standard lipid measures, lipid ratios, and CRP as risk factors for cardiovascular disease in women. *JAMA*, *294*(3), 326–333. https://doi.org/10.1001/jama.294.3.326

Salazar, M. R., Carbajal, H. A., Espeche, W. G., Leiva Sisnieguez, C. E., March, C. E., Balbín, E., Dulbecco, C. A., Aizpurúa, M., Marillet, A. G., & Reaven, G. M. (2013). Comparison of the abilities of the plasma triglyceride/high-density lipoprotein cholesterol ratio and the metabolic syndrome to identify insulin resistance.

Diabetes & Vascular Disease Research, *10*(4), 346–352. https://doi.org/10.1177/1479164113479809

Salazar-Flores, J., Dondiego-Aldape, R., Rubi-Castellanos, R., Anaya-Palafox, M., Nuño-Arana, I., Canseco-Avila, L. M., Flores-Flores, G., Morales-Vallejo, M. E., Barojas-Pérez, N., Muñoz-Valle, J. F., Campos-Gutiérrez, R., & Rangel-Villalobos, H. (2010). Population structure and paternal admixture landscape on present-day Mexican-Mestizos revealed by Y-STR haplotypes. *American Journal of Human Biology : The Official Journal of the Human Biology Council*, *22*(3), 401–409. https://doi.org/10.1002/ajhb.21013

Samson, S. L., & Garber, A. J. (2014). Metabolic syndrome. *Endocrinology and Metabolism Clinics of North America*, *43*(1), 1–23. https://doi.org/10.1016/j.ecl.2013.09.009

Samuel, V. T., Petersen, K. F., & Shulman, G. I. (2010). Lipid-induced insulin resistance: unravelling the mechanism. *Lancet (London, England)*, *375*(9733), 2267–2277. https://doi.org/10.1016/S0140-6736(10)60408-4

Samuel, V. T., & Shulman, G. I. (2016). The pathogenesis of insulin resistance: integrating signaling pathways and substrate flux. *The Journal of Clinical Investigation*, *126*(1), 12–22. https://doi.org/10.1172/JCI77812

Sharma, R. B., & Alonso, L. C. (2014). Lipotoxicity in the pancreatic beta cell: not just survival and function, but proliferation as well? *Current Diabetes Reports*, *14*(6), 492. https://doi.org/10.1007/s11892-014-0492-2

Sherling, D. H., Perumareddi, P., & Hennekens, C. H. (2017). Metabolic Syndrome. *Journal of Cardiovascular Pharmacology and Therapeutics*, *22*(4), 365–367. https://doi.org/10.1177/1074248416686187

Simental-Mendía, L. E., Gómez-Díaz, R., Wacher, N. H., & Guerrero-Romero, F. (2022). The Triglycerides and Glucose Index is Negatively Associated with Insulin Secretion in Young Adults with Normal Weight. *Hormone and Metabolic Research = Hormon- Und Stoffwechselforschung = Hormones et Metabolisme*, *54*(1), 33–36. https://doi.org/10.1055/a-1713-7821

Simental-Mendía, L. E., Rodríguez-Morán, M., & Guerrero-Romero, F. (2008). The product of fasting glucose and triglycerides as surrogate for identifying insulin resistance in apparently healthy subjects. *Metabolic Syndrome and Related Disorders*, *6*(4), 299–304. https://doi.org/10.1089/met.2008.0034

Tejera, C. H., Minnier, J., Fazio, S., Safford, M. M., Colantonio, L. D., Irvin, M. R., Howard, V., Zakai, N. A., & Pamir, N. (2021). High triglyceride to HDL cholesterol ratio is associated with increased coronary heart disease among White but not Black adults. *American Journal of Preventive Cardiology*, *7*, 100198. https://doi.org/10.1016/j.ajpc.2021.100198

von Bibra, H., Saha, S., Hapfelmeier, A., Müller, G., & Schwarz, P. E. H. (2017). Impact of the Triglyceride/High-Density Lipoprotein Cholesterol Ratio and the Hypertriglyceremic-Waist Phenotype to Predict the Metabolic Syndrome and Insulin Resistance. *Hormone and Metabolic Research = Hormon- Und Stoffwechselforschung = Hormones et Metabolisme*, *49*(7), 542–549. https://doi.org/10.1055/s-0043-107782

Wang, L., Cong, H.-L., Zhang, J.-X., Hu, Y.-C., Wei, A., Zhang, Y.-Y., Yang, H., Ren, L.-B., Qi, W., Li, W.-Y., Zhang, R., & Xu, J.-H. (2020). Triglyceride-glucose index predicts adverse cardiovascular events in patients with diabetes and acute coronary syndrome. *Cardiovascular Diabetology*, *19*(1), 80. https://doi.org/10.1186/s12933-020-01054-z

Wu, T.-T., Zheng, Y.-Y., Xiu, W.-J., Wang, W.-R., Xun, Y.-L., Ma, Y.-Y., Kadir, P., Pan, Y., Ma, Y.-T., & Xie, X. (2021). White Blood Cell Counts to High-Density Lipoprotein Cholesterol Ratio, as a Novel Predictor of Long-Term Adverse Outcomes in Patients After Percutaneous Coronary Intervention: A Retrospective Cohort Study. *Frontiers in Cardiovascular Medicine*, *8*, 616896. https://doi.org/10.3389/fcvm.2021.616896

Yang, Y., Wang, B., Yuan, H., & Li, X. (2021). Triglycerides to High-Density Lipoprotein Cholesterol Ratio Is the Best Surrogate Marker for Insulin Resistance in Nonobese Middle-Aged and Elderly Population: A Cross-Sectional Study. *International Journal of Endocrinology*, *2021*, 6676569. https://doi.org/10.1155/2021/6676569

Yeh, W.-C., Tsao, Y.-C., Li, W.-C., Tzeng, I.-S., Chen, L.-S., & Chen, J.-Y. (2019). Elevated triglyceride-to-HDL cholesterol ratio is an indicator for insulin resistance in middle-aged and elderly Taiwanese population: a cross-sectional study. *Lipids in Health and Disease*, *18*(1), 176. https://doi.org/10.1186/s12944-019-1123-3

Young, K. A., Maturu, A., Lorenzo, C., Langefeld, C. D., Wagenknecht, L. E., Chen, Y.-D. I., Taylor, K. D., Rotter, J. I., Norris, J. M., & Rasouli, N. (2019). The triglyceride to high-density lipoprotein cholesterol (TG/HDL-C) ratio as a predictor of insulin resistance, β-cell function, and diabetes in Hispanics and African Americans. *Journal of Diabetes and Its Complications*, *33*(2), 118–122. https://doi.org/10.1016/j.jdiacomp.2018.10.018

Zou, Y., Zhong, L., Hu, C., Zhong, M., Peng, N., & Sheng, G. (2021). LDL/HDL cholesterol ratio is associated with new-onset NAFLD in Chinese non-obese people with normal lipids: a 5-year longitudinal cohort study. *Lipids in Health and Disease*, *20*(1), 28. https://doi.org/10.1186/s12944-021-01457-1

Annexes

Table 1. Anthropometric and biochemical characteristics of the study groups according to MetS.

Variable	Control group	MetS	*p*
n	350	269	-
Sex (M:F)[a]	134 : 216	94 : 175	0.402
Age[b]	45.50 (35.00-54.25)	43.00 (32.00-52.00)	<0.05
BMI (Kg/m^2)[b]	26.36 (23.62-29.80)	30.06 (27.01-33.16)	<0.001
WC (cm)[b]	91.00 (83.00-101.0)	100.0 (95.00-108.0)	<0.001
WHR[b]	0.895 (0.842-0.952)	0.933 (0.894-0.980)	<0.001
WBC (x10^9/L)[b]	5.400 (4.475-6.525)	5.300 (4.200-6.600)	0.4423
FBG (mg/dL)[b]	89.00 (81.75-98.00)	121.0 (103.0-174.0)	<0.001
Hb1Ac (%)[b]	5.90 (5.40-6.60)	7.00 (6.20-8.85)	<0.001
TC (mg/dL)[b]	182.0 (161.5-205.0)	194.0 (168.0-217.8)	<0.001
HDL-c (mg/dL)[b]	56.40 (50.60-65.95)	44.90 (39.53-52.38)	<0.001
LDL-c (mg/dL)[b]	97.60 (76.55-117.9)	104.5 (84.33-122.5)	<0.05
TG (mg/dL)[b]	125.0 (92.00-154.3)	206.5 (168.0-268.8)	<0.001
TyG[b]	4.685 (4.504-4.854)	5.105 (4.942-5.274)	<0.001
TC/HDL-c[b]	3.196 (2.723-3.680)	4.229 (3.657-4.807)	<0.001
TG/HDL-c[b]	2.171 (1.481-2.959)	4.329 (3.535-6.152)	<0.001
LDL/HDL-c[b]	1.719 (1.304-2.116)	2.222 (1.756-2.769)	<0.001
FBG/HDL-c[b]	1.566 (1.320-1.917)	2.631 (2.183-3.773)	<0.001
WBC/HDL-c[b]	93.44 (71.34-121.8)	114.5 (90.85-149.7)	<0.001

Data are presented as median (interquartile range) or proportions. The p value was calculated using the X^2 test[a] or the Mann-Whitney U test[b]. M, male; F, female; BMI, body mass index; WC, waist circumference; WHR, waist-to-hip ratio; WBC, white blood cell count; FBG, fasting blood glucose; Hb1Ac, glycosylated hemoglobin; TC, total cholesterol; HDL-c, high-density lipoprotein-cholesterol; LDL-c, low-density lipoprotein-cholesterol; TG, triglycerides.

Table 2. Correlations of the study variables: TyG, TC/HDL-c, TG/HDL-c, LDL-c/HDL-c, FBG/HDL-c and WBC/HDL-c with the MetS components and the anthropometric and biochemical characteristics of the study subjects.

Variable	TyG		TC/HDL-c		TG/HDL-c		LDL/HDL-c		FBG/HDL-c		WBC/HDL-c	
	rho	*p*	rho	*p*	rho	*p*	rho	*p*	rho	*p*	rho	*p*
Age	-0.078	0.054	-0.001	0.988	-0.037	0.352	-0.007	0.858	-0.072	0.072	-0.007	0.856
BMI	0.337	<0.001	0.292	<0.001	0.359	<0.001	0.216	<0.001	0.301	<0.001	0.147	<0.001
WC	0.360	<0.001	0.288	<0.001	0.355	<0.001	0.210	<0.001	0.360	<0.001	0.135	<0.01
WHR	0.290	<0.001	0.272	<0.001	0.278	<0.001	0.233	<0.001	0.345	<0.001	0.132	<0.01
WBC	-0.050	0.215	-0.080	<0.05	-0.030	0.456	-0.083	<0.05	-0.089	<0.05	0.768	<0.001
FBG	0.735	<0.001	0.333	<0.001	0.344	<0.001	0.264	<0.001	0.834	<0.001	0.059	0.144
Hb1Ac	0.577	<0.001	0.262	<0.001	0.256	<0.001	0.208	<0.001	0.642	<0.001	0.040	0.317
TC	0.361	<0.001	0.514	<0.001	0.211	<0.001	0.576	<0.001	0.051	0.203	-0.136	<0.01
HDL-c	-0.356	<0.001	-0.704	<0.001	-0.688	<0.001	-0.551	<0.001	-0.662	<0.001	-0.535	<0.001
LDL-c	0.191	<0.001	0.575	<0.001	0.115	<0.01	0.776	<0.001	0.108	<0.01	-0.051	0.202
TG	0.850	<0.001	0.589	<0.001	0.919	<0.001	0.319	<0.001	0.439	<0.001	0.227	<0.001

Spearman's rank correlation coefficient. BMI (kg/m^2), body mass index; WC (cm), waist circumference; WHR, waist-to-hip ratio; WBC ($x10^9/L$), white blood cells; FBG (mg/dL), fasting blood glucose; Hb1Ac (%), glycosylated hemoglobin; TC (mg/dL), total cholesterol; HDL-c (mg/dL), high-density lipoprotein-cholesterol; LDL-c (mg/dL), low-density lipoprotein-cholesterol; TG (mg/dL), triglycerides.

Table 3. Associations between the study variables: TyG, TC/HDL-c, TG/HDL-c, LDL-c/HDL-c, FBG/HDL-c and WBC/HDL-c with the MetS.

Variable	Odds Ratio	Confidence Interval (95%)		*p*
TyG	2.504	1.131	5.544	<0.05
TC/HDL-c	2.449	1.245	4.818	<0.01
TG/HDL-c	7.383	3.428	15.903	<0.001
LDL/HDL-c	2.164	1.024	4.573	<0.05
FBG/HDL-c	23.533	10.025	55.243	<0.001
WBC/HDL-c	1.867	1.109	3.144	<0.05

Values adjusted for sex and age. Binomial logistic regression test (the model considers the relationships with WC, BMI, FBG, TC, HDL-c, LDL-c and TG). OR, odds ratio.

Table 4. Diagnostic accuracy of the study variables: TyG, TC/HDL-c, TG/HDL-c, LDL-c/HDL-c, FBG/HDL-c and WBC/HDL-c in MetS.

Variable	AUC	CI (95%)		*p*	Cut-off	Sensitivity (%)	Specificity (%)
TyG	0.904	0.881	0.927	<0.001	≥4.823	91.40	74.30
TC/HDL-c	0.812	0.779	0.846	<0.001	≥3.701	74.30	75.70
TG/HDL-c	0.903	0.880	0.926	<0.001	≥3.311	82.50	84.00
LDL/HDL-c	0.713	0.673	0.754	<0.001	≥2.007	63.20	70.00
FBG/HDL-c	0.885	0.859	0.911	<0.001	≥2.001	85.10	79.70
WBC/HDL-c	0.660	0.617	0.703	<0.001	≥101.6	66.20	58.00

Receiver operating characteristics (ROC) curves analysis. AUC, area under curve; CI, confidence interval.

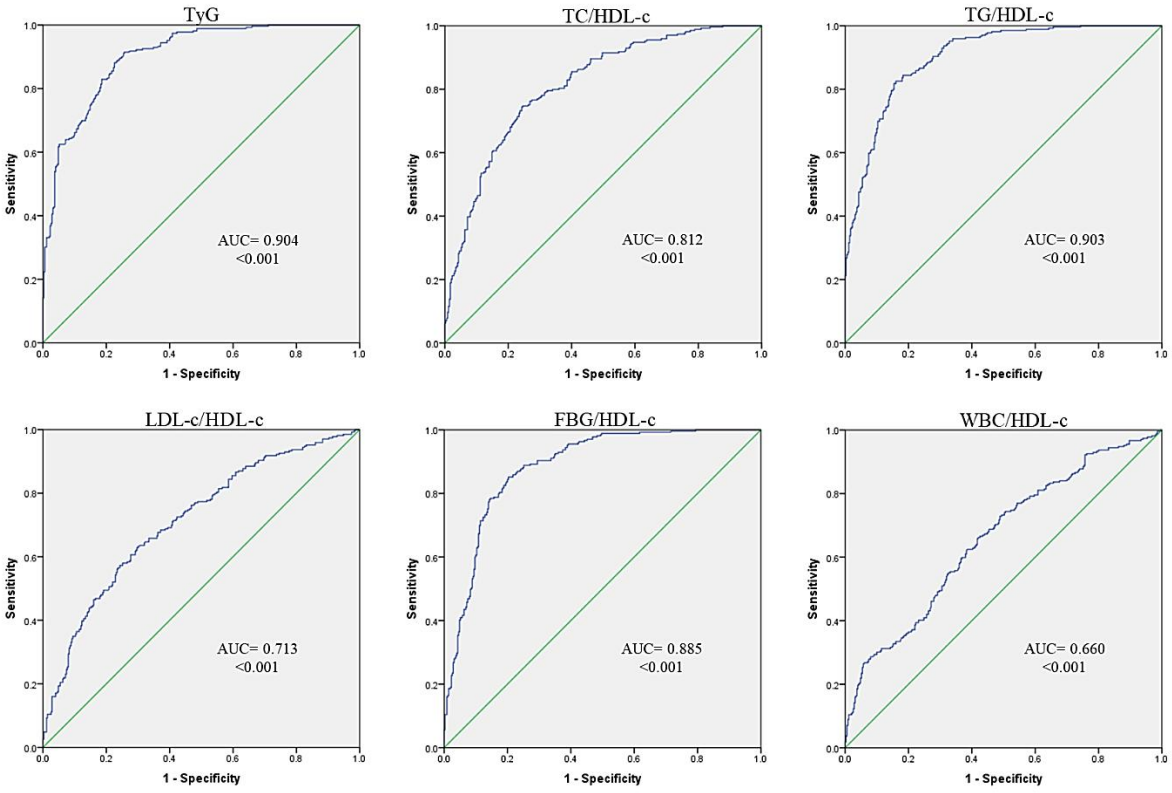

Figure legends

Figure 1. ROC curves of the different markers derived from the lipid profile. Receiver Operating Characteristics curves for TyG index and TC/HDL-c, TG/HDL-c, LDL-c/HDL-c, FBG/HDL-c and WBC/HDL-c ratios as indicators of high risk of MetS.

METABOLIC SYNDROME AND RELATED DISORDERS
Volume 22, Number 7, 2024

Pp. 510–515
DOI: 10.1089/met.2024.0045

ORIGINAL ARTICLES

Open camera or QR reader and scan code to access this article and other resources online.

Clinical Significance of the Lipid Profile Ratios and Triglyceride Glucose Index in the Diagnosis of Metabolic Syndrome

Abraham Cardenas-Juarez, MD,[1] Diana Patricia Portales-Pérez, PhD,[2,3] Bruno Rivas-Santiago, PhD,[1] and Mariana Haydee García-Hernández, PhD[1]

Abstract

Introduction: Metabolic syndrome (MetS) is a pathophysiological condition defined by a set of metabolic alterations such as hypertriglyceridemia, hyperglycemia, hypertension, low HDL-c levels, and visceral obesity. Its presence identifies people with an increased risk of developing cardiovascular diseases and type 2 diabetes; however, the lack of practical and reliable methods for its diagnosis limits the identification of people with this condition. In this sense, the objective of this study was to analyze the diagnostic utility of markers derived from the lipid profile [triglyceride–glucose (TyG) index and the ratios total cholesterol (TC)/high-density lipoprotein cholesterol (HDL-c), triglyceride (TG)/HDL-c, low-density lipoprotein cholesterol/HDL-c, fasting blood glucose (FBG)/HDL-c, and white blood cell/HDL-c] in the determination of MetS.
Methods: A retrospective study was designed that included 619 individuals. A logistic regression model was used to evaluate the associations of the different markers with MetS, and the cutoff points of the markers were determined through an analysis of receiver operating characteristic curves and the Youden Index.
Results: A positive and significant association was observed between all markers and the presence of MetS. The cutoff values for the markers that best predicted MetS were TyG ≥ 4.8 (sensitivity = 91.4%, specificity = 74.3%), TC/HDL-c ≥ 3.7 (sensitivity = 74.3%, specificity = 75.7%), TG/HDL-c ≥ 3.3 (sensitivity = 82.5%, specificity = 84.0%), and FBG/HDL-c ≥ 2.0 (sensitivity = 85.1%, specificity = 79.7%).
Conclusion: Our study demonstrated the diagnostic relevance of the different markers in detecting MetS, suggesting that these ratios may be useful in clinical practice for the opportune and accurate diagnosis of MetS.

Keywords: metabolic syndrome, lipid profile, TyG index, TC/HDL-c ratio, TG/HDL-c ratio, FBG/HDL-c ratio

Introduction

Metabolic syndrome (MetS) is a pathophysiological condition in which four main characteristics are distinguished: insulin resistance (IR), central obesity, atherogenic dyslipidemia, and endothelial dysfunction.[1] The MetS is defined by a set of metabolic alterations, according to the third report of the National Cholesterol Education Program Adult Treatment Panel (NCEP ATP-III), the diagnosis of this condition is granted if three or more of the following five criteria are met: blood pressure greater than 130/85 mmHg, waist circumference (WC) ≥40 inches in men and ≥35 inches in women, fasting blood glucose (FBG) levels ≥100 mg/dL, fasting triglyceride (TG) levels ≥150 mg/dL, and fasting high-density lipoprotein cholesterol (HDL-c) levels <40 mg/dL in men and <50 mg/dL in women.[2] Its presence discriminates

[1]Unidad de Investigación Biomédica, Delegación Zacatecas, México. Instituto Mexicano del Seguro Social, IMSS, Zacatecas, México.
[2]Facultad de Ciencias Químicas, Universidad Autónoma de San Luis Potosí, Zona Universitaria, San Luis Potosí, México.
[3]Centro de Investigación en Ciencias de la Salud y Biomedicina, Universidad Autónoma de San Luis Potos, San Luis Potosí, México.

between a specific group of patients with a shared pathophysiology, those with an increased risk of developing cardiovascular disease (CVD) and type 2 diabetes (T2D). However, the lack of practical methods for its diagnostic implementation limits its application in the field of preventive medicine. In this context, different markers derived from the lipid profile have been proposed for the opportune and accurate diagnosis of different metabolic pathologies; for example, the following have been evaluated: the triglyceride–glucose (TyG) index as a marker of IR,[3] MetS[4] and coronary events in patients with T2D, and in patients with acute coronary syndrome;[5] TG/HDL-c ratio as a marker of IR,[6–8] MetS,[9,10] diabetes,[11] development of CVD,[12,13] and nonalcoholic fatty liver;[14] total cholesterol (TC)/HDL-c ratio as a predictor of premature myocardial infarction[15] and CVD;[16,17] low-density lipoprotein cholesterol (LDL-c)/HDL-c ratio as a marker of nonalcoholic fatty liver[18] and as a predictor of coronary artery disease subsequent to acute myocardial infarction;[19] likewise, FBG/HDL-c and white blood cell (WBC) count/HDL-c ratios have been evaluated as predictors of mortality resulting from coronary artery disease.[20,21] However, previous studies have shown that the cutoff points for determining people at risk can vary depending on their ethnic origin;[22,23] therefore, the objective of this study was to determine and compare the accuracy diagnosis of the different markers derived from the lipid profile (TyG, TC/HDL-c, TG/HDL-c, LDL-c/HDL-c, FBG/HDL-c, and WBC/HDL-c) in the diagnosis of MetS in the adult population of Mexico.

Participants and Methods

Study population

This retrospective study included the participation of 619 subjects (228 men and 391 women) aged 44.0 ± 13.0 years, from the metropolitan area of the city of Zacatecas, Mexico. None of the individuals had vascular complications, pregnancy, hypothyroidism, or clinical infections disease. In addition, the individuals were not regular smokers, and they did not ingest alcohol on regular basis. People under regular pharmacological treatment for metabolic disorders (e.g., statins, hypoglycemic agents, and insulin) were included and people under hormonal treatment (e.g., corticosteroids and levothyroxine), chemotherapy, as well as lactating women were excluded. All participants were informed about the study and signed an informed consent. The protocol was approved by the Bioethics Committee of the Mexican Institute of Social Security (IMSS), with the registration numbers R-2018-785-072 and SALUD-2012-01-182554.

Anthropometric and biochemical characteristics

Anthropometric measurements were obtained by trained personnel. Body mass index (BMI, kg/m^2) and waist–hip ratio (WHR, waist cm/hip cm) were determined; a BMI <25 was considered normal weight, a BMI ≥25 and <30 was considered overweight, and a BMI ≥30 was considered obese. After fasting for 10–12 h, a blood sample was taken by venipuncture for the determination of WBC and levels of FBG, glycated hemoglobin (Hb1Ac), TC, HDL-c, LDL-c, and TG, in accordance with the conventional protocols of the IMSS Zone 1 General Hospital. The TyG index was used as a surrogate marker for the determination of TG-driven IR; a TyG index ≥4.6 indicates IR. This index was calculated as Ln [fasting triglycerides (mg/dL) × fasting glucose (mg/dL)]/2 [3]. For their part, the ratios TC/HDL-c, TG/HDL-c, LDL-c/HDL-c, FBG/HDL-c, and WBC/HDL-c were calculated by dividing the levels of TC (mg/dL), TG (mg/dL), LDL-c (mg/dL), FBG (mg/dL), and WBC (×10^7/dL) between the levels of HDL-c (mg/dL), respectively. The diagnosis of MetS was established according to the NCEP ATP-III criteria,[2] with values adjusted to the Mexican population.[24]

Statistical analysis

Statistical analysis was performed using SPSS software (IBM Statistics version 20.0). The Shapiro–Wilk test was used to determine the distribution of quantitative variables; because all variables presented a non-normal distribution, quantitative variables were compared using the nonparametric Mann–Whitney *U* test, whereas the chi-squared test (χ^2) was used for qualitative variables. The Spearman rank test was used to analyze the correlations between the TyG index and the TC/HDL-c, TG/HDL-c, LDL-c/HDL-c, FBG/HDL-c, and WBC/HDL-c ratios with the different quantitative variables established. The association between the TyG index and the TC/HDL-c, TG/HDL-c, LDL-c/HDL-c, FBG/HDL-c, and WBC/HDL-c ratios with MetS was analyzed using a logistic regression analysis. To define the cutoff point at which the greatest sensitivity and specificity of the index and the ratios evaluated is obtained, the receiver operating characteristic (ROC) curve analysis and the Youden Index were performed, and an area under the curve (AUC) ≥0.7 was considered acceptable. A value of $p < 0.05$ was considered significant.

Results

Anthropometric and biochemical characteristics

A total of 619 people participated in this study, of whom 36.8% were men and 63.2% were women, whose average age was 44 ± 13.0 years. The individuals consisted in Mexican Mestizo population, which is defined as people born in the country having a Spanish-derived last name, with family antecedents of Mexican ancestors.[25] Participants were classified according to the presence of MetS (43.5%, 94 males; 175 females) or its absence (control group) (56.5%, 134 males; 216 females). Participants diagnosed with MetS presented values of the TyG index and ratios of TC/HDL-c, TG/HDL-c, LDL-c/HDL-c, FBG/HDL-c, and WBC/HDL-c, significantly higher compared with the control group ($p < 0.001$). Both groups differ in obesity indicators such as BMI, WC, and WHR, whose values were higher in the group with MetS ($p < 0.001$) compared with the control group. Likewise, blood levels of FBG, Hb1Ac, TC, LDL-c, and TG were found to be statistically higher in the MetS group compared with the control group; however, HDL-c blood levels were higher in the control group compared with people diagnosed with MetS ($p < 0.001$) (Table 1).

Bivariate correlation analysis

The results of the bivariate correlation analysis demonstrated a statistically significant relationship between the TyG index and the TC/HDL-c, TG/HDL-c, LDL-c/HDL-c, FBG/HDL-c, and WBC/HDL-c ratios with the MetS components: WC

Table 1. Anthropometric and Biochemical Characteristics of the Study Groups According to the MetS

Variable	*Control group*	*MetS*	P
n	350	269	—
Sex (M:F)[a]	134:216	94:175	0.402
Age[b]	45.50 (35.00–54.25)	43.00 (32.00–52.00)	<0.05
BMI (kg/m^2)[b]	26.36 (23.62–29.80)	30.06 (27.01–33.16)	<0.001
WC (cm)[b]	91.00 (83.00–101.0)	100.0 (95.00–108.0)	<0.001
WHR[b]	0.895 (0.842–0.952)	0.933 (0.894–0.980)	<0.001
WBC (×10^9/L)[b]	5.400 (4.475–6.525)	5.300 (4.200–6.600)	0.442
FBG (mg/dL)[b]	89.00 (81.75–98.00)	121.0 (103.0–174.0)	<0.001
Hb1Ac (%)[b]	5.90 (5.40–6.60)	7.00 (6.20–8.85)	<0.001
TC (mg/dL)[b]	182.0 (161.5–205.0)	194.0 (168.0–217.8)	<0.001
HDL-c (mg/dL)[b]	56.40 (50.60–65.95)	44.90 (39.53–52.38)	<0.001
LDL-c (mg/dL)[b]	97.60 (76.55–117.9)	104.5 (84.33–122.5)	<0.05
TG (mg/dL)[b]	125.0 (92.00–154.3)	206.5 (168.0–268.8)	<0.001
TyG[b]	4.685 (4.504–4.854)	5.105 (4.942–5.274)	<0.001
TC/HDL-c[b]	3.196 (2.723–3.680)	4.229 (3.657–4.807)	<0.001
TG/HDL-c[b]	2.171 (1.481–2.959)	4.329 (3.535–6.152)	<0.001
LDL-c/HDL-c[b]	1.719 (1.304–2.116)	2.222 (1.756–2.769)	<0.001
FBG/HDL-c[b]	1.566 (1.320–1.917)	2.631 (2.183–3.773)	<0.001
WBC/HDL-c[b]	93.44 (71.34–121.8)	114.5 (90.85–149.7)	<0.001

Data are presented as median (interquartile range) or proportions.
The *p* value was calculated using the χ^2 test or the Mann–Whitney *U* test.
[a]χ^2 test.
[b]Mann–Whitney *U* test.
BMI, body mass index; F, female; FBG, fasting blood glucose; Hb1Ac, glycated hemoglobin; HDL-c, high-density lipoprotein cholesterol; LDL-c, low-density lipoprotein cholesterol; M, male; METs, metabolic syndrome; TC, total cholesterol; TG, triglycerides; WBC, white blood cell count; WC, waist circumference; WHR, waist-to-hip ratio.

(rho = 0.360, $p < 0.001$; rho = 0.288, $p < 0.001$; rho = 0.355, $p < 0.001$; rho = 0.210, $p < 0.001$; rho = 0.360, $p < 0.001$; rho = 0.135, $p < 0.01$, respectively); FBG (rho = 0.735, $p < 0.001$; rho = 0.333, $p < 0.001$; rho = 0.344, $p < 0.001$; 0.264, $p < 0.001$; rho = 0.834, $p < 0.001$; rho = 0.059, $p = 0.144$, respectively); HDL-c (rho = –0.356, $p < 0.001$; rho = –0.704, $p < 0.001$; rho = –0.688, $p < 0.001$; rho = –0.551, $p < 0.001$; rho = –0.662, $p < 0.001$; rho = –0.535, $p < 0.001$, respectively); and TG (rho = 0.850, $p < 0.001$; rho = 0.589, $p < 0.001$; rho = 0.919, $p < 0.001$; rho = 0.319, $p < 0.001$; rho = 0.439, $p < 0.001$; rho = 0.227, $p < 0.001$, respectively). Likewise, significant correlations with the other established variables were observed (Table 2).

Multivariable association analysis

After observing that the study variables were correlated with the MetS components and, to investigate their association as risk factors for the development of this condition, a logistic regression analysis was performed. It was found that the association between MetS and the study variables remained significant, even after adjustment for sex and age: TyG [odds ratio

Table 2. Correlations of the Study Variables: TyG, TC/HDL-c, TG/HDL-c, LDL-c/HDL-c, FBG/HDL-c, and WBC/HDL-c with the MetS Components and the Anthropometric and Biochemical Characteristics of the Study Subjects

	TyG		*TC/HDL-c*		*TG/HDL-c*		*LDL-c/HDL-c*		*FBG/HDL-c*		*WBC/HDL-c*	
Variable	*rho*	P	*rho*	P	*rho*	P	*rho*	P	*rho*	P	*rho*	P
Age	–0.078	0.054	–0.001	0.988	–0.037	0.352	–0.007	0.858	–0.072	0.072	–0.007	0.856
BMI (kg/m^2)	0.337	<0.001	0.292	<0.001	0.359	<0.001	0.216	<0.001	0.301	<0.001	0.147	<0.001
WC (cm)	0.360	<0.001	0.288	<0.001	0.355	<0.001	0.210	<0.001	0.360	<0.001	0.135	<0.01
WHR	0.290	<0.001	0.272	<0.001	0.278	<0.001	0.233	<0.001	0.345	<0.001	0.132	<0.01
WBC (×10^9/L)	–0.050	0.215	–0.080	<0.05	–0.030	0.456	–0.083	<0.05	–0.089	<0.05	0.768	<0.001
FBG (mg/dL)	0.735	<0.001	0.333	<0.001	0.344	<0.001	0.264	<0.001	0.834	<0.001	0.059	0.144
Hb1Ac (%)	0.577	<0.001	0.262	<0.001	0.256	<0.001	0.208	<0.001	0.642	<0.001	0.040	0.317
TC (mg/dL)	0.361	<0.001	0.514	<0.001	0.211	<0.001	0.576	<0.001	0.051	0.203	–0.136	<0.01
HDL-c (mg/dL)	–0.356	<0.001	–0.704	<0.001	–0.688	<0.001	–0.551	<0.001	–0.662	<0.001	–0.535	<0.001
LDL-c (mg/dL)	0.191	<0.001	0.575	<0.001	0.115	<0.01	0.776	<0.001	0.108	<0.01	–0.051	0.202
TG (mg/dL)	0.850	<0.001	0.589	<0.001	0.919	<0.001	0.319	<0.001	0.439	<0.001	0.227	<0.001

Spearman's rank correlation coefficient.
BMI, body mass index; FBG, fasting blood glucose; Hb1Ac, glycated hemoglobin; HDL-c, high-density lipoprotein cholesterol; LDL-c, low-density lipoprotein cholesterol; METs, metabolic syndrome; TC, total cholesterol; TG, triglycerides; WBC, white blood cells; WC, waist circumference; WHR, waist-to-hip ratio.

Table 3. Associations Between the Study Variables: TyG, TC/HDL-c, TG/HDL-c, LDL-c/HDL-c, FBG/HDL-c, and WBC/HDL-c with the MetS

Variable	*OR*	*CI (95%)*	P
TyG	2.504	1.131–5.544	<0.05
TC/HDL-c	2.449	1.245–4.818	<0.01
TG/HDL-c	7.383	3.428–15.90	<0.001
LDL-c/HDL-c	2.164	1.024–4.573	<0.05
FBG/HDL-c	23.53	10.02–55.24	<0.001
WBC/HDL-c	1.867	1.109–3.144	<0.05

Values adjusted for sex and age. Binomial logistic regression test (the model considers the relationships with WC, BMI, FBG, TC, HDL-c, LDL-c, and TG).

CI, confidence interval; FBG, fasting blood glucose; HDL-c, high-density lipoprotein cholesterol; LDL-c, low-density lipoprotein cholesterol; METs, metabolic syndrome; OR, odds ratio; TC, total cholesterol; TG, triglycerides; WBC, white blood cells.

(OR) = 2.504, confidence interval (CI) = 1.131–5.544, $p < 0.05$]; TC/HDL-c (OR = 2.449, CI = 1.245–4.818, $p < 0.01$); TG/HDL-c (OR = 7.383, CI = 3.428–15.90, $p < 0.001$); LDL-c/HDL-c (OR = 2.164, CI = 1.024–4.573, $p < 0.05$); FBG/HDL-c (OR = 23.53, CI = 10.02–55.24, $p < 0.001$); and WBC/HDL-c (OR = 1.867, CI = 1.109-3.144, $p < 0.05$) (Table 3).

ROC curve analysis

According to the Youden Index of the ROC curves, the optimal cutoff values of the TyG index and the ratios of the lipid profile in which the greatest joint sensitivity and specificity are obtained were the following: TyG (≥4.823), TC/HDL-c (≥3.701), TG/HDL-c (≥3.311), LDL-c/HDL-c (≥2.007), FBG/HDL-c (≥2.001), and WBC/HDL-c (≥101.06). Furthermore, the AUC was significant for TyG (0.904), TC/HDL-c (0.812), TG/HDL-c (0.903), LDL-c/HDL-c (0.713), FBG/HDL-c (0.885), and WBC/HDL-c (0.660), with a significance value of $p < 0.001$ in all cases. The TyG index (sensitivity = 91.40%, specificity = 74.30%) and the TC/HDL-c (sensitivity = 74.3%, specificity = 75.7%), TG/HDL-c (sensitivity = 82.50%, specificity = 84.00%), and FBG/HDL-c (sensitivity = 85.10%, specificity = 79.70%) ratios were the markers that demonstrated the highest diagnostic accuracy (Table 4, Fig. 1).

Discussion

In this study, we analyzed the association of different markers of the lipid profile with MetS, and our results demonstrated the diagnostic accuracy of the TyG index and the TC/HDL-c, TG/HDL-c, and FBG/HDL-c ratios to identify individuals at high risk of developing MetS in the Mexican Mestizo population. The cutoff values for the markers that best predicted MetS were TyG index ≥4.8, TC/HDL-c ratio ≥3.7, TG/HDL-c ratio ≥3.3, and FBG/HDL-c ratio ≥2.0. Previous studies have established different cutoff points for some of these markers for the diagnosis of MetS. For example, in a study carried out in an adult population between 18 and 59 years of age in Brazil, the cutoff value for the TyG index ≥4.52 (sensitivity = 84.3%, specificity = 75.7%) was proposed,[4] and compared with the cutoff point that we propose in our study (≥4.8), we obtained greater sensitivity and specificity. Likewise, cutoff values have been established for the TG/HDL-c ratio in the diagnosis of MetS; in a study carried out in Mexican Mestizo adults, a value of ≥3.0 was proposed (sensitivity = 86.9%, specificity = 66.8%),[9] which was similar to that observed in our analyzes (≥3.3), however, we obtained greater specificity and similar sensitivity with the cutoff point that we propose, likewise, cutoff points have also been established for this same ratio in the population of Germany,[8] Argentina,[26] and China;[10] however, as mentioned, the cutoff points must be established for each specific population because of the impact generated by ethnic origin on the distribution of the variables.[22,23] Otherwise, it is important to mention that our study is the first to consider the FBG/HDL-c ratio as a diagnostic marker for MetS; our results demonstrated its high diagnostic accuracy at the cutoff point ≥2.0 (sensitivity = 85.1%, specificity = 79.7%; OR = 23.53) in our study population. From a clinical point of view, physicians and patients can benefit from establishing practical diagnostic methods that accurately identify individuals with MetS, facilitating the approach to pharmacological treatment, and recommending preventive lifestyle changes.

The main strength of our study is the participation of people in a risk state who were overweight or obese but did not have MetS, which allowed us to demonstrate the robustness of the different markers as diagnostic tests. In contrast, our study proposes novel markers as diagnostic tests for MetS. Some of the limitations of our work is that our analysis model only adjusts for age, sex, and presence of obesity and does not consider other variables that could influence (physical activity, diet, and hereditary family history).

Conclusion

In conclusion, our study demonstrated that the relative ratios of lipid profile are positively associated with the

Table 4. Diagnostic Accuracy of the Study Variables: TyG, TC/HDL-c, TG/HDL-c, LDL-c/HDL-c, FBG/HDL-c, and WBC/HDL-c in MetS

Variable	*AUC*	*CI (95%)*	P	*Cutoff*	*Sensitivity*	*Specificity*
TyG	0.904	0.881–0.927	<0.001	≥4.823	91.40	74.30
TC/HDL-c	0.812	0.779–0.846	<0.001	≥3.701	74.30	75.70
TG/HDL-c	0.903	0.880–0.926	<0.001	≥3.311	82.50	84.00
LDL-c/HDL-c	0.713	0.673–0.754	<0.001	≥2.007	63.20	70.00
FBG/HDL-c	0.885	0.859–0.911	<0.001	≥2.001	85.10	79.70
WBC/HDL-c	0.660	0.617–0.703	<0.001	≥101.06	66.20	58.00

Receiver operating characteristic curve analysis.

AUC, area under the curve; CI, confidence interval; FBG, fasting blood glucose; HDL-c, high-density lipoprotein cholesterol; LDL-c, low-density lipoprotein cholesterol; METs, metabolic syndrome; TC, total cholesterol; TG, triglycerides; WBC, white blood cells.

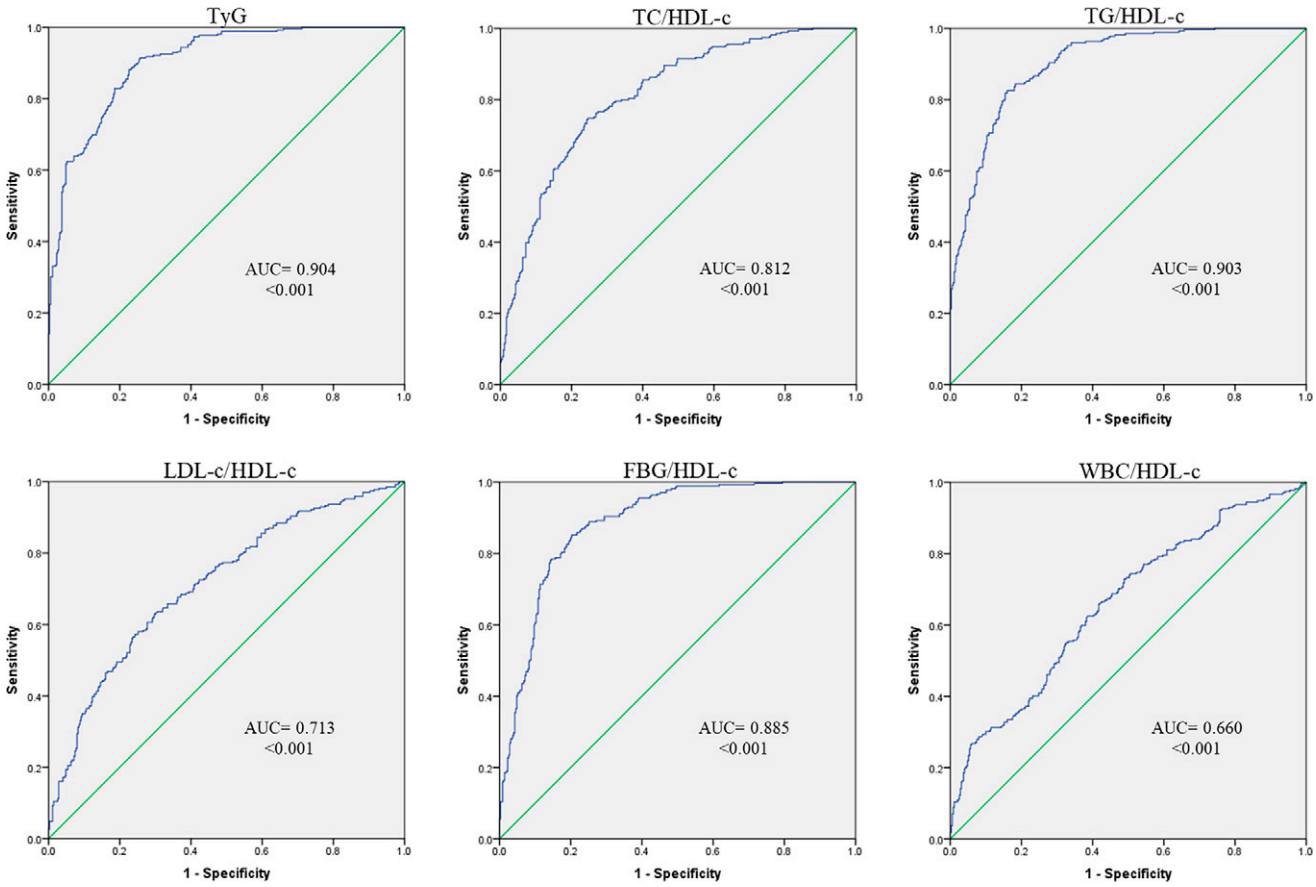

FIG. 1. Receiver operating characteristic curves of the different markers derived from the lipid profile. Receiver operating characteristic curves for TyG index and TC/HDL-c, TG/HDL-c, LDL-c/HDL-c, FBG/HDL-c, and WBC/HDL-c ratios as indicators of high risk of MetS. FBG, fasting blood glucose; HDL-c, high-density lipoprotein cholesterol; LDL-c, low-density lipoprotein cholesterol; TC, total cholesterol; TG, triglyceride; TyG, triglyceride–glucose; WBC, white blood cell.

high risk of presenting MetS in Mexican Mestizo adults. The cutoff values for the markers that best predict MetS and in which the highest diagnostic accuracy was presented were TyG index ≥4.8 and TC/HDL-c ≥3.7, TG/HDL-c ≥3.3, and FBG/HDL-c ≥2.0 ratios; these values maintained their significant association even after adjustment for age, sex, and presence of overweight or obesity, suggesting that these ratios may be useful in clinical practice for a timely, accurate, and reproducible diagnosis of MetS.

Authors' Contributions

The authors confirm contribution to the article as follows: Material preparation, data collection, and analysis were performed by A.C.-J. The first draft of the manuscript was written by A.C.-J., and all authors commented on the previous versions of the article. Study conception and design were performed by M.H.G.-H. and A.C.-J. Draft manuscript preparation was performed by A.C.-J., and D.P.P.-PO. and B.R.-S. reviewed and approved the final version of the article. All authors read and approved the final article.

Author Disclosure Statement

No conflicting financial interests exist.

Funding Information

The research reported in this article did not receive any financial support.

References

1. Huang PL. A comprehensive definition for metabolic syndrome. Dis Model Mech 2009;2(5–6):231–237; doi: 10.1242/dmm.001180
2. Alberti KG, Eckel RH, Grundy SM, et al. Harmonizing the metabolic syndrome: A joint interim statement of the International Diabetes Federation Task Force on Epidemiology and Prevention; National Heart, Lung, and Blood Institute; American Heart Association; World Heart Federation; International Atherosclerosis Society; and International Association for the Study of Obesity. Circulation 2009;120(16):1640–1645; doi: 10.1161/CIRCULATIONAHA.109.192644
3. Simental-Mendia LE, Gomez-Diaz R, Wacher NH, et al. The triglycerides and glucose index is negatively associated with insulin secretion in young adults with normal weight. Horm Metab Res 2022;54(1):33–36; doi: 10.1055/a–1713–7821
4. Ferreira JRS, Zandonade E, de Paula Alves Bezerra OM, et al. Cutoff point of TyG index for metabolic syndrome in Brazilian farmers. Arch Endocrinol Metab 2021;65(6):704–712; doi: 10.20945/2359-3997000000401

5. Wang L, Cong HL, Zhang JX, et al. Triglyceride-glucose index predicts adverse cardiovascular events in patients with diabetes and acute coronary syndrome. Cardiovasc Diabetol 2020;19(1):80; doi: 10.1186/s12933-020-01054-z
6. Yang Y, Wang B, Yuan H, et al. triglycerides to high-density lipoprotein cholesterol ratio is the best surrogate marker for insulin resistance in nonobese middle-aged and elderly population: A cross-sectional study. Int J Endocrinol 2021;2021:6676569; doi: 10.1155/2021/6676569
7. Young KA, Maturu A, Lorenzo C, et al. The triglyceride to high-density lipoprotein cholesterol (TG/HDL-C) ratio as a predictor of insulin resistance, beta-cell function, and diabetes in Hispanics and African Americans. J Diabetes Complications 2019;33(2):118–122; doi: 10.1016/j.jdiacomp.2018.10.018
8. von Bibra H, Saha S, Hapfelmeier A, et al. impact of the triglyceride/high-density lipoprotein cholesterol ratio and the hypertriglyceremic-waist phenotype to predict the metabolic syndrome and insulin resistance. Horm Metab Res 2017;49(7):542–549; doi: 10.1055/s-0043-107782
9. Baez-Duarte BG, Zamora-Ginez I, Rodriguez-Ramirez SO, et al. TG/HDL index to identify subjects with metabolic syndrome in the Mexican population. Gac Med Mex 2022; 158(5):259–264; doi: 10.24875/GMM.M22000693
10. Nie G, Hou S, Zhang M, et al. High TG/HDL ratio suggests a higher risk of metabolic syndrome among an elderly Chinese population: A cross-sectional study. BMJ Open 2021; 11(3):e041519; doi: 10.1136/bmjopen-2020-041519
11. Chen Z, Hu H, Chen M, et al. Association of Triglyceride to high-density lipoprotein cholesterol ratio and incident of diabetes mellitus: A secondary retrospective analysis based on a Chinese cohort study. Lipids Health Dis 2020;19(1): 33; doi: 10.1186/s12944-020-01213-x
12. Azarpazhooh MR, Najafi F, Darbandi M, et al. Triglyceride/-high-density lipoprotein cholesterol ratio: A clue to metabolic syndrome, insulin resistance, and severe atherosclerosis. Lipids 2021;56(4):405–412; doi: 10.1002/lipd.12302
13. McLaughlin T, Reaven G, Abbasi F, et al. Is there a simple way to identify insulin-resistant individuals at increased risk of cardiovascular disease? Am J Cardiol 2005;96(3):399–404 ; doi: 10.1016/j.amjcard.2005.03.085
14. Catanzaro R, Selvaggio F, Sciuto M, et al. Triglycerides to high-density lipoprotein cholesterol ratio for diagnosing nonalcoholic fatty liver disease. Minerva Gastroenterol (Torino) 2022;68(3):261–268; doi: 10.23736/S2724-5985 .21.02818-X
15. Hatmi ZN, Jalilian N, Pakravan A. The relationship between premature myocardial infarction with TC/HDL-C ratio subgroups in a multiple risk factor model. Adv J Emerg Med 2019;3(3):e24; doi: 10.22114/ajem.v0i0.149
16. Ingelsson E, Schaefer EJ, Contois JH, et al. Clinical utility of different lipid measures for prediction of coronary heart disease in men and women. Jama 2007;298(7):776–785; doi: 10.1001/jama.298.7.776
17. Ridker PM, Rifai N, Cook NR, et al. Non-HDL cholesterol, apolipoproteins A-I and B100, standard lipid measures, lipid ratios, and CRP as risk factors for cardiovascular disease in women. Jama 2005;294(3):326–333; doi: 10.1001/jama.294 .3.326
18. Zou Y, Zhong L, Hu C, et al. LDL/HDL cholesterol ratio is associated with new-onset NAFLD in Chinese non-obese people with normal lipids: A 5-year longitudinal cohort study. Lipids Health Dis 2021;20(1):28; doi: 10 .1186/s12944–021–01457–1
19. Gao P, Wen X, Ou Q, et al. Which one of LDL-C/HDL-C ratio and non-HDL-C can better predict the severity of coronary artery disease in STEMI patients. BMC Cardiovasc Disord 2022;22(1):318; doi: 10.1186/s12872–022–02760–0
20. Wu TT, Zheng YY, Xiu WJ, et al. White blood cell counts to high-density lipoprotein cholesterol ratio, as a novel predictor of long-term adverse outcomes in patients after percutaneous coronary intervention: A retrospective cohort study. Front Cardiovasc Med 2021;8:616896; doi: 10.3389/fcvm .2021.616896
21. Guo QQ, Zheng YY, Tang JN, et al. Fasting blood glucose to HDL-C ratio as a novel predictor of clinical outcomes in non-diabetic patients after PCI. Biosci Rep 2020;40(12); doi: 10.1042/BSR20202797
22. Tejera CH, Minnier J, Fazio S, et al. High triglyceride to HDL cholesterol ratio is associated with increased coronary heart disease among White but not Black adults. Am J Prev Cardiol 2021;7:100198; doi: 10.1016/j.ajpc.2021.100198
23. Li C, Ford ES, Meng YX, et al. Does the association of the triglyceride to high-density lipoprotein cholesterol ratio with fasting serum insulin differ by race/ethnicity? Cardiovasc Diabetol 2008;7:4; doi: 10.1186/1475-2840-7-4
24. Baez-Duarte BG, Sanchez-Guillen Mdel C, Perez-Fuentes R, et al. beta-cell function is associated with metabolic syndrome in Mexican subjects. Diabetes Metab Syndr Obes 2010;3:301–309; doi: 10.2147/DMSOTT.S12375
25. Salazar-Flores J, Dondiego-Aldape R, Rubi-Castellanos R, et al. Population structure and paternal admixture landscape on present-day Mexican-Mestizos revealed by Y-STR haplotypes. Am J Hum Biol 2010;22(3):401–409; doi: 10.1002/ ajhb.21013
26. Salazar MR, Carbajal HA, Espeche WG, et al. Comparison of the abilities of the plasma triglyceride/high-density lipoprotein cholesterol ratio and the metabolic syndrome to identify insulin resistance. Diab Vasc Dis Res 2013;10(4): 346–352; doi: 10.1177/1479164113479809

Address correspondence to:
Mariana Haydee García-Hernández, PhD
Unidad de Investigación Biomédica
Delegación Zacatecas
Instituto Mexicano del Seguro Social
IMSS
Interior Alameda No. 45. 98000 Zacatecas
Zac
México

E-mail: mariana.haydee.gh@gmail.com

METABOLIC SYNDROME AND RELATED DISORDERS
Volume 00, Number 00, 2025

Pp. 000–000
DOI: 10.1177/15578518251405802

Establishing Cut-Off Points for Lipid Profile-Derived Markers to Diagnose Prehypertension in Young Adults

Abraham Cardenas-Juarez, MSc,[1,*] Mariana Haydee García-Hernández, PhD,[1,*] Flor Itzel Lira-Hernandez, PhD,[1] Edgar Eduardo Lara-Ramirez, PhD,[2] Bruno Rivas-Santiago, PhD,[1] Juan Manuel Vargas-Morales, PhD,[3] and Diana Patricia Portales-Pérez, PhD[3,4]

Abstract

Introduction: Prehypertension (pre-HTN) affects between 25% and 50% of the adult population worldwide and constitutes a significant risk factor for the development of cardiovascular diseases and chronic kidney disease. Although it is not considered a disease, its identification is crucial as it reflects a state of alert to identify individuals at high risk of developing cardiovascular disease. However, the difficulties associated with its diagnosis limit its use in preventive medicine. In this context, the present study aims to analyze the diagnostic utility of markers derived from the lipid profile (TyG index and the ratios triglycerides (TG)/high-density lipoprotein-cholesterol (HDL-c), total cholesterol (TC)/HDL-c, low-density lipoprotein cholesterol (LDL-c)/HDL-c, non-HDL-c/HDL-c, and fasting blood glucose (FBG)/HDL-c) in determining pre-HTN.
Methods: A retrospective study was designed that included the participation of 668 young adults. A logistic regression model was used to examine the associations between the different markers and pre-HTN. The cut-off points of the markers were determined by receiver operating characteristic curve analysis and the Youden index.
Results: A positive and significant association was observed between all markers with the presence of pre-HTN. The cut-off values for the markers that best predicted pre-HTN status were TG/HDL-c ≥2.055 (sensitivity = 62.28%, specificity = 87.03%); TC/HDL-c ≥3.466 (sensitivity = 60.48%, specificity = 91.82%); non-HDL-c/HDL-c ≥2.466 (sensitivity = 60.48%, specificity = 91.82%); and FBG/HDL-c ≥1.726 (sensitivity = 68.26%, specificity = 73.25%).
Conclusions: Our study demonstrated the diagnostic relevance of the different markers for the detection of pre-HTN, suggesting that these markers may be useful in clinical practice for the timely and accurate diagnosis of pre-HTN.

Keywords: prehypertension, lipid profile, TG/HDL-c ratio, TC/HDL-c ratio, non-HDL-c/HDL-c ratio, FBG/HDL-c ratio

Introduction

High blood pressure, or hypertension, is the major preventable risk factor for the development of cardiovascular diseases (CVD) and chronic kidney disease and for mortality from these causes.[1] It is estimated that approximately one-third of the adult population over 18 years of age has hypertension worldwide.[2] However, its incidence, prevalence, and adverse health effects are increasing; this is due, in part, to deficiencies in prevention, diagnosis, and management strategies for hypertension.[3]

Classically, blood pressure has been classified as: optimal (systolic blood pressure [SBP] <120 mmHg and diastolic blood pressure [DBP] <80 mmHg); normal (SBP 120–129 mmHg and/or DBP 80–84 mmHg); high normal (SBP 130–139 mmHg and/or DBP 85–89 mmHg) and hypertension (SBP ≥140 mmHg and/or DBP ≥90 mmHg).[4,5] However, in 2003, the Seventh Report of the Joint National Committee on Prevention, Detection, Evaluation, and Treatment of High Blood Pressure (JNC7) proposed a new classification based in several studies demonstrating an association between the development of cardiovascular complications and blood

[1]Unidad de Investigación Biomédica, Instituto Mexicano del Seguro Social, Delegación Zacatecas, Zacatecas, México.
[2]Instituto Politécnico Nacional, Centro de Biotecnología Genómica, Laboratorio de Biotecnología Farmacéutica, Tamaulipas, México.
[3]Facultad de Ciencias Químicas, Universidad Autónoma de San Luis Potosí, Zona Universitaria, San Luis Potosí, México.
[4]Centro de Investigación En Ciencias de la Salud y Biomedicina, Universidad Autónoma de San Luis Potos, San Luis Potosí, México.
*These authors contributed equally to this study.

pressure levels previously considered normal.[6,7] This new classification included the term "prehypertension" (pre-HTN), which distinguishes those people with a SBP between 120 and 139 mmHg and/or a DBP between 80 and 89 mmHg, but, it is important note that pre-HTN is not classified as a disease, rather it is considered a state of alert to identify people at high risk of developing hypertension and other CVD.[5]

Pre-HTN can be detected through screening, and its detection allows preventive treatment to begin before symptoms appear. In Mexico, hypertension is a major clinical and public health problem. For example, among beneficiaries of the Mexican Social Security Institute, approximately 34–38 percent have hypertension.[8] In addition, hypertension is the leading cause of visits to primary care clinics, and its complications are among the leading causes of hospitalization.[9] Furthermore, the cost of medical care is considerable.[10] In this context, the timely detection of pre-HTN or hypertension and the use of antihypertensive therapy can reduce cardiovascular events.[11,12] Additionally, non-pharmacological therapies, such as magnesium supplementation, may serve as useful strategies to prevent hypertension.[13,14] Similarly, alternative treatments involving lifestyle modifications, including weight loss, dietary changes, and increased physical activity, may be effective in managing pre-HTN.[15] Prevention is critical to reduce health care costs and prevent the onset of clinical disease. The implementation of screening programs requires the identification of reliable markers to detect individuals with pre-HTN and hypertension. Young adults have greater autonomy over their decisions and begin to establish their own lifestyle habits, which can significantly impact their long-term health. To effectively prevent and manage various chronic conditions that emerge in the middle-aged, such as hypertension, metabolic syndrome and diabetes, it is essential to adopt and maintain a healthy lifestyle from an early age.

Several cohort studies have shown that people with pre-HTN often have an altered clinical and metabolic profile compared to people with normal blood pressure. This profile is manifested by an increase in several anthropometric indicators of obesity, such as body mass index (BMI), waist circumference, and waist-to-hip ratio. In addition, increase in serum levels of fasting blood glucose (FBG), fasting insulin, triglycerides (TG), total cholesterol (TC), and low-density lipoprotein cholesterol (LDL-c) are observed, while high-density lipoprotein cholesterol (HDL-c) levels are reduced compared to subjects with optimal blood pressure.[16–22] These features are closely associated with metabolic syndrome and other related conditions.

Previously, we demonstrated that the change in the metabolic profile determined by different markers derived from the lipid profile can be a reliable and accurate tool of the diagnosis of the metabolic syndrome,[23] but studies on these types of markers in the determination of pre-HTN are less common. In this sense, the objective of this study was to determine and compare the diagnostic accuracy of the different markers derived from the lipid profile (TyG index and the ratios TG/HDL-c, TC/HDL-c, LDL-c/HDL-c, non-HDL-c/HDL-c, and FBG/HDL-c) in the determination of pre-HTN in the Mexican mestizo population.

Participants and Methods

Study population

A retrospective study was designed that included the participation of 668 individuals who were younger than middle-aged (aged between 25 and 30 years old), from the metropolitan area of San Luis Potosí, Mexico. Individuals with inflammatory, endocrine, and/or chronic degenerative diseases were excluded (except for obesity, dyslipidemia, and diabetes), as were pregnant or lactating women. Individuals receiving regular pharmacological treatment for metabolic disorders (*e.g.,* statins, hypoglycemic agents, insulin, etc.) were allowed to participate, whereas those receiving hormonal treatment (*e.g.,* corticosteroids and levothyroxine) and chemotherapy were excluded. All participants were informed of the implications of the study and signed an informed consent form. The protocol was approved by the Ethics Committee of the Faculty of Chemical Sciences of the Autonomous University of San Luis Potosí, with registration number CEID-FCQ-CEID2015060.

Anthropometric and biochemical characteristics

Blood pressure measurements were performed by licensed and highly trained medical personnel. Patients were given instructions prior to the measurement, such as avoiding caffeine, smoking, and physical activity for at least 30 min beforehand. Blood pressure was recorded with the patient seated in a chair with a backrest, feet flat on the floor, and legs uncrossed. After a 5-min rest period, the patient's arm was supported at heart level, and they were instructed to remain silent during the measurement. At least two measurements were taken, 1 min apart, and the average value was recorded as the final measurement. A sphygmomanometer (Microlife AG, Heerbrugg, Switzerland) and a stethoscope (3 M Littmann Classical II, Neuss, Germany) were used. The record of blood pressure was conducted in accordance with the NOM-030-SSA2-2009 (applicable in Mexico) and aligned with the recommendations of the American College of Cardiology/American Heart Association Joint Committee on Clinical Practice Guidelines.[24] BMI (kg/m^2) was determined using a digital electronic scale (Beurer, BF1000, Germany). The value of BMI ≥18.5 and <25 was considered normal weight, a BMI ≥25 and <30 was considered overweight, and a BMI ≥30 was considered obese. After fasting for 10 to 12 h, a blood sample was taken by venipuncture for the determination of serum levels of FBG, TC, HDL-c, LDL-c, TG, uric acid (UA) and creatinine by spectrophotometric methods using the Mindray BS 300 Auto Chemistry Analyzer (Mindray®, Shenzhen, China), according to the conventional protocols of the University Clinical Laboratory of the Autonomous University of San Luis Potosí. The TyG index was calculated as Ln[fasting triglycerides (mg/dL)*fasting glucose (mg/dL)]/2.[25] The TG/HDL-c, TC/HDL-c, LDL-c/HDL-c, non-HDL-c/HDL-c, and FBG/HDL-c ratios were calculated by dividing the levels of TG (mg/dL), TC (mg/dL), LDL-c (mg/dL), non-HDL-c [TC-HDL-c (mg/dL)], and FBG (mg/dL), respectively by HDL-c levels (mg/dL). The diagnosis of pre-HTN was made according to the JNC7 criteria.[5]

Statistical analysis

Statistical analysis was performed using SPSS software (IBM Statics version 20.0). The Shapiro-Wilk test was used to assess the distribution of quantitative variables; since all these variables had a non-normal distribution, they were then compared using the non-parametric Mann–Whitney *U* test, while the chi-squared test was used for the qualitative variables. The Spearman rank test was used to analyze the

correlations between the TyG index and the ratios TG/HDL-c, TC/HDL-c, LDL-c/HDL-c, non-HDL-c/HDL-c and FBG/HDL-c, with the different established quantitative variables, while the Kendall's tau-b test was used for the qualitative variables. The association between the different lipid profile markers and the presence of pre-HTN was analyzed using a logistic regression analysis. A receiver operating characteristic (ROC) curve analysis and the Youden index were used to define the cut-off point at which the highest joint sensitivity and specificity of each of the markers evaluated were obtained; an area under the curve (AUC) ≥0.7 was considered acceptable, and a value of $p < 0.05$ was considered statistically significant in all cases.

Results

Anthropometric and biochemical characteristics

A total of 668 people (337 men and 331 women), with a mean age of 27 ± 4.0 years, participated in this study. Participants were classified according to the presence of pre-HTN (25%, 110 males; 57 females) or its absence (75%, 227 males; 274 females). Participants classified as having pre-HTN were more likely to be male compared with female ($P < 0.001$), while the TyG index and the ratios of TG/HDL-c, TC/HDL-c, LDL-c/HDL-c, non-HDL-c/HDL-c, and FBG/HDL-c were statistically higher in the pre-HTN group than in the control group ($p < 0.001$). Both groups differed in their clinical and metabolic profile, with significantly higher SBP, DBP, and BMI values observed in the pre-HTN group compared with the control group ($p < 0.001$); it was also observed that serum levels of FBG, TC, LDL-c, TG, UA, and creatinine were statistically higher in the pre-HTN group compared to the control group, but HDL-c levels were lower in the pre-HTN group compared with the control group ($p < 0.001$) (Table 1).

Bivariate correlation analysis

The results of the correlation analysis showed a positive and statistically significant relationship between the different markers derived from the lipid profile and the diagnosis of pre-HTN (TyG index rho = 0.436, $p < 0.001$; TG/HDL-c ratio rho = 0.440, $p < 0.001$; TC/HDL-c ratio rho = 0.445, $p < 0.001$; LDL-c/HDL-c ratio rho = 0.384, $p < 0.001$; non-HDL-c/HDL-c ratio rho = 0.445, $p < 0.001$; and FBG/HDL-c ratio rho = 0.374, $p < 0.001$), likewise, a positive and significant correlation was also observed between the variables of sex, SBP, DBP, BMI, FBG, TC, LDL-c, non-HDL-c, TG, UA, and creatinine with pre-HTN; however, the variable HDL-c was negatively correlated in pre-HTN cases (rho = –0.316, $p < 0.001$) (Table 2).

Multivariate association analysis

Having identified a significant correlation between the study variables and a deteriorated health status, a logistic regression analysis was performed to determine the strength of association of the different markers derived from the lipid profile as risk factors for the development of pre-HTN in young adults, and to evaluate their predictive capacity. To establish the regression models, the covariates that showed a stronger association, such as BMI and UA, were considered (TG was not included to avoid the effect of multicollinearity), and an adjustment was made for sex and age. Model 1 includes BMI, sex, UA, and age; model 2 eliminates the confounding variable of age; and model 3 eliminates the confounding variable of UA. Model 3 was the one that showed the best association and predictive ability of each of the lipid profile-derived markers with the presence of pre-HTN in a

Table 1. Anthropometric and Biochemical Characteristics of the Study Groups According to the pre-HTN

Variable	*Control group*	*Pre-HTN*	p
n	501	167	—
Sex (M:F)[a]	227 : 274	110 : 57	<0.001
Age[b]	27.0 (26.0–27.0)	27.0 (27.0–28.0)	0.063
SBP (mmHg)[b]	100 (90–110)	120 (120–120)	<0.001
DBP (mmHg)[b]	60 (60–70)	80 (80–80)	<0.001
BMI (kg/m^2)[b]	21.16 (19.80–22.89)	27.15 (24.68–30.00)	<0.001
FBG (mg/dL)[b]	85.00 (80.00–90.00)	89.00 (84.00–94.00)	<0.001
TC (mg/dL)[b]	155.0 (140.0–170.0)	167.5 (151.0–190.3)	<0.001
HDL-c (mg/dL)[b]	54.40 (48.70–62.03)	46.60 (38.95–53.83)	<0.001
LDL-c (mg/dL)[b]	83.55 (72.50–96.60)	96.30 (84.08–114.3)	<0.001
non-HDL-c (mg/dL)[b]	97.85 (85.23–110.1)	120.8 (102.6–144.6)	<0.001
TG (mg/dL)[b]	74.00 (60.00–92.00)	115.0 (81.00–178.0)	<0.001
Uric Acid (mg/dL)[b]	5.000 (4.140–5.940)	6.415 (5.635–7.405)	<0.001
Creatinine (mg/dL)[b]	0.970 (0.860–1.098)	1.055 (0.920–1.150)	<0.001
TyG[b]	4.356 (4.240–4.483)	4.624 (4.418–4.874)	<0.001
TG/HDL-c[b]	1.313 (0.988–1.758)	2.456 (1.470–4.028)	<0.001
TC/HDL-c[b]	2.829 (2.466–3.118)	3.646 (3.028–4.427)	<0.001
LDL-c/HDL-c[b]	1.523 (1.247–1.793)	2.106 (1.639–2.696)	<0.001
non-HDL-c/HDL-c[b]	1.831 (1.474–2.118)	2.663 (2.032–3.471)	<0.001
FBG/HDL-c[b]	1.549 (1.359–1.748)	1.942 (1.619–2.407)	<0.001

[a]Data are presented as median (interquartile range) or proportions. The p value was calculated using the χ^2 test.
[b]The Mann–Whitney U test.
M, male; F, female; SBP, systolic blood pressure; DPB, diastolic blood pressure; BMI, body mass index; FBG, fasting blood glucose; TC, total cholesterol; HDL-c, high-density lipoprotein-cholesterol; LDL-c, low-density lipoprotein-cholesterol; non-HDL-c [TC-HDL-c]; TG, triglycerides.

Table 2. Correlations of the Study Variables: TyG, TG/HDL-c, TC/HDL-c, LDL-c/HDL-c, non-HDL-c/HDL-c and FBG/HDL-c with Diagnosis of pre-HTN and the Anthropometric and Biochemical Characteristics of the Study Subjects

Variable	*Rho/tau-b*	p
Sex[a]	0.178	<0.001
Age[b]	0.072	0.063
SBP (mmHg)[b]	0.775	<0.001
DBP (mmHg)[b]	0.796	<0.001
BMI (kg/m^2)[b]	0.632	<0.001
FBG (mg/dL)[b]	0.243	<0.001
TC (mg/dL)[b]	0.262	<0.001
HDL-c (mg/dL)[b]	–0.316	<0.001
LDL-c (mg/dL)[b]	0.257	<0.001
non-HDL-c (mg/dL)[b]	0.375	<0.001
TG (mg/dL)[b]	0.409	<0.001
Uric Acid (mg/dL)[b]	0.457	<0.001
Creatinine (mg/dL)[b]	0.184	<0.001
TyG[b]	0.436	<0.001
TG/HDL-c[b]	0.440	<0.001
TC/HDL-c[b]	0.445	<0.001
LDL-c/HDL-c[b]	0.384	<0.001
non-HDL-c/HDL-c[b]	0.445	<0.001
FBG/HDL-c[b]	0.374	<0.001

[a]Kendall's Tau-b correlation.
[b]Spearman's rank correlation coefficient.

statistically significant manner for TyG (odds ratio [OR] = 2.862, confidence interval [CI]: 1.457–5.622), TG/HDL-c (OR = 3.029, CI: 1.611–5.694), TC/HDL-c (OR = 4.497, CI: 2.331–8.674), LDL-c/HDL-c (OR = 2.751, CI: 1.503–5.038), non-HDL-c/HDL-c (OR = 4.436, CI: 2.305–8.536) and FBG/HDL-c (OR = 2.216, CI: 1.224–4.012). We also observed that BMI and sex had a joint effect on the development of pre-HTN, with the presence of obesity and male sex being risk factors that increased the likelihood of developing pre-HTN in all cases (Table 3).

Receiver operating characteristic curve analysis

According to the Youden index of the ROC curves, the optimal cut-off values for the identification of pre-HTN for each of the markers evaluated, where the maximum joint sensitivity and specificity are achieved, were as follows TyG index ≥4.591; sensitivity = 56.89%, specificity = 90.62%, TG/HDL-c ratio ≥2.055; sensitivity = 62.28%, specificity = 87.03%, TC/HDL-c ratio ≥3.466; sensitivity = 60.48%, specificity = 91.82%, LDL-c/HDL-c ratio ≥1.949; sensitivity = 59.28%, specificity = 84.43%, non-HDL-c/HDL-c ratio ≥2.466; sensitivity = 60.48%, specificity = 91.82% and FBG/HDL-c ratio ≥1.726; sensitivity = 68.26%, specificity = 73.25%, with a significance value of $p < 0.001$ in all cases (Table 4). As shown in Figure 1, the AUC of the markers showing the highest diagnostic accuracy were TG/HDL-c ratio AUC = 0.793 (CI = 0.749–0.838), TC/HDL-c ratio AUC = 0.797 (CI = 0.751–0.842), non-HDL-c/HDL-c ratio AUC = 0.797 (CI = 0.751–0.842), and FBG/HDL-c ratio AUC = 0.749 (CI = 0.701–0.798).

Discussion

Epidemiological studies executed in different countries have reported a high incidence of pre-HTN among young adults, ranging from approximately 25% to 50%[19,20,26–29]; untreated pre-HTN can lead to the development of hypertension[30,31] CVD,[7] and renal disorders.[32]

Johnson and colleagues previously demonstrated that young adults (aged 18–39 years) exhibit a significantly lower rate of initial hypertension diagnosis compared to middle-aged (40–59 years) and older adults (≥60 years). Moreover, approximately 40% of young adults remain undiagnosed over a 4-year period.[33] The age-related disparities in undiagnosed hypertension among young adults may be attributed to several factors such as limited access to a regular source of primary care and/or lower utilization of primary care services,[34] underestimation of elevated blood pressure by health care providers (the white coat effect),[35] and poor adherence to clinical guidelines.[36] This delay in diagnosis may contribute to the onset and progression of uncontrolled health conditions later in life.

Blood pressure is a biological variable that may appear simple to measure, but because of its intrinsic variability, it is susceptible to measurement error, making its readings unreliable and prone to misinterpretation.[37] This variability is caused by various factors related to the patient (*e.g.,* acute ingestion of food or alcohol, acute use or exposure to nicotine, bladder distention, etc.), to the procedure (*e.g.,* body position, inadequate rest, etc.), or to the measurement device.[36,38] In this context, it is essential to implement new diagnostic strategies that enable the timely and accurate identification of pre-HTN in young adults, who often remain undiagnosed.

In this study, we investigated the relationship between different lipid profile markers and the presence of pre-HTN. Our results showed the positive association of the TyG index and the ratios TG/HDL-c, TC/HDL-c, LDL-c/HDL-c, non-HDL-c/HDL-c, and FBG/HDL-c with the increased risk of developing pre-HTN, with a stronger association observed with the ratios: TG/HDL-c (OR = 3.029), TC/HDL-c (OR = 4.497), and non-HDL-c/HDL-c (OR = 4.436). There are a few studies regarding the relationship between these types of markers and pre-HTN. A study by Zhang and colleagues showed that the risk of pre-HTN in the highest quartiles of TyG and TG/HDL was OR = 3.909 (95% CI: 3.151–4.849) and OR = 3.651 (95% CI: 2.948–4.521), respectively, compared to the lowest quartiles.[39] In contrast, Yang and colleagues found a lower level of association for these markers: TyG OR = 1.398 (95% CI: 1.208–1.617) and TG/HDL-c OR = 1.418 (95% CI: 1.241–1.621).[40] For their part, Xu and collaborators found a stronger association between the TyG index and pre-HTN, with an OR = 2.53 (95% CI: 2.38–2.69).[41] On the other hand, to our knowledge, no association values have been reported for the TC/HDL-c, non-HDL-c/HDL-c, and FBG/HDL-c ratios with pre-HTN.

Additionally, we found that the obesity status and male sex in the young population play an important role as risk factors, in agreement with previous studies on the development of hypertension.[42–47] On the other hand, we also evaluated its accuracy as a diagnostic tool, the cut-off values for the markers that best predicted pre-HTN were: TG/HDL-c ratio ≥2.055 (sensitivity = 62.28%, specificity = 87.03%); TC/HDL-c ratio ≥3.466 (sensitivity = 60.48%, specificity = 91.82%); non HDL-c/HDL-c ratio ≥2.466 (sensitivity = 60.48%, specificity = 91.82%); and FBG/HDL-c ratio ≥1.726 (sensitivity = 68.26%, specificity = 73.25%), notably,

Table 3. Associations Between the Study Variables: TyG, TG/HDL-c, TC/HDL-c, LDL-c/HDL-c, non-HDL-c/HDL-c, and FBG/HDL-c with pre-HTN

		Model 1			*Model 2*			*Model 3*		
Variable	*Exposure*	*OR*	*CI (95%)*	p	*OR*	*CI (95%)*	p	*OR*	*CI (95%)*	p
TyG	TyG	2.467	1.214–5.012	<0.05	2.470	1.216–5.017	<0.05	2.862	1.457–5.622	<0.05
	BMI	2.082	1.786–2.426	<0.001	2.090	1.794–2.434	<0.001	2.140	1.842–2.488	<0.001
	Sex	0.409	0.187–0.898	<0.05	0.409	0.186–0.897	<0.05	0.292	0.153–0.555	<0.001
	UA	1.266	0.922–1.739	0.145	1.267	0.923–1.740	0.144			
	Age	1.046	0.849–1.288	0.674						
TG/HDL-c	TG/HDL-c	2.711	1.412–5.207	<0.01	2.711	1.412–5.204	<0.01	3.029	1.611–5.694	<0.001
	BMI	2.080	1.783–2.426	<0.001	2.088	1.791–2.434	<0.001	2.147	1.846–2.498	<0.001
	Sex	0.407	0.184–0.902	<0.05	0.408	0.184–0.903	<0.05	0.284	0.149–0.543	<0.001
	UA	1.276	0.931–1.749	0.130	1.278	0.933–1.752	0.127			
	Age	1.049	0.846–1.301	0.662						
TC/HDL-c	TC/HDL-c	4.057	2.038–8.077	<0.001	4.070	2.047–8.095	<0.001	4.497	2.331–8.674	<0.001
	BMI	2.032	1.746–2.365	<0.001	2.037	1.752–2.368	<0.001	2.071	1.787–2.401	<0.001
	Sex	0.352	0.155–0.798	<0.05	0.351	0.155–0.795	<0.05	0.273	0.142–0.528	<0.001
	UA	1.177	0.852–1.627	0.322	1.178	0.853–1.628	0.319			
	Age	1.028	0.828–1.278	0.801						
LDL-c/HDL-c	LDL-c/HDL-c	2.490	1.335–4.648	<0.01	2.468	1.324–4.601	<0.01	2.751	1.503–5.038	<0.001
	BMI	2.080	1.786–2.423	<0.001	2.094	1.800–2.436	<0.001	2.151	1.853–2.497	<0.001
	Sex	0.405	0.182–0.900	<0.05	0.402	0.181–0.893	<0.05	0.275	0.145–0.522	<0.001
	UA	1.285	0.940–1.755	0.116	1.286	0.941–1.757	0.115			
	Age	1.063	0.865–1.306	0.560						
non-HDL-c/HDL-c	non-HDL-c/HDL-c	3.999	2.013–7.943	<0.001	4.012	2.022–7.961	<0.001	4.436	2.305–8.536	<0.001
	BMI	2.037	1.750–2.370	<0.001	2.041	1.756–2.373	<0.001	2.077	1.792–2.407	<0.001
	Sex	0.351	0.155–0.796	<0.05	0.350	0.154–0.793	<0.05	0.272	0.141–0.526	<0.001
	UA	1.179	0.853–1.629	0.319	1.180	0.854–1.630	0.317			
	Age	1.029	0.828–1.278	0.799						
FBG/HDL-c	FBG/HDL-c	2.002	1.087–3.687	<0.05	1.992	1.082–3.668	<0.05	2.216	1.224–4.012	<0.001
	BMI	2.125	1.824–2.476	<0.001	2.136	1.834–2.486	<0.001	2.208	1.901–2.565	<0.001
	Sex	0.442	0.199–0.980	<0.05	0.439	0.198–0.974	<0.05	0.290	0.152–0.555	<0.001
	UA	1.320	0.968–1.800	0.079	1.321	0.969–1.801	0.078			
	Age	1.055	0.859–1.296	0.608						

Binomial logistic regression test. Model 1: adjusted for BMI, sex, UA, and age; model 2: adjusted for BMI, sex and UA; model 3: adjusted for BMI and sex. UA, uric acid; OR, odds ratio; CI, confidence interval. The sex variable is relative to female.

we observed high specificity values compared to sensitivity values, which means that these markers can be useful as confirmatory tests in clinic practice, achieving discrimination against false positives.[48,49]

Several mechanisms could explain how increases in different lipid profile markers contribute to the risk of developing hypertension, with elevated TG levels as a common underlying factor. To begin, under hypertriglyceridemia conditions, hepatic production of very LDLs (vLDLs) increases. These particles can cross the vascular endothelium and enter the subendothelial space, where they are susceptible to oxidation mediated by enzymes such as lipoxygenases, NADPH oxidase, and xanthine oxidase.[50] The subsequent formation and accumulation of oxidized LDL particles reduce the bioavailability of nitric oxide (NO), a key vasodilator, leading to impaired endothelial function and, consequently, the development of hypertension.[51]

Second, the bioavailability of HDL particles decreases. The cardioprotective effect of HDL is largely attributed to its role in reverse cholesterol transport (RCT) and its antioxidant properties. Cholesterol ester transport protein mediates the exchange of TG from vLDL for cholesteryl esters (CE) from HDL. As a result, HDL becomes enriched with TG, while vLDL becomes enriched with CE. TG-enriched HDL particles serve as better substrates for hepatic lipase, which accelerates their clearance from circulation and reduces the number of HDL particles available to participate in RCT.[52] Furthermore, HDL exerts a protective effect on the endothelium by inducing the expression and activation of endothelial nitric oxide synthase. This effect is mediated by activation of

Table 4. Diagnostic Accuracy of the Study Variables: TyG, TG/HDL-c, TC/HDL-c, LDL-c/HDL-c, non-HDL-c/HDL-c, and FBG/HDL-c with pre-HTN

Variable	*AUC*	*CI (95%)*	p	*Cut-off*	*Sensitivity (%)*	*Specificity (%)*
TyG	0.791	(0.747–0.835)	<0.001	≥4.591	56.89	90.62
TG/HDL-c	0.793	(0.749–0.838)	<0.001	≥2.055	62.28	87.03
TC/HDL-c	0.797	(0.751–0.842)	<0.001	≥3.466	60.48	91.82
LDL-c/HDL-c	0.756	(0.707–0.804)	<0.001	≥1.949	59.28	84.43
non-HDL-c/HDL-c	0.797	(0.751–0.842)	<0.001	≥2.466	60.48	91.82
FBG/HDL-c	0.749	(0.701–0.798)	<0.001	≥1.726	68.26	73.25

ROC curves analysis.
AUC, area under curve; ROC, receiver operating characteristics.

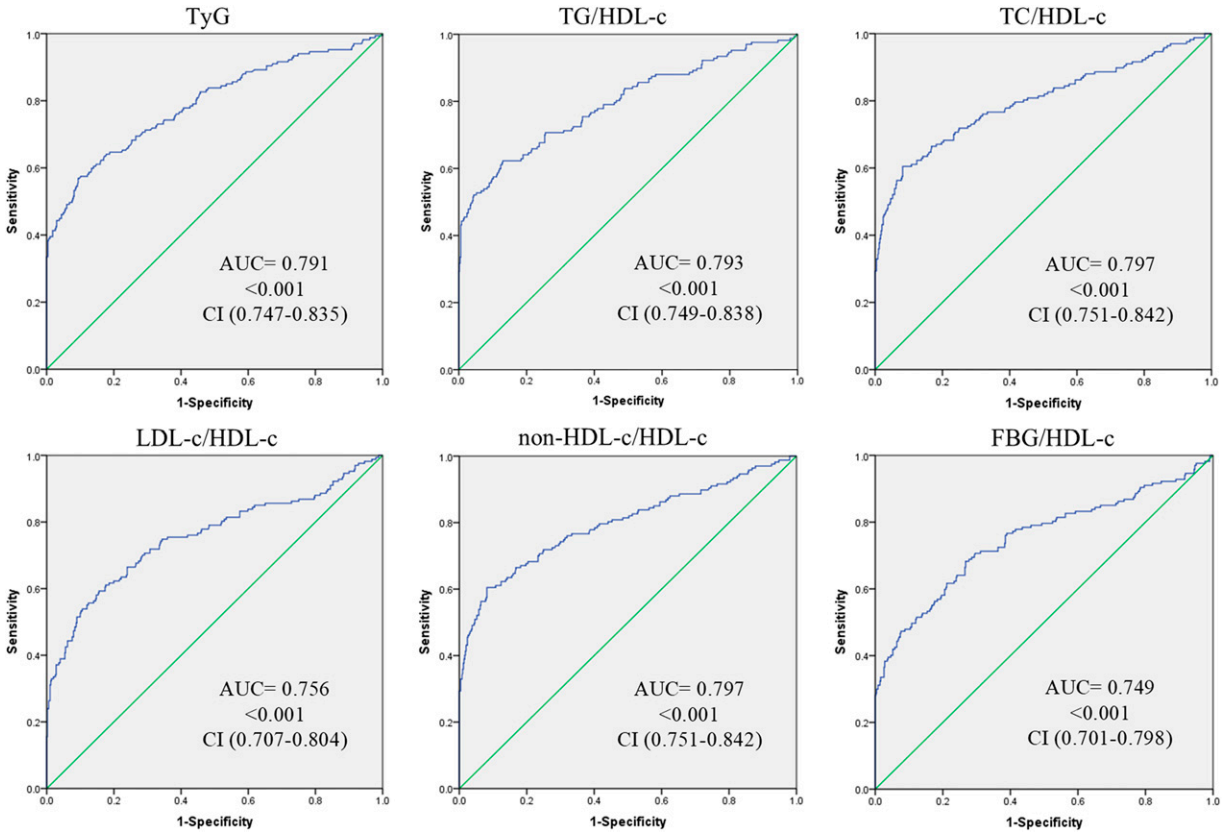

FIG. 1. Receiver operating characteristic (ROC) curves of the different markers derived from the lipid profile. ROC curves for TyG index and TG/HDL-c, TC/HDL-c, LDL-c/HDL-c, non-HDL-c/HDL-c, and FBG/HDL-c ratios as high-risk indicators of pre-HTN.

the PI3K/Akt pathway in endothelial cells following HDL interaction with surface receptors such as scavenger receptor class B type 1 and ATP-binding cassette transporter type A1.[53,54] These alterations in HDL-related mechanisms further compromise endothelial homeostasis.

Third, sympathetic nervous system (SNS) activity increases. Hypertriglyceridemia can induce insulin resistance,[55] which involves a reduction in the efficiency of glucose uptake and utilization by peripheral tissues in response to insulin. As a compensatory mechanism, insulin secretion increases, resulting in hyperinsulinemia. This, in turn, stimulates SNS activity and promotes the secretion of adrenaline and noradrenaline, thereby increasing cardiac output and peripheral vascular resistance.[56,57]

Nevertheless, this study has several limitations that should be acknowledged. For instance, the sample was limited to a Mexican population; therefore, these findings need to be replicated in different cohorts to assess their generalizability to other ethnic groups. Additionally, serum sodium and potassium levels were not measured, which prevents us from assessing the participant's sodium-potassium balance and limits our ability to evaluate its potential influence on the development of pre-HTN.

Conclusion

In conclusion, our study showed the strong association of different lipid profile-derived markers with pre-HTN, demonstrating their effect as risk factors. In our study, the cut-off values for the markers that predicted pre-HTN with the best diagnostic accuracy were TG/HDL-c ratio ≥2.055, TC/HDL-c ratio ≥3.466, non-HDL-c/HDL-c ratio ≥2.466, and FBG/HDL-c ratio ≥1.726. This study is of great importance for the early detection of prehypertension in young people in Mexico. The clinical application of the cut-off points for the different markers evaluated may be useful in the field of preventive medicine to mitigate the development of cardiovascular complications in people at risk.

Authors' Contributions

The authors confirm contribution to the article as follows: Material preparation and data collection J.M.V.-M., and D.P.P.-P., analysis was performed by A.C.-J., data curation A.C.-J., M.H.G.-H., F.I.L.-H., and E.E.L.-R. The first draft of the article was written by A.C.-J., and all the authors commented on previous versions of the article. Study conception and design A.C.-J., and M.H.G.-H. Draft article preparation: A.C.-J., M.H.G.-H., D.P.P.-P., and B.R.-S., All the authors read and approved the final article.

Author Disclosure Statement

None of the authors has any potential financial conflict of interest related to this article.

Funding Information

The research reported in this article was not supported.

References

1. Zhou B, Perel P, Mensah GA, et al. Global epidemiology, health burden and effective interventions for elevated blood pressure and hypertension. Nat Rev Cardiol 2021;18(11): 785–802; doi: 10.1038/s41569-021-00559-8
2. Mills KT, Stefanescu A, He J. The global epidemiology of hypertension. Nat Rev Nephrol 2020;16(4):223–237; doi: 10.1038/s41581-019-0244-2
3. Olsen MH, Angell SY, Asma S, et al. A call to action and a lifecourse strategy to address the global burden of raised blood pressure on current and future generations: The Lancet Commission on hypertension. Lancet 2016;388(10060): 2665–2712; doi: 10.1016/S0140-6736(16)31134-5
4. Kanegae H, Oikawa T, Kario K. Should Pre-hypertension Be Treated? Curr Hypertens Rep 2017;19(11):91; doi: 10 .1007/s11906-017-0789-z
5. Chobanian AV, Bakris GL, Black HR, et al.; National High Blood Pressure Education Program Coordinating Committee. Seventh report of the Joint National Committee on prevention, detection, evaluation, and treatment of high blood pressure. Hypertension 2003;42(6):1206–1252; doi: 10 .1161/01.HYP.0000107251.49515.c2
6. Lewington S, Clarke R, Qizilbash N, et al.; Prospective Studies Collaboration. Age-specific relevance of usual blood pressure to vascular mortality: A meta-analysis of individual data for one million adults in 61 prospective studies. Lancet 2002; 360(9349):1903–1913; doi: 10.1016/s0140-6736(02)11911-8
7. Vasan RS, Larson MG, Leip EP, et al. Impact of high-normal blood pressure on the risk of cardiovascular disease. N Engl J Med 2001;345(18):1291–1297; doi: 10.1056/ NEJMoa003417
8. Jimenez-Corona A, Lopez-Ridaura R, Stern MP, et al. Risk of progression to hypertension in a low-income Mexican population with prehypertension and normal blood pressure. Am J Hypertens 2007;20(9):929–936; doi: 10.1016/j.amjhyper.2007 .03.019
9. Castro-Rios A, Doubova SV, Martinez-Valverde S, et al. Potential savings in Mexico from screening and prevention for early diabetes and hypertension. Health Aff (Millwood) 2010;29(12):2171–2179; doi: 10.1377/hlthaff.2010.0819
10. Cortes-Hernandez DE, Lundelin KJ, Picazzo-Palencia E, et al. The burden of blood-pressure-related cardiovascular mortality in Mexico. Int J Hypertens 2014;2014(427684): 1–9; doi: 10.1155/2014/427684
11. Sipahi I, Swaminathan A, Natesan V, et al. Effect of antihypertensive therapy on incident stroke in cohorts with prehypertensive blood pressure levels: A meta-analysis of randomized controlled trials. Stroke 2012;43(2):432–440; doi: 10.1161/ STROKEAHA.111.636829
12. Law M, Wald N, Morris J. Lowering blood pressure to prevent myocardial infarction and stroke: A new preventive strategy. Health Technol Assess 2003;7(31):1–94; doi: 10.3310/hta7310
13. Rodriguez-Ramirez M, Simental-Mendia LE, Gonzalez-Ortiz M, et al. Prevalence of prehypertension in Mexico and its association with hypomagnesemia. Am J Hypertens 2015; 28(8):1024–1030; doi: 10.1093/ajh/hpu293
14. Rodriguez-Moran M, Guerrero-Romero F. Hypomagnesemia and prehypertension in otherwise healthy individuals. Eur J Intern Med 2014;25(2):128–131; doi: 10.1016/j.ejim.2013.08.706
15. Pimenta E, Oparil S. Prehypertension: Epidemiology, consequences and treatment. Nat Rev Nephrol 2010;6(1):21–30; doi: 10.1038/nrneph.2009.191
16. Sit JW, Sijian L, Wong EM, et al. Prevalence and risk factors associated with prehypertension: Identification of foci for primary prevention of hypertension. J Cardiovasc Nurs 2010;25(6):461–469; doi: 10.1097/JCN.0b013e3181dcb551
17. Isezuo SA, Sabir AA, Ohwovorilole AE, et al. Prevalence, associated factors and relationship between prehypertension and hypertension: A study of two ethnic African populations in Northern Nigeria. J Hum Hypertens 2011;25(4): 224–230; doi: 10.1038/jhh.2010.56
18. Ishikawa Y, Ishikawa J, Ishikawa S, et al.; Jichi Medical School Cohort Investigators Group. Prevalence and determinants of prehypertension in a Japanese general population: The Jichi medical school cohort study. Hypertens Res 2008;31(7):1323–1330; doi: 10.1291/hypres.31.1323
19. Erem C, Hacihasanoglu A, Kocak M, et al. Prevalence of prehypertension and hypertension and associated risk factors among Turkish adults: Trabzon hypertension study. J Public Health (Oxf) 2009;31(1):47–58; doi: 10.1093/pubmed/fdn078
20. Ferguson TS, Younger NO, Tulloch-Reid MK, et al. Prevalence of prehypertension and its relationship to risk factors for cardiovascular disease in Jamaica: Analysis from a cross-sectional survey. BMC Cardiovasc Disord 2008; 8(20):20; doi: 10.1186/1471-2261-8-20
21. Janghorbani M, Amini M, Gouya MM, et al. Nationwide survey of prevalence and risk factors of prehypertension and hypertension in Iranian adults. J Hypertens 2008;26(3): 419–426; doi: 10.1097/HJH.0b013e3282f2d34d
22. Tsai PS, Ke TL, Huang CJ, et al. Prevalence and determinants of prehypertension status in the Taiwanese general population. J Hypertens 2005;23(7):1355–1360; doi: 10 .1097/01.hjh.0000173517.68234.c3
23. Cardenas-Juarez A, Portales-Perez DP, Rivas-Santiago B, et al. Clinical significance of the lipid profile ratios and triglyceride glucose index in the diagnosis of metabolic syndrome. Metab Syndr Relat Disord 2024;22(7):510–515; doi: 10.1089/met.2024.0045
24. Writing Committee M, Jones DW, Ferdinand KC, et al. 2025 AHA/ACC/AANP/AAPA/ABC/ACCP/ACPM/AGS/AMA/ASPC/NMA/PCNA/SGIM guideline for the prevention, detection, evaluation and management of high blood pressure in adults: A report of the American college of cardiology/American heart association joint committee on clinical practice guidelines. Hypertension 2025;82(10): e212–e316; doi: 10.1161/HYP.0000000000000249
25. Simental-Mendia LE, Gomez-Diaz R, Wacher NH, et al. The triglycerides and glucose index is negatively associated with insulin secretion in young adults with normal weight. Horm Metab Res 2022;54(01):33–36; doi: 10.1055/a-1713-7821
26. Paquissi FC, Manuel V, Manuel A, et al. Prevalence of cardiovascular risk factors among workers at a private tertiary center in Angola. Vasc Health Risk Manag 2016;12:497–503; doi: 10.2147/VHRM.S120735
27. Meng XJ, Dong GH, Wang D, et al. Epidemiology of prehypertension and associated risk factors in urban adults from 33 communities in China–the CHPSNE study. Circ J 2012; 76(4):900–906; doi: 10.1253/circj.cj-11-1118
28. Wang Y, Wang QJ. The prevalence of prehypertension and hypertension among US adults according to the new joint national committee guidelines: New challenges of the old problem. Arch Intern Med 2004;164(19):2126–2134; doi: 10.1001/archinte.164.19.2126

29. Nedialkova M, Dobreva A, Bakalova S, et al. Functional criteria for differentiating blast cells in acute leukemia. Vutr Boles 1983;22(4):63–66.
30. Winegarden CR. From "prehypertension" to hypertension? Additional evidence. Ann Epidemiol 2005;15(9):720–725; doi: 10.1016/j.annepidem.2005.02.010
31. Vasan RS, Larson MG, Leip EP, et al. Assessment of frequency of progression to hypertension in non-hypertensive participants in the Framingham Heart Study: A cohort study. Lancet 2001;358(9294):1682–1686; doi: 10.1016/S0140-6736(01)06710-1
32. Leiba A, Twig G, Vivante A, et al. Prehypertension among 2.19 million adolescents and future risk for end-stage renal disease. J Hypertens 2017;35(6):1290–1296; doi: 10.1097/HJH.0000000000001295
33. Johnson HM, Thorpe CT, Bartels CM, et al. Undiagnosed hypertension among young adults with regular primary care use. J Hypertens 2014;32(1):65–74; doi: 10.1097/HJH.0000000000000008
34. Steckelings UM, Stoppelhaar M, Sharma AM, et al.; HYDRA Study Group. HYDRA: Possible determinants of unsatisfactory hypertension control in German primary care patients. Blood Press 2004;13(2):80–88; doi: 10.1080/08037050310030982
35. Tsai PS. White coat hypertension: Understanding the concept and examining the significance. J Clin Nurs 2002;11(6):715–722; doi: 10.1046/j.1365-2702.2002.00660.x
36. Kallioinen N, Hill A, Horswill MS, et al. Sources of inaccuracy in the measurement of adult patients' resting blood pressure in clinical settings: A systematic review. J Hypertens 2017;35(3):421–441; doi: 10.1097/HJH.0000000000001197
37. Muldoon MF, Kronish IM, Shimbo D. Of signal and noise: Overcoming challenges in blood pressure measurement to optimize hypertension care. Circ Cardiovasc Qual Outcomes 2018;11(5):e004543; doi: 10.1161/CIRCOUTCOMES.117.004543
38. Liu J, Li Y, Li J, et al. Sources of automatic office blood pressure measurement error: A systematic review. Physiol Meas 2022;43(9); doi: 10.1088/1361-6579/ac890e
39. Zhang X, Yu C, Ye R, et al. Correlation between non-insulin-based insulin resistance indexes and the risk of prehypertension: A cross-sectional study. J Clin Hypertens (Greenwich) 2022;24(5):573–581; doi: 10.1111/jch.14449
40. Yang S, Zhang Y, Zhou Z, et al. Association of triglyceride-glucose index, triglyceride to high-density lipoprotein cholesterol ratio, and related parameters with prehypertension and hypertension. J Clin Hypertens (Greenwich) 2025;27(1):e14926; doi: 10.1111/jch.14926
41. Xu J, Xu W, Chen G, et al. Association of TyG index with prehypertension or hypertension: A retrospective study in Japanese normoglycemia subjects. Front Endocrinol (Lausanne) 2023;14:1288693; doi: 10.3389/fendo.2023.1288693
42. Virani SS, Alonso A, Aparicio HJ, et al.; American Heart Association Council on Epidemiology and Prevention Statistics Committee and Stroke Statistics Subcommittee. Heart disease and stroke Statistics-2021 update: A report from the American heart association. Circulation 2021;143(8):e254–e743; doi: 10.1161/CIR.0000000000000950
43. Ostchega Y, Fryar CD, Nwankwo T, et al. Hypertension prevalence among adults aged 18 and over: United States, 2017-2018. NCHS Data Brief 2020(364):1–8.
44. Writing Group M, Mozaffarian D, Benjamin EJ, et al. Heart disease and stroke statistics-2016 update: A report from the American heart association. Circulation 2016;133(4):e38-360; doi: 10.1161/CIR.0000000000000350
45. Hall JE, do Carmo JM, da Silva AA, et al. Obesity-induced hypertension: Interaction of neurohumoral and renal mechanisms. Circ Res 2015;116(6):991–1006; doi: 10.1161/CIRCRESAHA.116.305697
46. Maranon R, Reckelhoff JF. Sex and gender differences in control of blood pressure. Clin Sci (Lond) 2013;125(7):311–318; doi: 10.1042/CS20130140
47. Garrison RJ, Kannel WB, Stokes J, et al. Incidence and precursors of hypertension in young adults: The framingham offspring study. Prev Med 1987;16(2):235–251; doi: 10.1016/0091-7435(87)90087-9
48. Naeger DM, Kohi MP, Webb EM, et al. Correctly using sensitivity, specificity, and predictive values in clinical practice: How to avoid three common pitfalls. AJR Am J Roentgenol 2013;200(6):W566–W70; doi: 10.2214/AJR.12.9888
49. Parikh R, Mathai A, Parikh S, et al. Understanding and using sensitivity, specificity and predictive values. Indian J Ophthalmol 2008;56(1):45–50; doi: 10.4103/0301-4738.37595
50. Jiang H, Zhou Y, Nabavi SM, et al. Mechanisms of oxidized LDL-Mediated endothelial dysfunction and its consequences for the development of atherosclerosis. Front Cardiovasc Med 2022;9:925923; doi: 10.3389/fcvm.2022.925923
51. Gallo G, Volpe M, Savoia C. Endothelial dysfunction in hypertension: Current concepts and clinical implications. Front Med (Lausanne) 2021;8:798958; doi: 10.3389/fmed.2021.798958
52. Welty FK. How do elevated triglycerides and low HDL-cholesterol affect inflammation and atherothrombosis? Curr Cardiol Rep 2013;15(9):400; doi: 10.1007/s11886-013-0400-4
53. Besler C, Heinrich K, Rohrer L, et al. Mechanisms underlying adverse effects of HDL on eNOS-activating pathways in patients with coronary artery disease. J Clin Invest 2011;121(7):2693–2708; doi: 10.1172/JCI42946
54. Yuhanna IS, Zhu Y, Cox BE, et al. High-density lipoprotein binding to scavenger receptor-BI activates endothelial nitric oxide synthase. Nat Med 2001;7(7):853–857; doi: 10.1038/89986
55. Li N, Fu J, Koonen DP, et al. Are hypertriglyceridemia and low HDL causal factors in the development of insulin resistance? Atherosclerosis 2014;233(1):130–138; doi: 10.1016/j.atherosclerosis.2013.12.013
56. da Silva AA, do Carmo JM, Li X, et al. Role of Hyperinsulinemia and Insulin Resistance in Hypertension: Metabolic Syndrome Revisited. Can J Cardiol 2020;36(5):671–682; doi: 10.1016/j.cjca.2020.02.066
57. Tack CJ, Smits P, Willemsen JJ, et al. Effects of insulin on vascular tone and sympathetic nervous system in NIDDM. Diabetes 1996;45(1):15–22; doi: 10.2337/diab.45.1.15

Address correspondence to:
Diana P. Portales-Pérez, PhD
Universidad Autónoma de San Luis Potosí
UASLP
Laboratorio de Inmunología y Biología Celular y Molecular
Facultad de Ciencias Químicas, UASLP
Av. Manuel Nava No. 6
C.P. San Luis Potosí 78210
México

E-mail: dportale@uaslp.mx

IMMUNOLOGICAL INVESTIGATIONS
https://doi.org/10.1080/08820139.2025.2515411

Taylor & Francis
Taylor & Francis Group

RESEARCH ARTICLE

Expression of the Transcription Factor FOXP3 in Human Peripheral Blood B-Cell Subtypes (CD19+CD39+ and CD19 +CD39-) and Evaluation of Their Regulatory Function

A. Cardenas-Juarez[a], E. E. Uresti-Rivera[b,c], F. Ochoa-González[d], F. I. Lira-Hernández[a], E. E. Lara-Ramírez[e,f], J. M. Vargas-Morales[b], B. Rivas-Santiago[a], D. P. Portales-Peréz[b,c], and M. H. García-Hernández[a]

[a]Unidad de Investigación Biomédica, Delegación Zacatecas, Instituto Mexicano del Seguro Social, IMSS; [b]Facultad de Ciencias Químicas, Universidad Autónoma de San Luís Potosí, UASLP, San Luis Potosi, México; [c]Centro de Investigación en Ciencias de la Salud y Biomedicina, Universidad Autónoma de San Luis Potosí, San Luis Potosí, México; [d]Área de Ciencias de la Salud, Universidad Autónoma de Zacatecas, UAZ, Zacatecas, México; [e]Unidad Académica Multidisciplinaria Mante, Universidad Autónoma de Tamaulipas, Mante, México; [f]Laboratorio de Biotecnología Farmacéutica, Centro de Biotecnología Genómica, Instituto Politécnico Nacional, Reynosa, México

ABSTRACT

Introduction: The aim of this study was to evaluate FOXP3 expression in $CD19^+CD39^+$ and $CD19^+CD39^-$ B cells, and to investigate its potential regulatory role.

Methods: Peripheral B cells were obtained from 25 volunteers. FOXP3 expression at the mRNA and protein levels was analyzed in $CD19^+CD39^+$ and $CD19^+CD39^-$ B cells by FACS and RT-qPCR. Suppressive activity was assessed through co-cultures of PBMC with $CD19^+CD39^+$ and $CD19^+CD39^-$ B cells stimulated with anti-CD3/CD28, evaluating T cell proliferation and the percentage of Th1 cells.

Results: The percentage of $CD19^+CD39^+$ $FOXP3^+$ B cells was higher compared to other phenotypes. There was a positive correlation between FOXP3 and CD39 in $CD19^+$ B cells. FOXP3 mRNA was increased in $CD19^+CD39^+$ B cells compared to $CD19^+CD39^-$ B cells. $CD19^+CD39^-$ B cells reduced the proliferation, the percentage of Th1 cells, and expressed higher IL-10 mRNA compared to $CD19^+CD39^+$ B cells. B cell phenotypes were inversely associated with Th1 cells and CRP. $CD19^+CD39^-$ was associated with HOMA-β. $CD19^+CD39^+$ was inversely associated with HbA1c.

Discussion: FOXP3 is expressed on both $CD19^+CD39^-$ and $CD19^+CD39^+$ B lymphocytes. $CD19^+CD39^-$ cells showed high levels of IL-10 and low levels of FOXP3 mRNA. $CD19^+CD39^-$ B cells decreased the Th1 cells and were associated with β-cell function.

KEYWORDS
BMI; CD39; FOXP3; HOMA-B; IL-10

Introduction

The Forkhead box p3 (Foxp3) transcription factor is widely recognized as the master regulator of T regulatory cells (Treg), making its expression a hallmark for identifying and quantifying these cells (Morina et al., 2023). Foxp3 expression has been linked to the downregulation of IFN-γ, IL-4 and IL-10 cytokines (Hori et al., 2003). Mice lacking

CONTACT M. H. García-Hernández mariana.haydee.gh@gmail.com Instituto Mexicano del Seguro Social, IMSS, Unidad de Investigación Biomédica, Delegación Zacatecas, Interior de la Alameda No. 45, Zacatecas, Zac 98000, México
Supplemental data for this article can be accessed online at https://doi.org/10.1080/08820139.2025.2515411

functional Foxp3$^+$ Treg cells exhibit severe autoimmunity (Fontenot et al., 2003), additionally, a diminution of FOXP3$^+$ Treg has been described in multiple human autoimmune diseases (Baecher-Allan & Hafler, 2006). While Foxp3 in mice is a specific marker for Treg cells, capable of driving naïve T cells toward Treg-cell phenotype (Fontenot et al., 2003; Hori et al., 2003), in humans, FOXP3 expression is not always linked to regulatory function. Activated human T cells can transiently express FOXP3 (Allan et al., 2007; Wang et al., 2007) and over expression of FOXP3 in T cells does not induce a suppressive FOXP3$^+$ Treg cells phenotype (Allan et al., 2005; Tran et al., 2007). Interestingly, FOXP3 expression is not restricted to T cells. Studies have reported FOXP3 expression in highly purified CD19$^+$ cells (Vadasz et al., 2015). Moreover, regulatory B cells (Breg), a subset of CD19$^+$CD5$^+$ B cells, are known to express Foxp3 and play critical roles in immunoregulation of T cells (Noh et al., 2012; Park et al., 2016). Foxp3$^+$CD19$^+$ B cells have been shown to attenuate pro-inflammatory cytokines production and enhance Foxp3 expression in CD4$^+$ T cells (Park et al., 2016). Furthermore, reduced percentages of FOXP3$^+$CD19$^+$ cells have been observed in patients with rheumatoid arthritis, with an inverse association to inflammatory markers such as C-reactive protein (CRP) and erythrocyte sedimentation rate (ESR) (Guo et al., 2015).

Breg are a heterogeneous group including different subtypes such as CD24^{High}CD38^{High} Bregs, B10 cells (CD24^{High}CD27$^+$) (Mauri & Menon, 2015). Their activity often relies on IL-10 and interaction with T cells via CD80-CD86 (Blair et al., 2010). Mechanisms that Bregs use to suppress T cell responses include expression of PD-L1, granzyme B, CD39, and CD73 (Lindner et al., 2013; Siewe et al., 2014). CD39 and CD73 are ectonucleotidases that hydrolyze exogenous ATP to adenosine, which in turn suppress T-cell proliferation and cytokine production (Saze et al., 2013). Notably, CD39 expression is directly regulated by Foxp3 (Borsellino et al., 2007), and it has been proposed as a surface marker of Foxp3$^+$ suppressor cells. Similar to FOXP3$^+$ T cells, FOXP3$^+$ B cells may express CD39 and mediate suppression of T cells through a CD39 dependent mechanism (Gandhi et al., 2010). It has been previously reported that CD19$^+$CD39$^+$ B cells have an immunosuppressive activity. Indeed, CD39^{High} B cells suppress T cell activity via adenosine and IL-10 (Figueiro et al., 2016). In this sense, CD19$^+$CD39$^+$ B cells synthesize adenosine whereas that CD19$^+$ B cells lacking CD39 cells do not (Pati et al., 2023). However, it has been described that in peripheral blood from healthy donors CD24^{High}CD38^{High} Bregs lack of expression CD39 determining that CD19$^+$CD39$^-$ cells are a short phenotype of the CD24^{High}CD38^{High} Breg subpopulation (Pati et al., 2023). IL-10 levels are higher in CD19$^+$CD39$^-$B cells compared to CD19$^+$CD39$^+$ B cells (Pati et al., 2023). Regulatory mechanisms in B cells shows parallels to type 1 regulatory T cells (Tr1) which secret high levels of IL-10 but lack Foxp3 expression (Vieira et al., 2004). Therefore, the expression of FOXP3 in CD19$^+$CD39$^-$ and CD19$^+$CD39$^+$ B cells and its regulatory role remain an area of interest.

Given the limited knowledge about FOXP3 expression in CD19$^+$CD39$^+$ and CD19$^+$CD39$^-$ B cells and its possible immunomodulatory activity, in this study we aimed to evaluate the expression of FOXP3 in CD19$^+$CD39$^+$and CD19$^+$CD39$^-$ B cells. Furthermore, we evaluated the suppressive activity of these subsets by analyzing CD4$^+$ T cells proliferation and Th1 cells percentages (IFN-γ$^+$ CD4$^+$ T cells) in co-cultures of PBMC and CD19$^+$CD39$^+$ or CD19$^+$CD39$^-$ B cells. Finally, we explored associations between these subsets (CD19$^+$CD39$^+$ B cells, CD19$^+$CD39$^-$ B cells, and CD19$^+$CD39$^+$ expressing FOXP3 B cells, CD19$^+$ CD39$^-$expressing FOXP3 B cells) and biochemical

parameters, including C-reactive protein (CRP) levels and Th1 cells of individuals enrolled in the study.

Material and methods

Individuals

Peripheral blood samples were drawn from 25 individuals (15 females and 10 males), aged 41 to 65 years, attending the CADIMSS at Instituto Mexicano del Seguro Social (IMSS) in Zacatecas, Zac., Mexico. All participants were non-smokers, without prior diagnosis of chronic diseases. Each assay (flow cytometry, gene expression, co-culture) was performed using cells derived from individual donors, without pooling. Anthropometric and biochemical parameters of the participants are summarized in Table 1. Insulin resistance and pancreatic β-cell functionality were evaluated using the Homeostatic Model Assessment (HOMA) formulae, which is based on the relationship between fasting plasma glucose (FPG) and insulin levels (Matthews et al., 1985). Additionally, the Triglyceride-Glucose (TyG) index, calculated as Ln [fasting triglycerides(mg/dL) × fasting glucose(mg/dL)]/2, was used as a surrogate marker for insulin resistance mediated by triglycerides (TG). Individuals with a history or diagnosis of chronic diseases such as rheumatoid arthritis, hypothyroidism or systemic lupus erythematosus were excluded. The overall study design is shown in Supplementary Figure 1. This study was approved by the Bioethics Committee of the National Commission for Scientific Research of IMSS (project *R*-2018–785–072), and all procedures adhered to the 1964 Helsinki declaration. Written informed consent was obtained from all participants.

Isolation of Peripheral blood mononuclear cell (PBMC)

The blood samples were obtained by peripheral venipuncture, diluted in phosphate-buffered saline (PBS) solution, and placed over a Ficoll-Paque density gradient (GE Healthcare Biosciences, Piscataway, NJ). The PBMC layer was carefully extracted, washed with PBS and evaluated for cell viability using the trypan blue exclusion assay. Viability above 99% was considered acceptable.

Table 1. Anthropometric and metabolic parameters of individuals.

Sex (F/M)	(15/10)	Insulin (UI/mL)	13.7 ± 6.95
Age (years)	52.83 ± 12.10	HDL-c (mg/dL)	51.9 ± 9.26
Weight (kg)	71.16 ± 11.00	TC (mg/dL)	161.4 ± 25.32
Height (m)	1.63 ± 0.09	LDL-c (mg/L)	76.5 ± 24.24
BMI (kg/m2)	26.64 ± 2.57	vLDL (mg/dL)	32.9 ± 538
WC (cm)	85.1 ± 9.65	CRP (mg/L)	4.09 ± 1.62
FPG (mg/dL)	99.6 ± 23.15	TG (mg/dL)	164.7 ± 26.91
HbA1c (%)	6.1 ± 1.62	TyG index	4.8 ± 0.16
HOMA-IR	3.5 ± 2.17		
HOMA-β	171.6 ± 105.12		

Data are presented as mean ± SEM. M, male; F, female; BMI, body mass index; WC, waist circumference; FPG, fasting plasma glucose; HbA1c, glycosylated hemoglobin; TC, total cholesterol; HDL-c, high-density lipoprotein-cholesterol; LDL-c, low-density lipoprotein-cholesterol; TG, triglycerides; CRP, c-reactive protein; TyG, triglyceride-glucose index, HOMA-IR, homeostatic model assessment insulin resistance; HOMA-β, homeostasis model assessment of beta-cell function.

Peripheral IFN-γ+ CD4+ T cells (Th1) evaluation

PBMC were seeded at $2X10^5$ cells/mL and stimulated with an anti-CD3 and anti-CD28 dynabeads (1:1 ratio, bead: cell) (Thermo Fisher Scientific) for 18 hours at 37 °C in a humidified incubator containing 5% CO_2. Brefeldin A (3 μg/mL) was added three hours before the end of the incubation. Stimulated PBMC were surface stained with anti-human CD4 conjugated with fluoresce in isothiocyanate (FITC) for 30 minutes at 4 °C in the dark. Then, PBMC were fixed and permeabilized using a fixation and permeabilization buffers (eBioscience, San Diego, CA, USA) before intracellular stained with anti-IFN-γ conjugated with phycoerythrin (PE) (eBioscience). The cells were acquired using a FACSCanto II flow cytometer (BD Biosciences) and data analysis was performed with DIVA software.

Evaluation of FOXP3 in $CD19^+CD39^+$ and $CD19^+CD39^-$cells

Fresh unstimulated PBMC were surface stained with anti-human CD19 conjugated with FITC (Miltenyi Biotec, San Diego, CA, USA) and anti-human CD39 conjugated with phycoerythrin-cyanine7 (PE-Cy7) (BioLegend, San Diego, CA, USA), then fixed and permeabilized using the FOXP3 Transcription Factor Staining Buffer Kit (Invitrogen), followed by intracellular staining with anti-FOXP3 conjugated with allophycocyanin (APC) (eBioscience). Immunostaining was conducted in accordance with the supplier's instructions. Cells were acquired in a FACSCanto II cytometer, and data were analyzed using DIVA software (BD Biosciences).

Isolation of $CD39^+$ or $CD39^-$ B $CD19^+$ cells

B cells were enriched from PBMC using the B cell Isolation Kit II, Human (Miltenyi Biotec). The purity (>88%) was evaluated by flow cytometry. B cells were immunostained with anti-human CD39-APC antibody (eBioscience). Subsequently, the cells were labeled with anti-APC MicroBeads (Miltenyi Biotec), and B cell subsets were separated from the cell suspension using a MACS Separator. The unlabeled fraction consisted of $CD39^-$ cells, while the APC-labeled fraction contained $CD39^+$ cells. All procedures were performed in accordance with the manufacturer's instructions.

Determination of gene expression by real-time quantitative PCR

To assess the mRNA expression levels of FOXP3 and IL-10 in $CD19^+CD39^+$ and $CD19^+CD39^-$ B cell subsets, total RNA was extracted from these cells using the TRIzol reagent (Invitrogen) according to manufacturer's protocol, followed by ethanol precipitation and quantification via NanoDrop spectrophotometer (Thermo Fisher). RNA integrity was confirmed by agarose gel electrophoresis. One microgram of RNA was reverse-transcribed into complementary DNA (cDNA) using SuperScript II Reverse Transcriptase and random hexamer primers (Invitrogen, Carlsbad, CA, USA), following the manufacturer's protocol. Quantitative real-time PCR (RT-qPCR) was performed using the LightCycler 480 II System (Roche, Indianapolis, IN, USA) with iQ SYBR Green Supermix (Bio-Rad, Hercules, CA, USA). The following gene-specific primers were used: FOXP3: Forward 5′-AGCTGCTCGCACAGATTAC-3′; Reverse 5′-

GTTGAGTGAGGGACAGGATTG-3′. IL-10: Forward 5′-TTTCCCTGACCTCCCTCTAA -3′; Reverse 5′-CGAGACACTGGAAGGTGAATTA-3′. β-actin (reference gene): Forward 5′-TCCACCGCAAATGCTTCT-3′; Reverse 5′-AGCCATGCCAATCTCATCTT-3′ Thermal cycling conditions were: initial denaturation at 95 °C for 3 min, followed by 40 cycles of denaturation at 95 °C for 15 s, and annealing/extension at 60 °C for 60 s. Relative expression levels of the each gene were calculated using the 2^−ΔCt method, normalized to the endogenous reference gene, where ΔCt = (Ct Target gene − Ct reference gene), and β-actin was used as the endogenous control gene. This method is appropriate for comparing normalized expression levels across independent biological samples, as recommended by Schmittgen and Livak (2008) when results are reported as individual data points. Data are presented as mean ± SEM.

Suppression activity of $CD19^+CD39^+$ and $CD19^+CD39^-$ B cells determination

To evaluate the possible suppression activity of $CD19^+CD39^+$ and $CD19^+CD39^-$ B cells the proliferation assay was performed. In brief, PBMC were labeled with 5 µM carboxyfluorescein diacetate (CFSE), co-cultured with $CD19^+CD39^+$ or $CD19^+CD39^-$ B cells at 1:1 ratio and stimulated with anti-CD3 and anti-CD28 dynabeads at 1:1 ratio, bead: cell (Thermo Fisher Scientific). The co-cultures were maintained for 72 hours at 37 °C in a humidified incubator containing 5% CO_2. Subsequently, cells were harvested and immunostained with anti-CD4 conjugated with allophycocyanin (APC). The percentage of divided $CD4^+$ T cells was assessed by FACS. Also, since the inhibition of production of IFN-γ^+ by $CD4^+$ T cells by Breg cells was reported. We decided to evaluate the percentages of IFN-γ producing $CD4^+$ T cells in the cell co-cultures in presence of $CD19^+CD39^+$ and $CD19^+CD39^-$ B cells. For this purpose, PBMC were stimulated with an anti-CD3 and anti-CD28 dynabeads (1:1 ratio, bead: cell) in the presence of $CD19^+CD39^+$ or $CD19^+CD39^-$ B cells (1:1 ratio). The co-cultures were maintained for 18 hours at 37 °C in a humidified incubator containing 5% CO_2. Three hours before the end of the incubation period, brefeldin A (3 µg/mL) was added. The cells were then harvested and immunostained with an anti-human CD4 antibody conjugated to fluorescein isothiocyanate (FITC). Intracellular IFN-γ staining was performed using fixation and permeabilization buffers (eBioscience) and an anti-human IFN-γ antibody conjugated with phycoerythrin (PE). The cells were acquired on FACSCanto II (BD Biosciences) and the percentage of IFN-γ^+ $CD4^+$ T cells was analyzed using DIVA software (BD Biosciences).

Statistical analysis

Statistical analyses were conducted using GraphPad Prism version 5.0 (San Diego, CA, USA). Data distribution was assessed using the Kolmogorov – Smirnov test. Based on the distribution, appropriate parametric or non-parametric tests were applied: Student's t-test or Mann – Whitney U test for comparisons between two groups, and one-way ANOVA or Kruskal – Wallis test for comparisons among three or more groups. All results are expressed as mean ± standard error of the mean (SEM), as indicated in the figure legends and text. A p-value <0.05 was considered statistically significant. To assess associations between cell percentages and inflammatory or

biochemical parameters, Spearman's rank correlation analysis was conducted, and correlation matrix plots were generated using the corrplot package in R. A p-value <0.05 was considered statistically significant in all cases.

Results

FOXP3 expression in B cell populations

The gating strategy to evaluate the expression of FOXP3 in $CD19^+CD39^-$, $CD19^+CD39^+$ B cells and $CD19^-CD39^+$ non-B cells is include Supplementary Figure 2. The percentage of $CD19^+CD39^+$B cells was significantly higher compared to $CD19^+CD39^-$B cells and $CD19^-CD39^+$ non-B cells (Figures 1(a,b)). Additionally, the percentage of $CD19^+CD39^+$ expressing FOXP3 B cells and $CD19^-CD39^+$ expressing FOXP3 non-B cells was elevated compared to the $CD19^+CD39^-$ expressing FOXP3B cells (Figures 1(a,c)). When FOXP3 expression was analyzed based on mean fluorescence intensity (MFI), $CD19^-CD39^+$ expressing FOXP3 non-B cells exhibited the highest levels, significantly surpassing both $CD19^+CD39^+$ expressing FOXP3 B cells and $CD19^+CD39^-$ expressing FOXP3 B cells (Figures 1(a,d)). In fact, the expression of FOXP3 as MFI was similar between $CD19^+CD39^+$ and $CD19^+CD39^-$ populations (Figure 1(d)). We found a direct positive correlation between FOXP3 expression and CD39 expression, both measured as percentages of $CD19^+$ cells (Figure 2(a)). Finally, the FOXP3 mRNA expression was high in $CD19^-CD39^+$ non-B cells compared to both $CD19^+CD39^+$ and $CD19^+CD39^-$ B cells (Figure 2(b)). Notably, $CD19^+CD39^+$ B cells expressed higher FOXP3 mRNA levels than $CD19^+CD39^-$ B cells (Figure 2(b)). These findings suggest that a subset of peripheral blood B cells co-express CD39 and FOXP3 and that FOXP3 expression is positively associated with CD39 in B cells.

Suppressiveactivity of $CD19^+CD39^+$ and $CD19^+CD39^-$ B Cells

To assess the possible suppressive activity of $CD19^+CD39^+$ and $CD19^+CD39^-$ B cells, we performed proliferation assays and measure the percentage of IFN-γ^+ $CD4^+$ T (Th1) cells in co-cultures of PBMC with each B cell phenotype. Interestingly, $CD19^+CD39^-$ B cells significantly reduced the percentage of Th1 cells compared to $CD19^+CD39^+$B cells and the positive control (PBMC αCD3/αCD28) (Figure 2(c)). In contrast, $CD19^+CD39^+$ B cells increased the percentage of Th1 cells compared to the positive control (Figure 2(c)). In CFSE assay an augment in the percentage of divided cells ($CD4^+$ T cells) was observed in PBMC cultures stimulated (positive control) compared to non-stimulated conditions (negative control) (Figure 2(d)). Interestingly, the presence of both $CD19^+CD39^-$ B cells and $CD19^+CD39^+$ B cells in PBMC cultures significantly increased the percentage of divided cells ($CD4^+$ T cells) compared to unstimulated and stimulated conditions (Figure 2(d)). However, $CD19^+CD39^+$ B cells induced greater $CD4^+$ T cell proliferation than $CD19^+CD39^-$ B cells (Figure 2(e)). Finally, IL-10 mRNA expression was higher in $CD19^+CD39^-$ B cells compared to $CD19^+CD39^+$ B cells (Figure 2(f)).

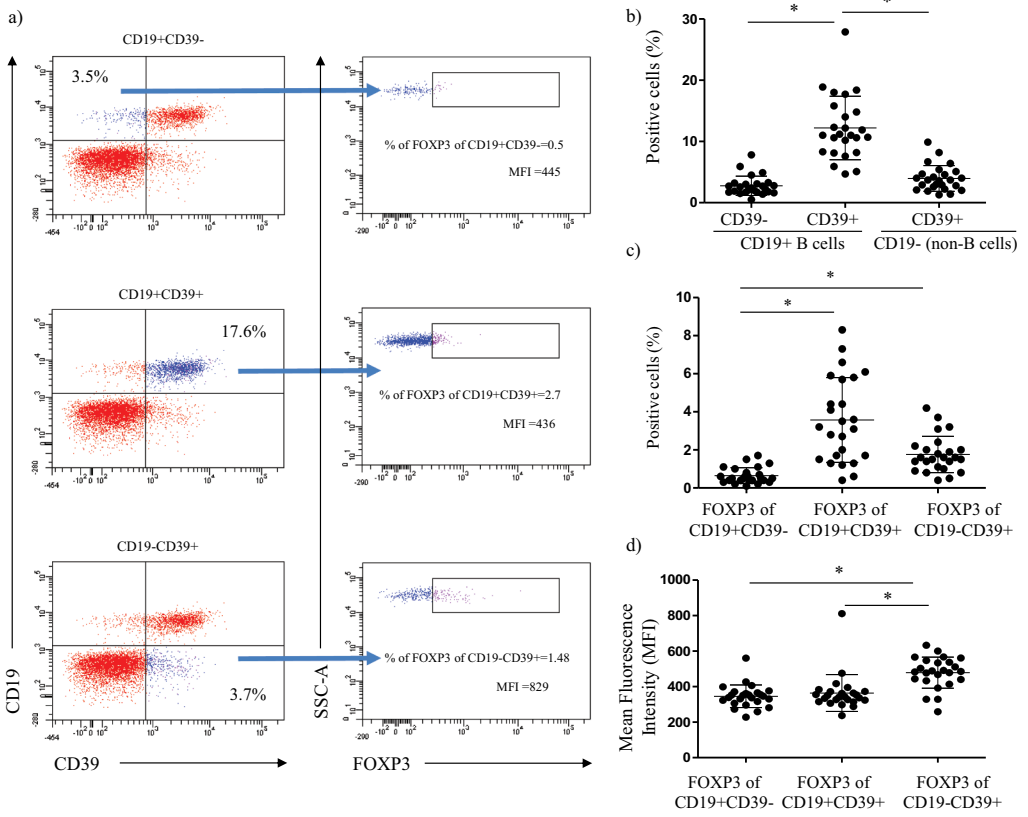

Figure 1. FOXP3 expression in $CD19^{+}CD39^{-}$, $CD19^{+}CD39^{+}$ B cells and $CD19^{-}CD39^{+}$ non-B cells. (a) Representative dot plot showing the gating strategy used to evaluate FOXP3 expression as percentage and the mean florescence intensity (MFI) in $CD19^{+}CD39^{-}$ and $CD19^{+}CD39^{+}$ B cells as well as $CD19^{-}CD39^{+}$ non-B cells. The dot plot illustrates the phenotypes of $CD19^{+}CD39^{-}$, $CD19^{+}CD39^{+}$ and $CD19^{-}CD39^{+}$ with quadrant gates defining each subpopulation. A second dot plot displaying FOXP3 expression as both percentage and MFI of $CD19^{+}CD39^{-}$, $CD19^{+}CD39^{+}$ and $CD19^{-}CD39^{+}$ phenotypes is presented. (b) Percentages of $CD19^{+}CD39^{-}$ B cells ($n = 25$), $CD19^{+}CD39^{+}$ B cells ($n = 25$), and $CD19^{-}CD39^{+}$ (non-B cells) ($n = 25$). (c) FOXP3 expression as percentage of $CD19^{+}CD39^{-}$ B cells ($n = 25$), $CD19^{+}CD39^{+}$ B cells ($n = 25$) and $CD19^{-}CD39^{+}$ non-B cells ($n = 25$). (d) FOXP3 expression as the mean fluorescence intensity (MFI) in $CD19^{+}CD39^{-}$ B cells ($n = 25$), $CD19^{+}CD39^{+}$ B cells ($n = 25$) and $CD19^{-}CD39^{+}$non-B cells ($n = 25$). The cells were acquired on FACSCanto II (BD biosciences), and data were processed using DIVA software (BD Biosciences). Results are presented as mean ± SEM. Statistical significance was evaluated using the Kruskal-wallis test or the t test for nonparametric data, with significant differences indicated by asterisks considering $*p < 0.05$ value.

Correlation analysis

We performed a correlation analysis between B cell phenotypes and inflammatory parameters such as C-reactive protein (CRP) and percentage of Th1 cells. The results revealed an inverse correlation between the percentages of $CD19^{+}CD39^{-}$ B cells and $CD19^{+}CD39^{+}$ B cells and the percentage of Th1 cells (Figure 3). Furthermore, the results showed an inverse correlation between the percentages of $CD19^{+}CD39^{-}FOXP3^{+}$ B cells and $CD19^{+}CD39^{+}FOXP3^{+}$ B cells and the percentage of Th1 cells (Figure 3).

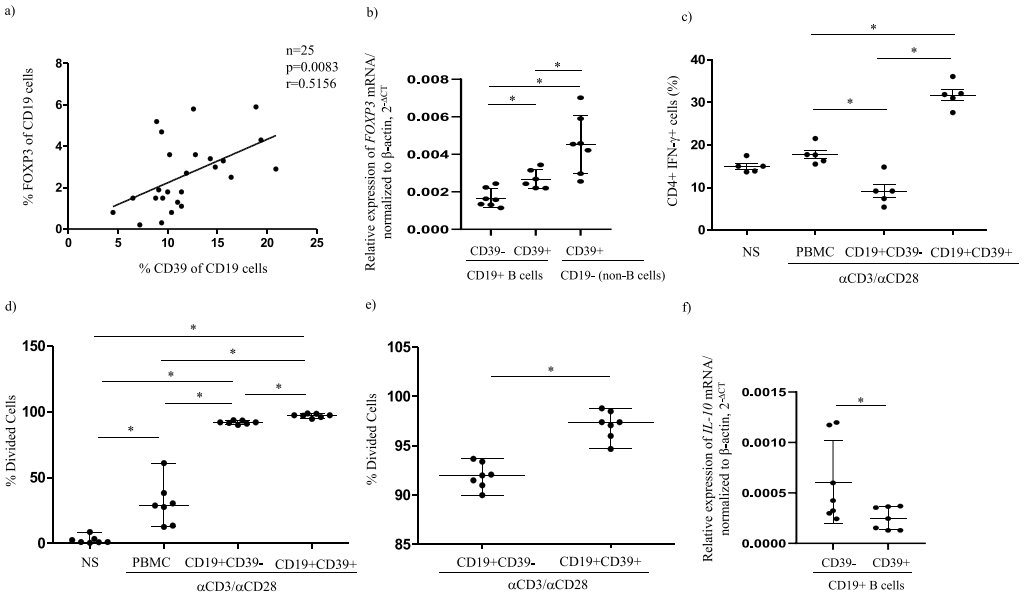

Figure 2. FOXP3 expression and regulatory function of CD19$^+$ CD39$^+$ and CD19$^+$ CD39$^-$ B cells. a) correlation analysis between the percentage of CD39$^+$ cells and FOXP3$^+$ cells within the CD19$^+$ B cell population, as determined by flow cytometry. The sample size (n), p-value, and correlation coefficient (r) are indicated. b) FOXP3 mRNA expression levels in different cell phenotypes ($n = 6$ or 7 per group). c) Percentage of IFN-γ$^+$ CD4$^+$ (Th1) cells in PBMC co-cultures with CD19$^+$ CD39$^-$ or CD19$^+$ CD39$^+$ B cells stimulated with anti-CD3/anti-CD28 microbeads ($n = 5$ per condition). d – e) Percentage of divided CD4$^+$ T cells in PBMC co-cultures with CD19$^+$ CD39$^-$ or CD19$^+$ CD39$^+$ B cells stimulated with anti-CD3/anti-CD28 microbeads. PBMC were stained with CFSE, and after incubation, immunostaining with anti-CD4-APC was performed as described in the materials and methods section. The percentage of divided cells was analyzed within the CD4$^+$ gate ($n = 7$ per condition). f) IL-10 mRNA expression levels in CD19$^+$ CD39$^-$ and CD19$^+$ CD39$^+$ B cells. Cells were acquired using a FACSCanto II flow cytometer (BD biosciences), and data were analyzed with DIVA software (BD Biosciences) ($n = 7$ per group). Results are presented as mean ± SEM. Statistical significance was evaluated using the Kruskal–wallis test or the t test for non-parametric data, with significant differences indicated by asterisks (*$p < .05$).

The percentages of Th1 were positively associated with CRP levels (Figure 3). In addition, the percentages of CD19$^+$CD39$^-$, CD19$^+$CD39$^+$ and CD19$^+$CD39$^-$FOXP3$^+$ B cells were inversely correlated with CRP serum levels (Figure 3). The percentages of CD19$^+$CD39$^-$ B cells were positively related to the functionality of β-cells (HOMA-β values) (Figure 4). HOMA-β values were inversely associated with TyG index, glycated hemoglobin (HbA1c) and FPG levels (Figure 4). The percentages of CD19$^+$CD39$^+$ were inversely associated with HbA1c values, with total cholesterol (TC), LDL-c and vLDL lipoproteins levels (Figure 4). The percentages of CD19$^+$CD39$^-$FOXP3$^+$ were inversely associated with TG, TC, LDL-c and vLDL levels (Figure 4). Also, the percentages of CD19$^+$CD39$^+$ expressing FOXP3 B cells were inversely associated with HbA1c values, TG, total cholesterol, LDL-c and vLDL levels (Figure 4). Finally, the FOXP3 expression as MFI in CD19$^+$CD39$^+$ B cells was inversely associated with body mass index (BMI) and waist circumference (WC) (Figure 4).

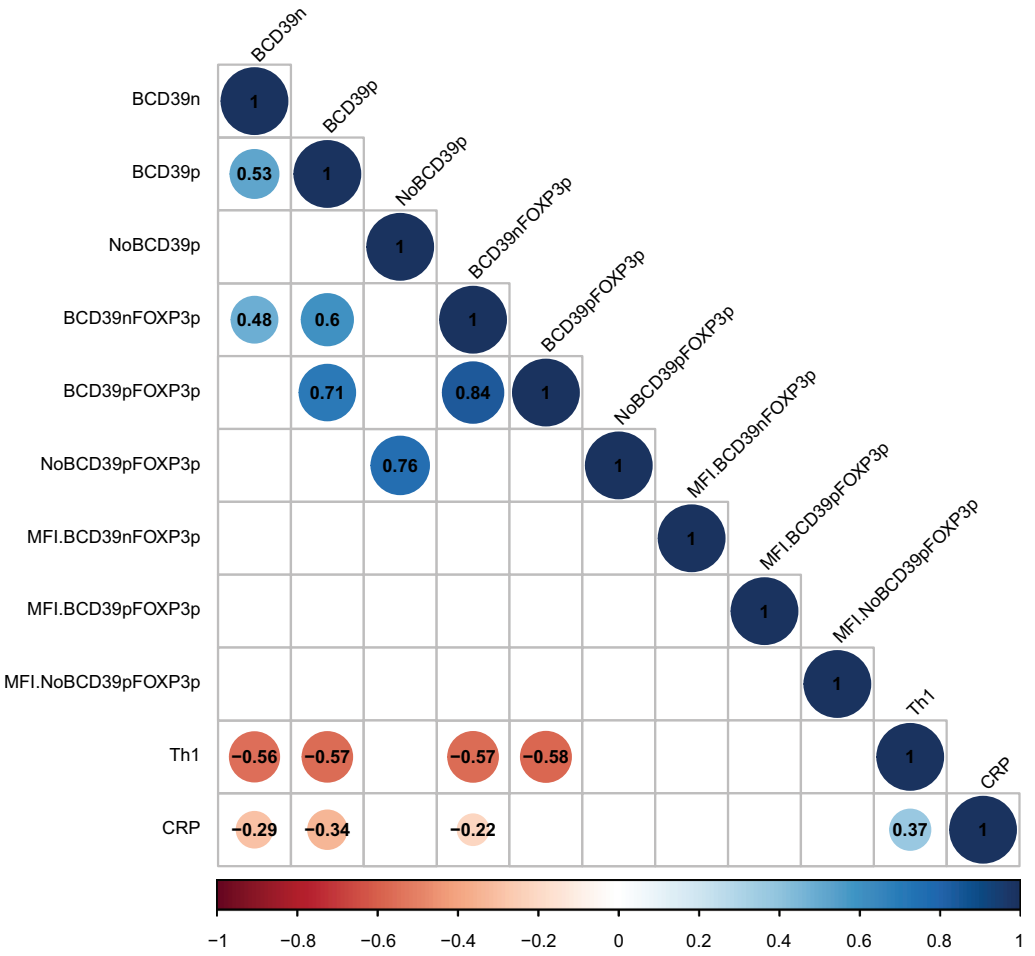

Figure 3. The Spearman correlation matrix of B phenotypes and Th1 cells and CRP serum levels. The matrix includes the following variables: BCD19n ($CD19^+CD39^-$ B cells), BCD39p ($CD19^+CD39^+$ B cells), NoBCD39p ($CD19^-CD39^+$non-B cells), BCD39nFOXP3p (% FOXP3 of $CD19^+CD39^-$ B cells), BCD39pFOXP3p (% FOXP3 of $CD19^+CD39^+$ B cells), NoBCD39pFOXP3p (% FOXP3 of $CD19^-CD39^+$ non-B cells). MFI_BCD39nFOXP3p (MFI FOXP3 of $CD19^+CD39^-$ B cells), MFI_BCD39pFOXP3p (MFI FOXP3 of $CD19^+CD39^+$ B cells), MFI_NoBCD39pFOXP3p (MFI FOXP3 of $CD19^-CD39^+$ non-B cells), Th1 (% IFN-γ^+CD4^+T cells), and serum C-reactive protein levels (CRP). The numbers inside the circles (red or blue) represent the Spearman correlation coefficient (r) for each pair of variables. Statistically significant correlations ($p < 0.05$) are represented by circles (red or blue) located at the intersection of two variables. Red circles indicate an inverse/negative association, while blue circles indicate a direct/positive association. The horizontal scale and color bar at the bottom indicate the direction (negative or positive) of the correlation values.

Discussion

Foxp3 is a transcription factor essential for the development of regulatory T cells and the negative modulation of inflammatory responses (Hori et al., 2003). While traditionally associated with T cells, recent studies have identified FOXP3 expression in specific B cells subsets, such as $CD19^+CD5^+$ B cells, suggesting potential regulatory roles that

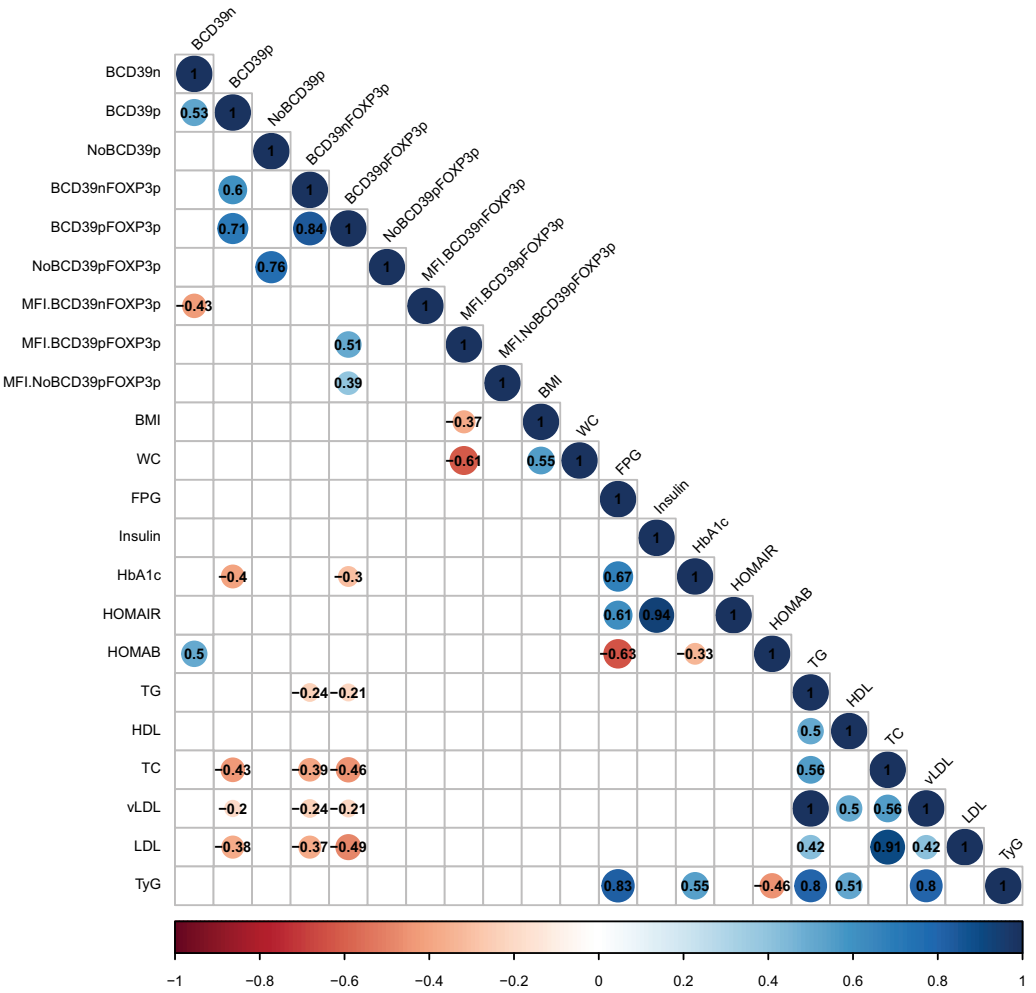

Figure 4. The Spearman correlation matrix for the percentage of B phenotypes and anthropometric and metabolic parameters. The matrix includes the following variables: BCD19n ($CD19^{+}CD39^{-}$ B cells), BCD39p ($CD19^{+}CD39^{+}$ B cells), NoBCD39p ($CD19^{-}CD39^{+}$non-B cells), BCD39nFOXP3p (% FOXP3 of $CD19^{+}CD39^{-}$ B cells), BCD39pFOXP3p (% FOXP3 of $CD19^{+}CD39^{+}$ B cells), NoBCD39pFOXP3p (% FOXP3 of $CD19^{-}CD39^{+}$ non-B cells). MFI_BCD39nFOXP3p (MFI FOXP3 of $CD19^{+}CD39^{-}$ B cells), MFI_BCD39pFOXP3p (MFI FOXP3 of $CD19^{+}CD39^{+}$ B cells), MFI_NoBCD39pFOXP3p (MFI FOXP3 of $CD19^{-}CD39^{+}$ non-B cells). The number within the circles (red or blue) represents the Spearman correlation coefficient (r) value for each pair of variables. Statistically significant correlations ($p < 0.05$) are shown as circles (red or blue) located at the intersection of two variables. Red circles represent an inverse/negative association, while blue circles indicate a direct/positive association. The horizontal scale and color bar at the bottom indicate the direction (negative or positive) of the correlation values.

remain under investigation (Noh et al., 2010). Our findings revealed an increased percentage of the $CD19^{+}CD39^{+}$ B cells expressing FOXP3 in peripheral blood, along with a direct correlation between FOXP3 and CD39 expression in B cells. Consistent with our results, other studies have shown Foxp3 responsible for the expression of the CD39 on mouse T regulatory cells (Treg cells) (Borsellino et al., 2007). Moreover, the

expression of Foxp3 was positively associated with CD39 in $CD4^+CD25^{High}$ T cells (Borsellino et al., 2007). In addition, CD39 expression in Treg cells contributes to immunomodulation through adenosine generation (Deaglio et al., 2007). Taken together, these results suggest that B cells co-expressing FOXP3 and CD39 could contribute to the immune regulation of immune responses. Interestingly, our results showed higher expression of FOXP3 in $CD19^-CD39^+$ non-B lymphocytes compared to B cell subsets ($CD19^+CD39^+$, $CD19^+CD39^-$). Furthermore, in purified cell subpopulations ($CD19^+CD39^+$, $CD19^+CD39^-$ and $CD19^-CD39^+$), FOXP3 mRNA expression was significantly elevated in non-B lymphocytes compared to others. These lymphocytes likely correspond to $CD4^+$ T lymphocytes, as Foxp3 is primarily expressed in the $CD25^+CD4^+$ T population in the periphery (Hori et al., 2003). Despite $CD19^+CD39^+$ and $CD19^+CD39^-$ B cells containing less levels of FOXP3 compared to non-B cells; $CD19^+CD39^+$B cells showed higher FOXP3 mRNA expression than $CD19^+CD39^-$ B cells, raising questions about the functional implications of FOXP3 expression in B cells. Previous studies have identified lymphocytes with low Foxp3 expression, such as $CD25^-CD4^+$ cells, which are part to the $CD45R^{Low}$ B population and have been described as having regulatory activity (Annacker et al., 2001; Hori et al., 2003; Stephens & Mason, 2000). This suggests that the low levels of FOXP3 in B cells do not necessarily exclude their possible regulatory activity.

When evaluating the suppressive activity of $CD19^+CD39^+$ and $CD19^+CD39^-$ B cells, we found that $CD19^+CD39^-$ B cells reduced IFN-γ production by $CD4^+$T cells (Th1 cells) and induced less $CD4^+$ T proliferation compared to $CD19^+CD39^+$ B cells. In line with this, we also observed that $CD19^+CD39^-$ B cells expressed higher levels of IL-10 compared to $CD19^+CD39^+$ B cells, which is consistent with a recent study showing IL-10-dependent suppressive activity of $CD19^+CD39^-$ B cells (Pati et al., 2023). In addition, IL-10 producing B cells were inversely associated with Th1 cells in agreement with our results (Wilde et al., 2013). Finally, it is important to note that there is evidence for the existence of T regulatory cells that do not express FOXP3 but do produce IL-10 (Groux et al., 1997). Although $CD19^+CD39^-$ B cells showed an immunomodulatory effect towards Th1 cells. On the other hand, CD39 exerts its immunomodulatory function by promoting ATP hydrolysis, which, in conjunction with CD73, leads to the production of adenosine (Fletcher et al., 2009). Adenosine, in turn, binds to A_{2A} receptors, thereby down regulating inflammation (Csoka et al., 2008). A previous report showed that $CD19^+CD39^+$ cells produce significant amounts of adenosine (Pati et al., 2023). Similarly, $CD19^+CD39^+$ cells expressed higher levels of FOXP3 mRNA levels compared to $CD19^+CD39^-$ B cells. We therefore speculate that they may have regulatory activities. However, our results showed that $CD19^+CD39^+$ B cells did not reduce IFN-γ production or $CD4^+$ T cell proliferation. In fact, $CD19^+CD39^+$ B cells increase the proliferation of $CD4^+$ T cells. And the proliferation of $CD4^+$ T cells was higher compared to $CD19^+CD39^-$ B cells. Removal of harmful ATP may be a possible function of CD39 expression in $CD19^+$ B cells. Furthermore, PatiS. et al show that $CD19^+CD39^+$ cells lack regulatory activity but produce higher levels of adenosine compared to $CD19^+CD39^-$ B cells (Pati et al., 2023). Although, adenosine may have inhibitory effects, it could also positively influence class switching recombination (CSR) in B cells and promote B cell differentiation and antibody production (Pati et al., 2023). It is worth noting that $CD19^+CD39^+$ cells expressed higher FOXP3 mRNA levels compared to $CD19^+CD39^-$ B cells, but, lacked significant suppressive activity (at least those evaluated in this study); therefore, we suggest that FOXP3 expression

could be associated with the CD39 expression on B cells and with the responsiveness of $CD19^+CD39^+$ B cells, but not directly correlated with the regulatory function. In support of this, FOXP3 expression in human cells alone is not sufficient to induce regulatory T cell activity or to identify regulatory T cells (Wang et al., 2007).

Finally, our correlation analysis showed an inverse association between $CD19^+CD39^-$B cells and $CD19^+CD39^+$ B cells, as well as between $CD19^+CD39^+$B cells expressing FOXP3 and $CD19^+CD39^-$ B cells expressing FOXP3 with inflammatory markers like the percentage of Th1 cells and the levels of C-reactive protein (CRP). Additionally, the percentage of Th1 cells was positively associated with CRP levels. CRP plays a role in host defense promoting phagocytosis and complement activation. In the context of low-grade inflammation, even slightly elevated CRP levels can be harmful (Ridker et al., 2013). Previous studies have demonstrated that the increase of CRP was associated with activation of Th17 cells and with inhibition of $CD4^+$ $Foxp3^+$ T lymphocytes (Zu & Zhang, 2022). In this context, we decided to analyze whether its levels were associated with the percentages of B subpopulations evaluated in this study. Rheumatoid arthritis (RA) patients have a reduced percentageof $CD19^+FOXP3^+$ B cells, which is negatively associated with the disease activity indicators of erythrocyte sedimentation rate (ESR) and CRP. Rheumatoid arthritis has long been classified as a Th1 mediated disease (Bazzazi et al., 2018); in this sense, the reduction in $CD19^+FOXP3^+$ Breg cells has been associated with Th1 mediated immunopathology (Wilde et al., 2013). An inverse association between FOXP3 expression as MFI in $CD19^+CD39^+$B cells and BMI and waist circumference (WC) was also observed. In addition, the percentage of the $CD19^+CD39^-$ B cells were directly associated with the β-cell functionality (HOMA-β). And the β-cell functionality was inversely associated with TyG, HbA1c and FPG. In previous studies we observed a decrease in the percentage of Bregs ($CD19^+CD27^+CD38^{High}$ and $CD19^+CD24^{High}CD38^{High}$) in obese individuals (BMI >30 Kg/m^2), and obese individuals also showed increased IL-17 and IFN-γ levels in $CD4^+$ T cell supernatants (Garcia-Hernandez et al., 2018). Furthermore, previous results suggest a direct correlation between the percentage of $CD19^+CD24^+CD38^+$ Breg cells and HOMA-β levels in patients with type 2 diabetes (T2D) (Mendez-Frausto et al., 2021). In this study, the T2D patients also showed increased levels of IL-6, increased percentage of $IL\text{-}17^+$ and $IL\text{-}17^+IFN\text{-}\gamma^+$ T cells and decreased levels of IL-10 and of the percentage of $CD19^+IL\text{-}10^+$ B cells (Mendez-Frausto et al., 2021). Taken together these results suggest that multiple phenotypes of B cells may be involved in the pathology of obesity and T2D. Future studies should investigate the potential role of these phenotypes in inflammatory and/or autoimmune diseases.

Conclusion

This study highlights the differential expression of FOXP3 in $CD19^+CD39^-$ and $CD19^+CD39^+$ B subpopulations, revealing a complex interplay between these subsets in immune regulation. While FOXP3 expression was less abundant in B cells compared to non-B $CD39^+$ lymphocytes, its presence may contribute to the phenotypic characteristics of B cells. We suggest that FOXP3 expression in $CD19^+CD39^+$ B cells appears to be associated with enhancing their ability to induce the immune response and to avoid the deleterious effects of ATP on cells. Conversely, our results indicate that $CD19^+CD39^-$ B cells have a suppressive function and are characterized by increased IL-10 production and low levels

of FOXP3. We also observed that B cell phenotypes were inversely associated with inflammatory markers. And $CD19^{+}CD39^{-}$ B cells were associated with metabolic parameters such as β-cell functionality and in turn with glycemic control and insulin resistance. The precise role of FOXP3 in B cell function remains to be fully elucidated, highlighting the need for further research to understand its implications in immune regulation.

Acknowledgments

CJA, UREE and MHGH made substantial contributions to the conception or design of the work; DPPP, VMJM, LREE, OGF, BRS contribute with the acquisition, analysis, or interpretation of data for the work; and CJA, UREE and MHGH drafting the work. UREE reviewing it critically for important intellectual content. CJA, UREE DPPP, VMJM, LREE, OGF, BRS and MHGH made the final approval of the version to be published. All authors agreed to be accountable for all aspects of the work in ensuring that questions related to the accuracy or integrity of any part of the work were appropriately investigated and resolved.

Disclosure statement

No potential conflict of interest was reported by the author(s).

Funding

The research reported in this manuscript was supported by a grant from the FONDO DE INVESTIGACION EN SALUD, Mexican Institute of Social Security (R-2018-785-072) to Garcia-Hernandez MH.

Author contributions

CRediT: **A. Cardenas-Juarez:** Conceptualization, Data curation, Formal analysis, Investigation, Methodology, Software, Writing – original draft, Writing – review & editing; **E. E. Uresti-Rivera:** Formal analysis, Methodology, Writing – review & editing; **F. Ochoa-González:** Visualization, Writing – review & editing; **F. I. Lira-Hernández:** Methodology, Writing – review & editing; **E. E. Lara-Ramírez:** Data curation, Formal analysis, Software, Writing – review & editing; **J. M. Vargas-Morales:** Writing – review & editing; **B. Rivas-Santiago:** Formal analysis, Investigation, Writing – review & editing; **D. P. Portales-Peréz:** Formal analysis, Investigation, Writing – review & editing; **M. H. García-Hernández:** Conceptualization, Data curation, Formal analysis, Funding acquisition, Investigation, Methodology, Project administration, Resources, Software, Supervision, Validation, Visualization, Writing – original draft, Writing – review & editing.

Ethics statement

The bioethical committee of the National Commission for Scientific Research of IMSS (project *R*-2018–785–072) approved this study. All procedures involving human participants were in accordance with the 1964 Helsinki declaration and its later amendments or comparable ethical standards. All subjects signed a written informed consent before their inclusion in the study.

ORCID

M. H. García-Hernández http://orcid.org/0000-0002-9244-5706

References

Allan, S. E., Crome, S. Q., Crellin, N. K., Passerini, L., Steiner, T. S., Bacchetta, R., Roncarolo, M. G., & Levings, M. K. (2007). Activation-induced FOXP3 in human T effector cells does not suppress proliferation or cytokine production. *International Immunology*, *19*(4), 345–354. https://doi.org/10.1093/intimm/dxm014

Allan, S. E., Passerini, L., Bacchetta, R., Crellin, N., Dai, M., Orban, P. C., Ziegler, S. F., Roncarolo, M. G., & Levings, M. K. (2005). The role of 2 FOXP3 isoforms in the generation of human CD4+ Tregs. *Journal of Clinical Investigation*, *115*(11), 3276–3284. https://doi.org/10.1172/JCI24685

Annacker, O., Pimenta-Araujo, R., Burlen-Defranoux, O., Barbosa, T. C., Cumano, A., & Bandeira, A. (2001). CD25+ CD4+ T cells regulate the expansion of peripheral CD4 T cells through the production of IL-10. *The Journal of Immunology*, *166*(5), 3008–3018. https://doi.org/10.4049/jimmunol.166.5.3008

Baecher-Allan, C., & Hafler, D. A. (2006). Human regulatory T cells and their role in autoimmune disease. *Immunological Reviews*, *212*(1), 203–216. https://doi.org/10.1111/j.0105-2896.2006.00417.x

Bazzazi, H., Aghaei, M., Memarian, A., Asgarian-Omran, H., Behnampour, N., & Yazdani, Y. (2018). Th1-Th17 ratio as a new insight in rheumatoid arthritis disease. *Iranian Journal of Allergy, Asthma, and Immunology*, *17*(1), 68–77.

Blair, P. A., Norena, L. Y., Flores-Borja, F., Rawlings, D. J., Isenberg, D. A., Ehrenstein, M. R., & Mauri, C. (2010). CD19(+)CD24(hi)CD38(hi) B cells exhibit regulatory capacity in healthy individuals but are functionally impaired in systemic Lupus Erythematosus patients. *Immunity*, *32*(1), 129–140. https://doi.org/10.1016/j.immuni.2009.11.009

Borsellino, G., Kleinewietfeld, M., DiMitri, D., Sternjak, A., Diamantini, A., Giometto, R., Hopner, S., Centonze, D., Bernardi, G., Dell'acqua, M. L., Rossini, P. M., Battistini, L., Rotzschke, O., & Falk, K. (2007). Expression of ectonucleotidase CD39 by Foxp3+ Treg cells: Hydrolysis of extracellular ATP and immune suppression. *Blood*, *110*(4), 1225–1232. https://doi.org/10.1182/blood-2006-12-064527

Csoka, B., Himer, L., Selmeczy, Z., Vizi, E. S., Pacher, P., Ledent, C., Deitch, E. A., Spolarics, Z., Nemeth, Z. H., & Hasko, G. (2008). Adenosine A2A receptor activation inhibits T helper 1 and T helper 2 cell development and effector function. *FASEB Journal: Official Publication of the Federation of American Societies for Experimental Biology*, *22*(10), 3491–3499. https://doi.org/10.1096/fj.08-107458

Deaglio, S., Dwyer, K. M., Gao, W., Friedman, D., Usheva, A., Erat, A., Chen, J. F., Enjyoji, K., Linden, J., Oukka, M., Kuchroo, V. K., Strom, T. B., & Robson, S. C. (2007). Adenosine generation catalyzed by CD39 and CD73 expressed on regulatory T cells mediates immune suppression. *Journal of Experimental Medicine*, *204*(6), 1257–1265. https://doi.org/10.1084/jem.20062512

Figueiro, F., Muller, L., Funk, S., Jackson, E. K., Battastini, A. M., & Whiteside, T. L. (2016). Phenotypic and functional characteristics of CD39(high) human regulatory B cells (Breg). *Oncoimmunology*, *5*(2), e1082703. https://doi.org/10.1080/2162402X.2015.1082703

Fletcher, J. M., Lonergan, R., Costelloe, L., Kinsella, K., Moran, B., O'Farrelly, C., Tubridy, N., & Mills, K. H. (2009). CD39+Foxp3+ regulatory T cells suppress pathogenic Th17 cells and are impaired in multiple sclerosis. *The Journal of Immunology*, *183*(11), 7602–7610. https://doi.org/10.4049/jimmunol.0901881

Fontenot, J. D., Gavin, M. A., & Rudensky, A. Y. (2003). Foxp3 programs the development and function of CD4+CD25+ regulatory T cells. *Nature Immunology*, *4*(4), 330–336. https://doi.org/10.1038/ni904

Gandhi, R., Kumar, D., Burns, E. J., Nadeau, M., Dake, B., Laroni, A., Kozoriz, D., Weiner, H. L., & Quintana, F. J. (2010). Activation of the aryl hydrocarbon receptor induces human type 1 regulatory T cell-like and Foxp3(+) regulatory T cells. *Nature Immunology*, *11*(9), 846–853. https://doi.org/10.1038/ni.1915

Garcia-Hernandez, M. H., Rodriguez-Varela, E., Garcia-Jacobo, R. E., Hernandez De la Torre, M., Uresti-Rivera, E. E., Gonzalez-Amaro, R., & Portales-Perez, D. P. (2018). Frequency of regulatory B cells in adipose tissue and peripheral blood from individuals with overweight, obesity and

normal-weight. *Obesity Research & Clinical Practice*, *12*(6), 513–519. https://doi.org/10.1016/j.orcp.2018.07.001

Groux, H., O'Garra, A., Bigler, M., Rouleau, M., Antonenko, S., de Vries, J. E., & Roncarolo, M. G. (1997). A CD4+ T-cell subset inhibits antigen-specific T-cell responses and prevents colitis. *Nature*, *389*(6652), 737–742. https://doi.org/10.1038/39614

Guo, Y., Zhang, X., Qin, M., & Wang, X. (2015). Changes in peripheral CD19(+)Foxp3(+) and CD19(+)TGFβ(+) regulatory B cell populations in rheumatoid arthritis patients with interstitial lung disease. *Journal of Thoracic Disease*, *7*(3), 471–477. https://doi.org/10.3978/j.issn.2072-1439.2015.02.11

Hori, S., Nomura, T., & Sakaguchi, S. (2003). Control of regulatory T cell development by the transcription factor Foxp3. *Science*, *299*(5609), 1057–1061. https://doi.org/10.1126/science.1079490

Lindner, S., Dahlke, K., Sontheimer, K., Hagn, M., Kaltenmeier, C., Barth, T. F., Beyer, T., Reister, F., Fabricius, D., Lotfi, R., Lunov, O., Nienhaus, G. U., Simmet, T., Kreienberg, R., Moller, P., Schrezenmeier, H., & Jahrsdorfer, B. (2013). Interleukin 21-induced granzyme B-expressing B cells infiltrate tumors and regulate T cells. *Cancer Research*, *73*(8), 2468–2479. https://doi.org/10.1158/0008-5472.CAN-12-3450

Matthews, D. R., Hosker, J. P., Rudenski, A. S., Naylor, B. A., Treacher, D. F., & Turner, R. C. (1985). Homeostasis model assessment: Insulin resistance and beta-cell function from fasting plasma glucose and insulin concentrations in man. *Diabetologia*, *28*(7), 412–419. https://doi.org/10.1007/BF00280883

Mauri, C., & Menon, M. (2015). The expanding family of regulatory B cells. *International Immunology*, *27*(10), 479–486. https://doi.org/10.1093/intimm/dxv038

Mendez-Frausto, G., Romero-Aguilera, G., Sanchez-Gutierrez, R., Garcia-Jacobo, R. E., Lara-Ramirez, E. E., Uresti-Rivera, E. E., Gonzalez-Amaro, R., Enciso-Moreno, J. A., & Garcia-Hernandez, M. H. (2021). B regulatory cells associated with changes in biochemical and inflammatory parameters in normal-glycemic individuals, pre-diabetes and T2DM patients. *Diabetes Research & Clinical Practice*, *173*, 108692. https://doi.org/10.1016/j.diabres.2021.108692

Morina, L., Jones, M. E., Oguz, C., Kaplan, M. J., Gangaplara, A., Fitzhugh, C. D., Kanakry, C. G., Shevach, E. M., & Buszko, M. (2023). Co-expression of Foxp3 and Helios facilitates the identification of human T regulatory cells in health and disease. *Frontiers in Immunology*, *14*, 1114780. https://doi.org/10.3389/fimmu.2023.1114780

Noh, J., Choi, W. S., Noh, G., & Lee, J. H. (2010). Presence of Foxp3-expressing CD19(+)CD5(+) B cells in human peripheral blood mononuclear cells: Human CD19(+)CD5(+)Foxp3(+) regulatory B cell (Breg). *Immune Network*, *10*(6), 247–249. https://doi.org/10.4110/in.2010.10.6.247

Noh, J., Noh, G., Kim, H. S., Kim, A. R., & Choi, W. S. (2012). Allergen-specific responses of CD19(+)CD5(+)Foxp3(+) regulatory B cells (Bregs) and CD4(+)Foxp3(+) regulatory T cell (Tregs) in immune tolerance of cow milk allergy of late eczematous reactions. *Cell Immunol*, *274*(1–2), 109–114. https://doi.org/10.1016/j.cellimm.2012.01.005

Park, M. K., Jung, Y. O., Lee, S. Y., Lee, S. H., Heo, Y. J., Kim, E. K., Oh, H. J., Moon, Y. M., Son, H. J., Park, M. J., Park, S. H., Kim, H. Y., Cho, M. L., & Min, J. K. (2016). Amelioration of autoimmune arthritis by adoptive transfer of Foxp3-expressing regulatory B cells is associated with the Treg/Th17 cell balance. *Journal of Translational Medicine*, *14*(1), 191. https://doi.org/10.1186/s12967-016-0940-7

Pati, S., Mukherjee, S., Dutta, S., Guin, A., Roy, D., Bose, S., Paul, S., Saha, S., Bhattacharyya, S., Datta, P., Chakraborty, J., Sarkar, D. K., & Sa, G. (2023). Tumor-associated CD19+CD39- B regulatory cells deregulate class-switch recombination to suppress antibody responses. *Cancer Immunology Research*, *11*(3), 364–380. https://doi.org/10.1158/2326-6066.CIR-21-1073

Ridker, P. M., Kastelein, J. J., Genest, J., & Koenig, W. (2013). C-reactive protein and cholesterol are equally strong predictors of cardiovascular risk and both are important for quality clinical care. *European Heart Journal*, *34*(17), 1258–1261. https://doi.org/10.1093/eurheartj/eht022

Saze, Z., Schuler, P. J., Hong, C. S., Cheng, D., Jackson, E. K., & Whiteside, T. L. (2013). Adenosine production by human B cells and B cell-mediated suppression of activated T cells. *Blood*, *122*(1), 9–18. https://doi.org/10.1182/blood-2013-02-482406

Siewe, B., Wallace, J., Rygielski, S., Stapleton, J. T., Martin, J., Deeks, S. G., Landay, A., & Unutmaz, D. (2014). Regulatory B cells inhibit cytotoxic T lymphocyte (CTL) activity and elimination of infected CD4 T cells after in vitro reactivation of HIV latent reservoirs. *PLOS ONE*, *9*(4), e92934. https://doi.org/10.1371/journal.pone.0092934

Stephens, L. A., & Mason, D. (2000). CD25 is a marker for CD4+ thymocytes that prevent autoimmune diabetes in rats, but peripheral T cells with this function are found in both CD25+ and CD25- subpopulations. *The Journal of Immunology*, *165*(6), 3105–3110. https://doi.org/10.4049/jimmunol.165.6.3105

Tran, D. Q., Ramsey, H., & Shevach, E. M. (2007). Induction of FOXP3 expression in naive human CD4+FOXP3 T cells by T-cell receptor stimulation is transforming growth factor-beta dependent but does not confer a regulatory phenotype. *Blood*, *110*(8), 2983–2990. https://doi.org/10.1182/blood-2007-06-094656

Vadasz, Z., Peri, R., Eiza, N., Slobodin, G., Balbir-Gurman, A., & Toubi, E. (2015). The expansion of CD25 high IL-10 high FoxP3 high B regulatory cells is in association with SLE disease activity. *Journal of Immunology Research*, *2015*, 254245. https://doi.org/10.1155/2015/254245

Vieira, P. L., Christensen, J. R., Minaee, S., O'Neill, E. J., Barrat, F. J., Boonstra, A., Barthlott, T., Stockinger, B., Wraith, D. C., & O'Garra, A. (2004). IL-10-secreting regulatory T cells do not express Foxp3 but have comparable regulatory function to naturally occurring CD4+CD25+ regulatory T cells. *The Journal of Immunology*, *172*(10), 5986–5993. https://doi.org/10.4049/jimmunol.172.10.5986

Wang, J., Ioan-Facsinay, A., van der Voort, E. I., Huizinga, T. W., & Toes, R. E. (2007). Transient expression of FOXP3 in human activated nonregulatory CD4+ T cells. *European Journal of Immunology*, *37*(1), 129–138. https://doi.org/10.1002/eji.200636435

Wilde, B., Thewissen, M., Damoiseaux, J., Knippenberg, S., Hilhorst, M., van Paassen, P., Witzke, O., & Cohen Tervaert, J. W. (2013). Regulatory B cells in ANCA-associated vasculitis. *Annals of the Rheumatic Diseases*, *72*(8), 1416–1419. https://doi.org/10.1136/annrheumdis-2012-202986

Zu, D. M., & Zhang, L. (2022). Assessment of mechanisms of infectious pneumonia based on expression of fibrinogen, procalcitonin, high-sensitivity C-reactive protein expression, T helper 17 cells, regulatory T cells interleukin-10, and interleukin-17. *Translational Pediatrics*, *11*(1), 73–84. https://doi.org/10.21037/tp-21-565

ACS OMEGA

Open Access

http://pubs.acs.org/journal/acsodf

Article

Consensus Virtual Screening and *Ex Vivo* Evaluation of Novel JAK2/STAT1,3 Inhibitors

Mariana H. García-Hernández, Elena Jaime-Sánchez, Abraham Cardenas-Juarez, Carmen J. Serrano, Lenci K. Vázquez-Jiménez, Gildardo Rivera, Juan E. López-Ramos, and Edgar E. Lara-Ramírez*

Cite This: *ACS Omega* 2025, 10, 51297−51308

Read Online

ACCESS | Metrics & More | Article Recommendations | Supporting Information

ABSTRACT: The Janus kinase (JAK)/signal transducer and activator of transcription (STAT) signaling pathway is a key therapeutic target for inflammatory and neoplastic diseases such as rheumatoid arthritis (RA) and certain types of cancer. Although several inhibitors have been approved for medical use, their associated adverse effects limit their therapeutic use. Therefore, it is essential to search for new, safer inhibitors. In this work, we applied computer-aided approaches consisting of consensus molecular docking and molecular dynamics using the JAK2 structure as a filter of 3330 drugs approved by the Food and Drug Administration (FDA) retrieved from the ZINC20 database. The best predicted virtual hits were evaluated in an *ex vivo* STAT1,3 phosphorylation functional model in human lymphocytes induced by IL-6 stimulation. The docking-based consensus-scoring strategy allowed the selection of pitavastatin (PIT), eltrombopag (ELT), flavoxate (FLA), and empagliflozin (EMP) as potential JAK2 inhibitors. Their stability was confirmed by running independent molecular dynamics simulations of 200 ns in triplicate, which showed comparable stability with baricitib (BAR) and showed that hydrogen bonding is involved in their binding with key amino acids of the ATP-binding site. In the *ex vivo* evaluations, pitavastatin (0.5004 μM), eltrombopag (0.2548 μM), flavoxate (0.1536 μM), and empagliflozin (0.2548 μM) affected the phosphorylation of downstream STAT1 and STAT3 signaling molecules, similarly to tofacitinib citrate (TOF) (1.2 nM). These results encourage further in-depth preclinical experiments aimed at exploring the additional effects of the JAK2-STAT1/3 signaling pathway.

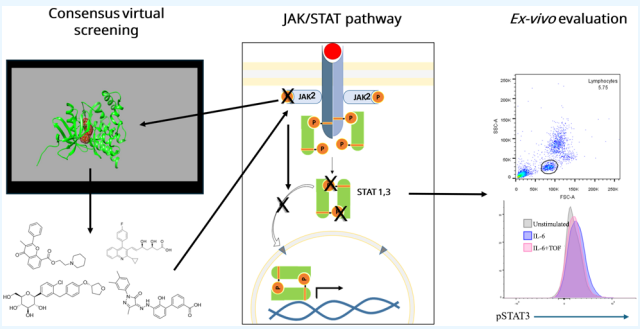

INTRODUCTION

The Janus kinase (JAK) signal transducer and activator of transcription (STAT) signaling pathway is involved in important processes of normal human homeostasis that include blood cell differentiation, metabolism, and immune regulation.[1] This pathway consists of several molecules embedded in the cell membrane and the cytosol. The JAK component is composed of four proteins, JAK1, 2, 3, and TYK2. The STAT component consists of the proteins STATs 1, 2, 3, 4, 5A, 5B, and 6. When this pathway is dysregulated, it produces several immune-mediated pathogenic processes that have been associated with the development of rheumatoid arthritis (RA), different types of blood cancer, intestinal inflammatory diseases, and dermatological diseases.[2] Thus, this pathway is an important drug target for the development of new treatments for important human diseases.

Currently, several nonselective, pan inhibitors and specific inhibitors of the JAK component are used for the treatment of several chronic human diseases.[3] For example, ruxolitinib, an inhibitor of JAK1 and JAK2, first approved for the treatment of myelofibrosis in 2011,[4] was later approved for the treatment of polycythemia vera in 2014.[5] Tofacitinib, a pan inhibitor of the three JAKs and TIK2, was the second inhibitor approved in 2012 for the treatment of RA;[6] then, this drug was approved for the treatment of psoriatic arthritis (2017), ulcerative colitis (2018), and juvenile idiopathic arthritis (2021).[7] Baricitinib (BAR) is another inhibitor of JAK1 and JAK2. It was approved for the treatment of moderate to severe RA[8] and was recently approved for the treatment of alopecia areata[9] and COVID-19.[10] Therefore, it is evident that JAK components are suitable disease-repurposing drug targets.

Among the JAK/STAT components, the JAK2 and its related STAT1 and STAT3 signaling molecules play a prominent role in normal and abnormal immune responses. These molecules are activated by specific cytokines. For example, when the IL-6 cytokine binds to the transmembrane receptor in cells, it induces homodimerization of the gp130

Received: July 8, 2025
Revised: September 29, 2025
Accepted: October 15, 2025
Published: October 24, 2025

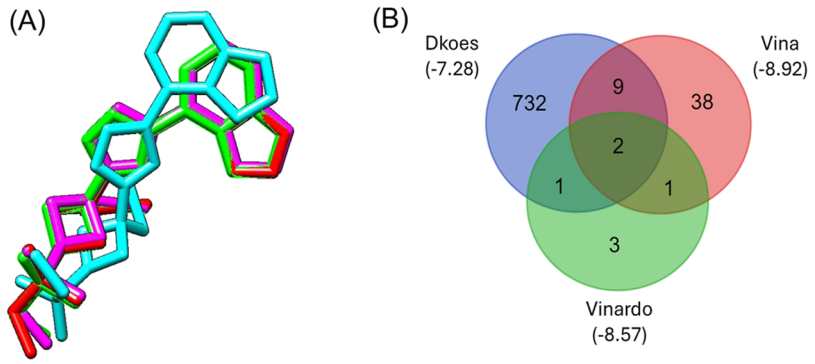

Figure 1. (A) Docking reproducibility for baricitinib (red) using Dkoes (cyan), Vina (green), and Vinardo (magenta) scoring functions. (B) Venn diagram showing the best virtual hits ranked based on the predicted binding energy (kcal/mol) for each scoring function.

subunit, leading to the activation (phosphorylation) of JAK2, which, in turn, phosphorylates the tyrosine-based motifs of SH2-containing substrates such as STAT1 and STAT3 and may itself or through associated JAK kinases become phosphorylated on tyrosine residues.[11] Subsequently, phosphorylated STATs dissociate from gp130 and dimerize with themselves or with related STATs and translocate to the nucleus to promote the transcription of genes.[12] The deregulation of the phosphorylation of JAK2/STAT1,3 molecules is related to distinct chronic inflammatory and neoplastic processes. Therefore, these molecules represent potentially attractive targets for immunosuppression in inflammatory and neoplastic human diseases.[13] JAK2 inhibitors act through blocking the ATP-binding site located in the kinase JH domain, impeding the subsequent STAT1,3 signaling cascade.[14] However, due to the vital importance of this signaling pathway, the use of these drugs had severe adverse effects. Therefore, it is necessary to continue searching for new safe inhibitors of JAK2/STAT1,3 signaling.

In this work, we performed a consensus docking structure-based approach to identify potential JAK2 inhibitors in the Food and Drug Administration (FDA) data set retrieved from the ZINC20 database. Then, molecular dynamics simulations were performed to confirm the most stable ligand-JAK2 complexes for *ex vivo* evaluations. Stable JAK2 binders were tested on a flow cytometry experiment using human leukocytes that confirmed their effects on the phosphorylation of downstream STAT1 and STAT3 signaling molecules.

RESULTS

Consensus Virtual Screening Identifies Potential JAK2 Binders. In this work, we used the Vina, Vinardo, and Dkoes scoring functions available on the Smina software.[15] These scores were used to evaluate the baricitinib binding pose reproducibility to set the cutoff values to identify the best binders among the used scoring functions. The pose reproducibility (Figure 1A) using Vina (DockRMSD = 0.376) and Vinardo scores (DockRMSD = 0.305) was similar and better than the Dkoes scoring function (DockRMSD = 1.8).

The highest number of FDA best virtual hits (Figure 1B) was produced with the Dkoes score (n = 744 < −7.28 kcal/mol), followed by the Vina score (n = 50 < −8.982 kcal/mol), and finally the Vinardo score (n = 7 < −8.57). The 3 scoring functions shared 13 compounds; thus, we decided to analyze those compounds with more detail, including the 3 exclusively produced by the Vinardo score, which was a more stringent scoring function (Figure 1B).

The final 16 selected compounds were ranked according to the consensus binding score (Tables 1 and S1). The best binders were desozine (ZINC000003830682), flavoxate (ZINC000000608382), pitavastin (ZINC000001534965), and empagliflozin (ZINC000036520252), which showed a better consensus score than baricitinib (ZINC000073069247). It was interesting that eltrombopag (ELT) (ZINC000011679756) was ranked in a better place than ruxolitinib (ZINC000043207851), just below baricitinib. Considering those observations, these compounds were selected for further binding pose interaction analysis in comparison with baricitinib.

Chemical Diversity of the Selected Binders Contributes to the Binding Mode Interaction. The top-ranked selected compounds showed diverse chemical structures. They showed polycyclic rings with amines, esters, ethers, nitriles, and sulfonamides as functional groups (Table 1 and Figure 2); for example, the best-ranked compound dezocine, a synthetic opioid, showed a rigid polycyclic fused ring in its chemical structure. This compound interacts mainly through hydrophobic interactions with the ATP-binding site and has one hydrophilic interaction with the amino acid Arg980 (Figure 2A). The other compounds also showed that the hydrophobic interaction dominates the binding poses with two or three hydrophilic interactions (Figure 2B−E). For example, the flavoxate benzopyrane moiety is anchored to Leu932 located at the hinge region through a hydrogen bond, like baricitinib (Figure 2B,E). This Leu932 hydrogen bonding is also observed with the chloride ion of empagliflozin (Figure 2D). Eltrombopag and pitavastatin (PIT) compounds also interact with Leu932 through hydrophobic interactions; in general, all of them shared similar amino acid interactions (red circles in Figure 2A−E), including Leu855, Gly856 of the P-loop, and Asp994 of the DFG motif, important for the known inhibitory mechanism of the approved JAK2 inhibitors.[16]

Molecular Dynamics Analysis. The selected top binders, including baricitinib (BAR) and eltrombopag coupled to the JAK2 receptor, were subjected to a first molecular simulation (MD) of 100 ns to evaluate their stabilization over time in a real water simulated environment. The values of the root mean square deviation (RMSD) (Figures S1 and 3A) reached stable patterns at the first 10 ns for the holo and apoprotein forms, except for dezocine (Figure S1); thus, this complex was discarded from the extended independent simulations of 200 ns per triplicate (Figure S2).

https://doi.org/10.1021/acsomega.5c06639
ACS Omega 2025, 10, 51297−51308

Table 1. Consensus Binding Score of FDA Compounds

Zinc code	Drug	Chemical structure	Consensus Z-score
ZINC000003830682	Dezocine	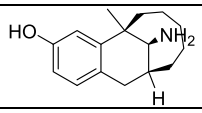	-1.5
ZINC000000608382	Flavoxate	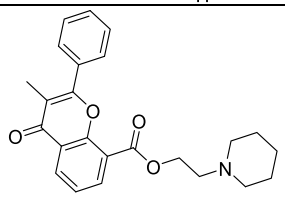	-0.5
ZINC000001534965	Pitavastatin	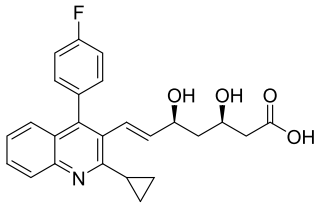	-0.3
ZINC000036520252	Empagliflozin	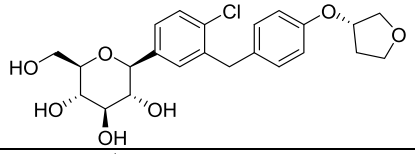	-0.2
ZINC000073069247	Baricitinib	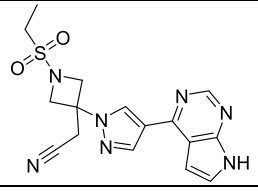	-0.1
ZINC000011679756	Eltrombopag	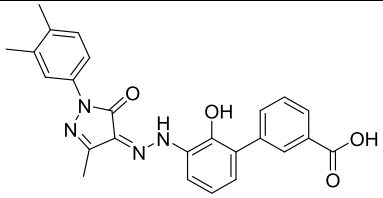	0.0
ZINC000002036732	Florantyrone	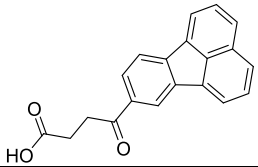	0.1
ZINC000003874715	Wartec-podofilotoxina	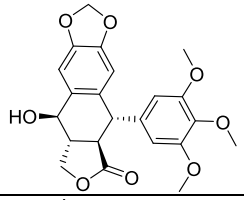	0.1
ZINC000043207851	Ruxolitinib	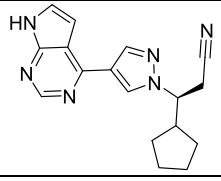	0.1

https://doi.org/10.1021/acsomega.5c06639
ACS Omega 2025, 10, 51297−51308

Table 1. continued

Zinc code	Drug	Chemical structure	Consensus Z-score
ZINC000003831241	Betalactam_analog	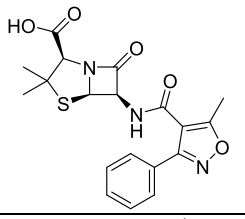	0.1
ZINC000001550499	Cinacalcet	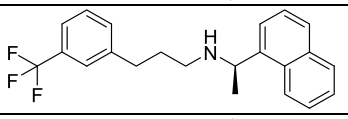	0.2
ZINC000003830826	Fazadinium	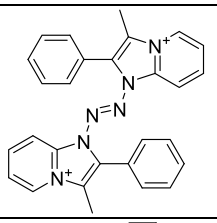	0.2
ZINC000003607120	Zymar-gatifloxacin	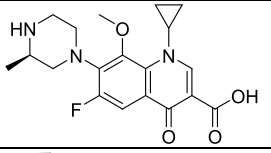	0.2
ZINC000003875980	Nafcillin	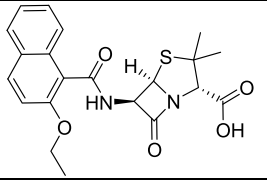	0.3
ZINC000002032615	Nix-permetrin (trans-Permethrin)	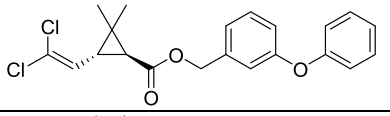	0.3
ZINC000001850376	Nix-permetrin (cis-Permethrin)	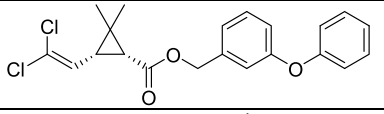	0.4
ZINC000100057530	Strychnine	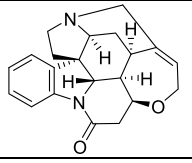	0.5

In extended simulations, all ligand−receptor complexes showed a tendency to stabilize with an RMSD in the range of 2−6 Å (Figure 3A), even better than the baricitinib-JAK2 complex (Figure S2). Root mean square fluctuation (RMSF) showed that amino acid atomic fluctuations (Figure 3B) are more flexible (>7 Å) at the N-terminal, which comprises amino acids 830−850. From the 880 to 1100 residues, where the important amino acids for binding are located, the protein fluctuates between 1 and 2 Å, indicating that the binding of the ligands to the ATP-binding site is structurally stable. Through simulation, all ligands established a range of 1−8 hydrogen bonds (Figure 3C). Transient hydrogen bonding is observed in the first nanoseconds of the simulation, before the ligand−protein complexes reach stabilization at 20 to the last 200 ns. In the stabilization phase, there is a presence of 1 or 2 H bonds for all ligand−protein complexes (Figure 3C).

Selected ligand−protein snapshots extracted from molecular dynamics at 40, 80, 120, 160, and 200 ns showed that all ligands are surrounded mainly by hydrophobic interactions (Figure S3A−E) and kept hydrogen-bond interactions with key residues of the ATP-binding site (Figure 4); for example, flavoxate with Leu932 (occupancy 60.19%); baricitinib with Ser 936 (occupancy 46.07%) located at the extended hinge region;[17] eltrombopag (occupancy 77.22%), pitavastatin (occupancy 64.81%), and empagliflozin (occupancy 25.21%) with Asp994 located at the DFG motif; additionally, empagliflozin had a hydrogen interactions with Arg980 (occupancy 48.52%). Thus, these residues could be the key to the binding of these chemical structures in the JAK2-binding site.

Selected FDA Drugs Changed *Ex Vivo* STAT1,3 Phosphorylation. Our simulation results indicate that the

https://doi.org/10.1021/acsomega.5c06639
ACS Omega 2025, 10, 51297−51308

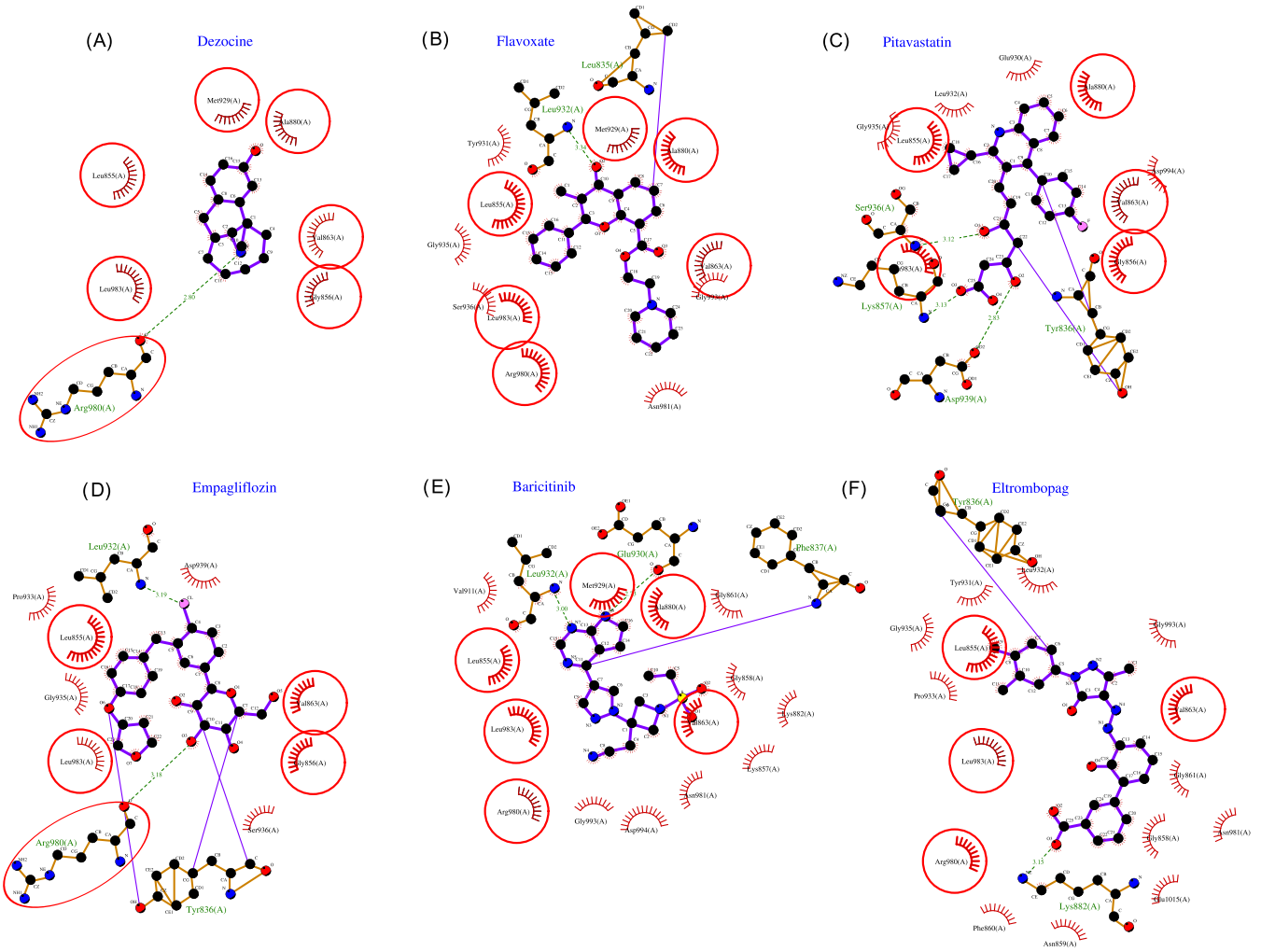

Figure 2. Binding mode interactions of the best selected ranked compounds. Red arcs indicate hydrophobic interactions; green dashed lines indicate hydrophilic interactions with the distance in Å; and red circles indicate shared amino acid interactions among binding poses. (A) Dezocine, (B) flavoxate, (C) pitavastatin, (D) empagliflozin, (E) baricitinib, and (F) eltrombopag. The binding poses images were produced with the ligplot (https://www.ebi.ac.uk/thornton-srv/software/LigPlus/), and the panels were done with the inkscape (https://inkscape.org/).

analyzed drugs may bind stably to the JAK2 kinase and, in turn, could inhibit the phosphorylation of downstream signaling transcription factors STAT1 and STAT3. Thus, we first confirmed through *ex vivo* assays induced by IL-6 (Figure 5A,B), an augmentation in the phosphorylation of STAT3 in lymphocytes (ΔpSTAT3) that changed when tofacitinib was added (Figure 5C).

Then, we tested each selected compound, using a unique concentration in the μM range derived from the docking Vina scores (Table 2). After the compounds were added, a statistically significant reduction in the level of phosphorylation of STAT1 (compared to the level of phosphorylation induced by IL-6) was observed in the cell cultures treated with pitavastatin (Figure 6B), eltrombopag (Figure 6D), and tofacitinib (Figure 6E). Moreover, the reduction in the phosphorylation of STAT3 in lymphocytes was observed in cell cultures stimulated with hrIL-6 in the presence of empagliflozin (Figure 6F), pitavastatin (Figure 6G), flavoxate (Figure 6H), eltrombopag (Figure 6I), and tofacitinib (Figure 6J).

DISCUSSION

In this work, through a consensus-scoring virtual screening approach, four potential inhibitors of JAK2 were identified. We used four scoring functions to calculate the consensus score that could improve the recovery of active drugs with the highest possibility of showing biological activity.[18] Among the scoring functions used, the Vinardo scoring function showed the lowest number of best virtual hits. The Vinardo score was designed for the Smina software, which was reported as better than Vina in consensus-scoring virtual screening campaigns.[19,20] Thus, our results are consistent with previous findings and support the strategy used to select potential inhibitors of JAK2.

Further detailed analysis of binding mode and molecular dynamics simulation helped us identify that these best binders showed comparable interactions and stability with baricitinib; hence, we validated through molecular modeling that the drugs selected could avoid the activation of JAK2. We observed that these compounds have a binding mode that interacts with amino acids located at the hinge region, p-loop, and the DFG motif of the JAK2 active site, which are important in the binding of JAK2 inhibitors in experimentally determined structures and molecular dynamics studies.[16,21] We found that

https://doi.org/10.1021/acsomega.5c06639
ACS Omega 2025, 10, 51297−51308

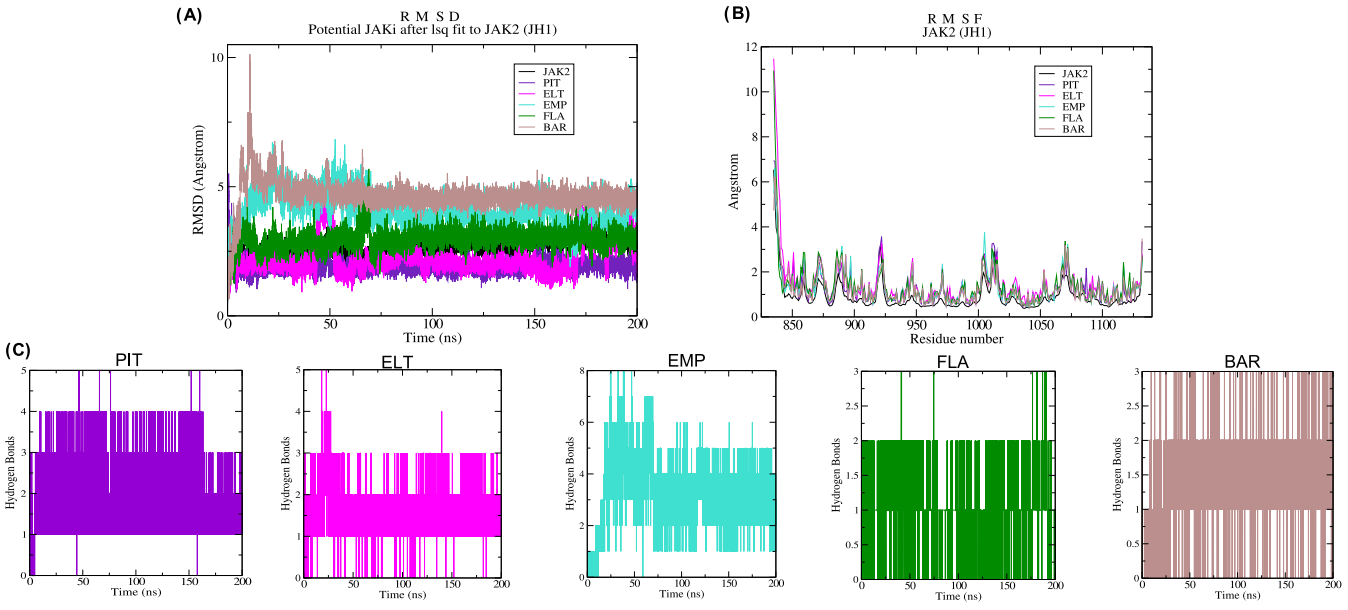

Figure 3. Molecular dynamics of the JAK2-ligand complexes. (A) RMSD and (B) RMSF for each JAK2-ligand complex represented by different color lines. (C) Hydrogen bond formation of pitavastatin (PIT, purple), eltrombopag (ELT, magenta), empaglifozin (EMP, cyan), flavoxate (FLA, green), and baricitinib (BAR, brown). The graphics were produced with the xmgrace (https://plasma-gate.weizmann.ac.il/Grace/), and the panels were done with the inkscape (https://inkscape.org/).

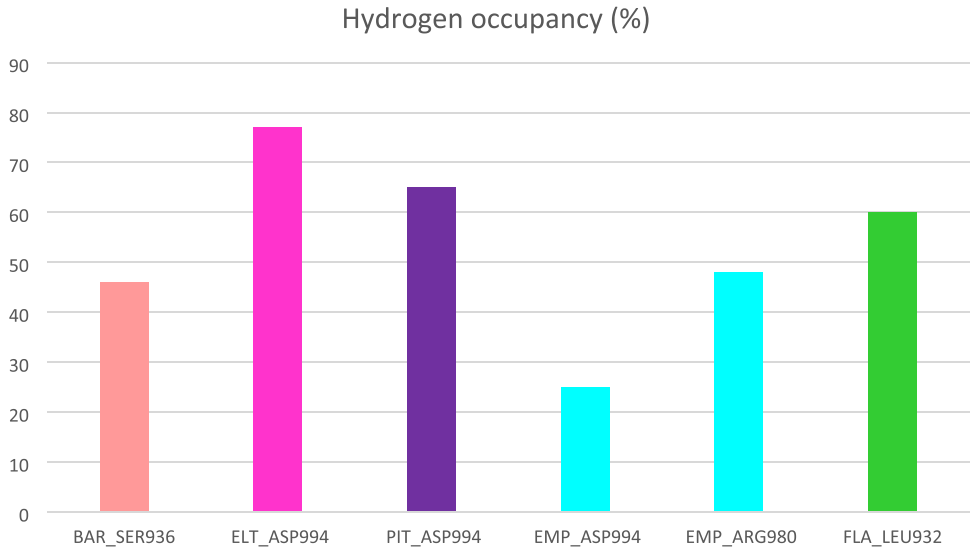

Figure 4. Hydrogen bond occupancy between the ligand and the protein using a cutoff of 30° for angle and 3 Å for distance. At the bottom of the bars are indicated the amino acids for baricitinib (BAR), eltrombopag (ELT), pitavastatin (PIT), empaglifozin (EMP), and flavoxate (FLA).

the chemical structures of the best predicted hits influence the binding interaction with these residues through hydrogen and hydrophobic bonding. Further studies should be directed to test these potential inhibitors in enzymatic assays to evaluate their selectivity or resistance in wild and mutated JAK2 proteins.

On the other hand, our *ex vivo* studies showed that these drugs indeed affected the JAK2 downstream-related molecules STAT1 and STAT3 by reducing their phosphorylation in human lymphocytes stimulated with IL-6, suggesting that these drugs could be useful as therapy in inflammatory diseases, potentially affecting apoptosis and lymphocyte proliferation. In this context, we found that the pitavastatin, a known inhibitor of HMG-CoA, has been implicated in the reduction of T-cell responses,[22] such as antigen presentation[23] and chemokine synthesis, in PBMC cultures[24] through the reduction of mevalonate, a precursor of cholesterol. Moreover, a property of statins unrelated to HMG-CoA inhibition is the blocking of LFA-1 and ICAM-1,[25] affecting the function of leukocytes. In agreement with our molecular modeling results, pitavastatin has been shown to inhibit the activity of other kinases such as ERK. The inhibition of ERK decreases the expression of IL-6, TNF-α, and MCP-1, as well as lymphocyte proliferation at a concentration of 10^{-9} M.[22] Statins have potential as novel therapeutic agents for rheumatoid arthritis (RA),[26] as the previously described JAK2 inhibitors.

Furthermore, we observed that eltrombopag induces the dephosphorylation of STAT1 and STAT3. In contrast, the known mechanism of action of the noncompetitive eltrombopag is through the binding in the allosteric site of c-MPL

https://doi.org/10.1021/acsomega.5c06639
ACS Omega 2025, 10, 51297−51308

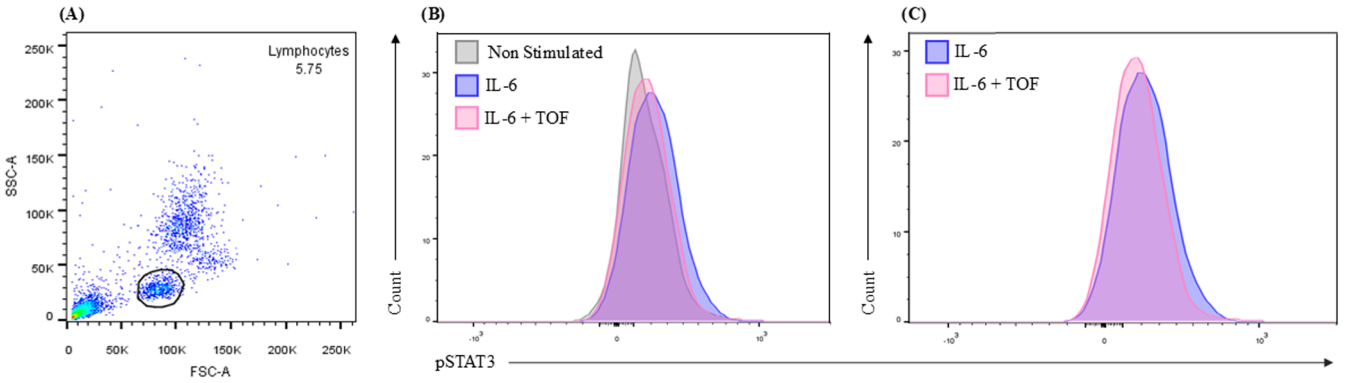

Figure 5. Representative dotted plot showing the gating strategy used to evaluate STAT3 phosphorylation (pSTAT3) in lymphocytes. (A) Lymphocyte subpopulation was selected using forward and side scatter. (B) Phosphorylated STAT3 (pSTAT3) was evaluated as the percentage of positive cells. The histograms of unstimulated lymphocytes (gray), stimulated with IL-6 (100 ng/mL) (purple), and IL-6 plus the drug tofacitinib (pink) are shown. (C) It shows the difference between pSTAT3-positive cells for the IL-6 condition and that for the IL-6 plus tofacitinib condition.

Table 2. Selected Compounds with Their Derived K_i Values from the Docking Vina Scores[a]

zinc code	drug name	MOLPORT ID	ΔG	K_i μM
ZINC000000608382	FLA	MOLPORT-003-986-802	−9.3	0.1536
ZINC000001534965	PIT	MOLPORT-006-822-984	−8.6	0.5004
ZINC000036520252	EMP	MOLPORT-027-720-828	−9	0.2548
ZINC000011679756	ELT	MOLPORT-009-679-439	−9	0.2548

[a]ΔG value from the Vina score. FLA: flavoxate; PIT: pitavastatin; EMP: empagliflozin; and ELT: eltrombopag.

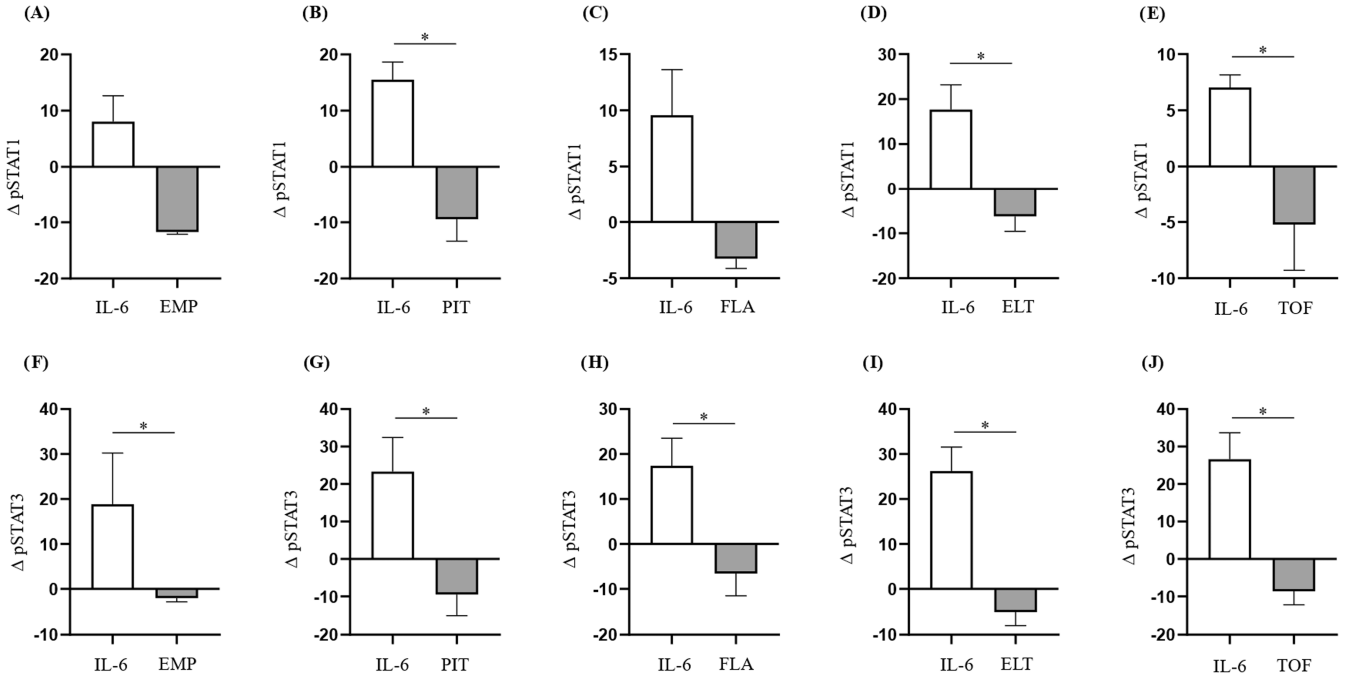

Figure 6. Changes in STAT1 and STAT3 phosphorylation produced by the selected FDA drugs. The changes in the phosphorylation of STAT1 (ΔpSTAT1) induced by (A) empagliflozin (EMP), (B) pitavastatin calcium (PIT), (C) flavoxate (FLA), (D) eltrombopag (ELT), and (E) tofacitinib citrate (TOF) are shown. In addition, the changes in the phosphorylation of STAT3 (ΔpSTAT3) induced by (F) empagliflozin, (G) pitavastatin calcium, (H) flavoxate, (I) eltrombopag, and (J) tofacitinib citrate are shown. Data is presented as mean ± SD. The Mann−Whitney *U* test was used for statistical analysis. *$p < 0.05$ was considered significant. The *p* values are shown as horizontal lines; an asterisk indicates statistically significant differences between the groups studied.

receptor in megakaryocytes.[27,28] However, in other studies, it was demonstrated that eltrombopag may stimulate megakaryopoiesis through the activation of the JAK/STAT signaling pathway.[27] Regarding this, low concentrations of eltrombopag (0.01 μM) may activate STAT5 in a Ba/F3 cell line, a murine interleukin-3-dependent pro-B cell line.[27] Moreover, the activation of MAPK (mitogen-activated protein kinase) pathways by eltrombopag through this was observed.[28] In our results, the dephosphorylation of STAT1 and STAT3 by eltrombopag was determined in lymphocytes, although variants

https://doi.org/10.1021/acsomega.5c06639
ACS Omega 2025, 10, 51297−51308

of MPL were detected in freshly isolated PBMC (lymphocytes and monocytes).[29] At this point, it is important to note that we do not verify the activation status of STAT5 in our cell cultures in the presence of eltrombopag. However, it could be relevant since eltrombopag could avoid the phosphorylation of JAK2/STAT3 while promoting STAT5 activation, leading to not only a decrease in proliferation and apoptosis but also the generation of T regulatory cells.[12,30,31]

Also, we observed a decrease in the level of pSTAT3 in cell cultures in the presence of empagliflozin. The results were consistent with the recent report where empagliflozin decreased pSTAT3 in lipopolysaccharide (LPS) stimulated RAW264.7 macrophages.[32] In addition, the treatment with empagliflozin of BALB/c mice with experimental autoimmune myocarditis showed a reduction in the pSTAT3. Moreover, the treatment with empagliflozin was able to diminish the levels of TNF-α, IL-1β, and iNOS *in vivo* and *in vitro* models.[32] Some anti-inflammatory effects of empagliflozin could be partially dependent on the inhibition of the glucose transporter SGLT-2,[33] since this is expressed in immune cells such as monocytes.[34] However, the anti-inflammatory effect of empagliflozin could also be independent of its interaction with SGLT-2. The expression of SGLT-2 at the protein level was described in monocytes/macrophages and lymphocytes.[35] In concordance with previous reports, we observed the activation of JAK2/STAT3/STAT1 induced by IL-6 in blood lymphocytes[36,37] and the reduction in the phosphorylation of STAT3 by empagliflozin. We suggest that in lymphocytes, the decrease of pSTAT3 would result from the inhibition of JAK2 phosphorylation by empagliflozin.[38]

Finally, we observed the reduction of pSTAT3 in blood lymphocytes stimulated with IL-6 when the cells were treated with flavoxate. Here, in a modeling design, flavoxate binds to Jh1 of JAK2, and the reduction in the phosphorylation of pSTAT3 can be a consequence of this. JAK inhibitors reduce the level of STAT signaling. Also, the inhibition of JAK/STAT signaling may have inflammatory responses by immune cells, as the activation of JAK/STAT signaling induced activation of nuclear factor of activated T cell (NFAT), and its translocation to the nucleus impacts $CD4^+$ T cell proliferation and function.[39,40] Flavoxate is a competitive phosphodiesterase (PDE) inhibitor. PDE breaks a phosphodiester bond in the second messenger cyclic AMP (cAMP).[41] cAMP is an important regulator of signal transduction. Increased levels of cAMP in effector $CD4^+$ T cells lead to nuclear localization of inducible cAMP early repressor (ICER)/cAMP response modulator (CREM) and the repression of NFAT and IL-2 secretion. Moreover, cAMP supports the suppressor function of regulatory T cells.[42,43] Then, we could speculate that flavoxate executes anti-inflammatory effects through the inhibition of cAMP degradation, enhancing suppressive activities of T regulatory cells over effector $CD4^+$ T cells[44] and suppressing the NFAT induced by JAK kinases.

The search for selective inhibitors of the JAK/STAT pathway was aimed at minimizing their associated adverse effects. The high conservation of the structurally JAK isoform components in their ATP-binding site makes this task difficult.[45] However, selectivity was achieved for a specific JAK isoform. For example, the chemical upadacitinib was predicted to attach to this region, considering the amino acid differences at the glycine-rich loop in JAK1 compared with the JAK2 isoform.[46] The subsequent dose-dependent *in vitro* and *ex vivo* studies confirmed the selectivity of upadacitib to JAK1, even in phase I and II trials.[46,47]

Our computational predictions suggested that pitavastatin, eltrombopag, empaglifozin, and flavoxate could be potential selective JAK2 inhibitors, as they showed impairment in phosphorylation of downstream-related molecules STAT1 and STAT3. Overall, these findings suggested a new off-target effect for these compounds. This is the main advantage of the repositioning approach, and it allows identifying new uses for molecules that have experimental information on their pharmacokinetics and pharmacodynamics, accelerating the identification of potential safer drugs.[48] However, since a new target is proposed for these drugs, changes in concentrations, formulation, and route of administration may be necessary, considering the diseases in which the JAK/STAT pathway could be dysregulated. Further, whether these compounds have off-target effects on the other JAK components is a pending task.

The limitations of this study are that we did not directly confirm the JAK2 enzyme inhibition and that we used a unique concentration derived from docking scores to evaluate the inhibitory effects of STAT1,3 phosphorylation in lymphocytes. Thus, it is critical to evaluate whether the parameters of potency and efficacy of inhibition of this signaling pathway by the drugs tested here are enough to reduce the secretion of inflammatory cytokines such as IL-6 and TNF-α, which might impact the pathological inflammatory processes. Finally, another upstream cytokine deregulation must be experimentally validated.

CONCLUSION

In this work, we performed a computer-aided strategy to repurpose potential JAK2/STAT1,3 inhibitors. The consensus-scoring strategy and molecular dynamics simulations helped us identify the best virtual hits to test in an *ex vivo* flow cytometry study using human lymphocytes. Like tofacitinib, the selected drugs pitavastatin, eltrombopag, flavoxate, and empagliflozin were shown to change the phosphorylation of downstream STAT1 and STAT3 signaling molecules. These results encourage further in-depth preclinical experiments aimed at exploring the effects of these drugs on inflammatory signaling pathways.

MATERIAL AND METHODS

Molecular Docking. The crystallized-JH1 kinase domain of the JAK2 receptor with baricitinib ligand was downloaded from the protein database under the PDBID 6vn8.[16] The receptor was prepared by removing the baricitinib ligand, water, and extra chains; then, polar hydrogens and Gasteiger charges were added using the option "dockprep" available in the Chimera software version 1.19.[49] The baricitinib ligand from chain A of the JAK2 crystal was also prepared with the "dockprep" option of the Chimera software. The search space at 1 Å for docking simulation was performed with the mgltools[50] using baricitinib located at the center coordinates x = 55.328, y = −24.384, z = −11.982, and a box size of X = 12, Y = 10, Z = 16 as the reference. Redocking of baricitib was performed with Smina software,[15,19] using the scoring functions Vina, Vinardo, and Dkoes. The reproducibility of the docking was assessed with the DockRMSD software[51] and the best pose with binding scores were used as reference to screen the best binders among 3330 ligands obtained from

https://doi.org/10.1021/acsomega.5c06639
ACS Omega 2025, 10, 51297−51308

FDA catalog available on the ZINC20 database.[52] The FDA ligands were prepared with the openbabel software version 3.1.1,[53] minimizing the energy, adding hydrogens, and transforming the files to the ".pdbqt" format required for Smina. The docking of all ligands was performed by using each scoring function at a time. After an initial screening using the mentioned scoring functions, the Fit dock scoring produced through template-based docking using the CB-Dock2 Web server[54] was included in the *z*-score calculation for the four binding scores with the formula

$$z = \frac{xi - \overline{x}}{s}$$

where *xi* is the predicted binding energy of a specific ligand (kcal/mol), $\overline{x}$ is the mean of a specific scoring function, and *s* is the standard deviation.

The consensus scoring *j* was calculated as the average of its scores normalized across the used *N* metrics as follows

$$\text{consensus scoring}_j = \frac{1}{N}(z_{j1} + z_{j2} + z_{j3} + z_{j4N})$$

where *N* is the total number of the scoring functions and *z*1−4 are the scoring functions used. Thus, the compounds were selected based on the lowest *Z* mean consensus score. The binding mode of the best-ranked compounds was analyzed with the ligplot software.[55]

Molecular Dynamics. The molecular dynamics was performed using GROMACS software version 2024.1.[56] For each Drug-JAK2 complex, the best-ranked poses produced by molecular docking were submitted to molecular dynamics. First, the parametrization of the receptor was done by centering the coordinates with the "Charm27" force field, solvated ion "TIP3P" water model, and taking Leu-835 as the terminal amino group and Gly-1132 as the terminal carbonyl of the JH1 domain of JAK2. The shape of the box used to perform the molecular dynamics was triclinic (X = 4.652, Y = 3.645, Z = 3.722), inside which approximately 14956 solvent molecules (H2O) were added. In each case, approximately 30 Cl ions and 31 Na ions were replaced between the water molecules of the solvent. The energy minimization of each system was performed until the molecules inside the box reached an F_{max} <10.0 kJ/mol, taking the "Verlet" "cutoff-scheme" parameter. The equilibration of the molecules was performed for 100 ps with the "Verlet" parameter, restricting the corresponding "LIG & REC", the "NVT" volume equilibration was performed with "V -rescale", the "NPT" pressure equilibration was performed with the "Berendsen" parameters, Maxwell Vel. at 26.85 °C. To produce molecular dynamics, it was run for 200 ns in triplicate for each complex, saving or capturing the coordinates every 10 ps to produce a total of 20,000 reading frames per run. The parameters of each run were performed according to "Verlet, PME, V-rescale, Parrinello−Rahman" at 26.85 °C. The molecular dynamics analysis was performed with GROMACS and xmgrace (https://plasma-gate.weizmann.ac.il/Grace/) to obtain the RMSD, RMSF, and hydrogen-bonding plots. The option "hydrogen bonds" of the VMD program[57] was used to calculate the occupancy of hydrogen bonds (>20%) using the angle cutoff of 30° and distance of 3 Å.

Blood Cell *Ex Vivo* STAT1,3 Activations by Exogenous IL-6 Stimulation and Drug Inhibition Confirmation. To obtain drug concentration for testing the inhibitory effects of the selected compound purchased from MOLPORT (https://www.molport.com/), we calculated the theoretical K_i values for the selected potential JAK2-inhibitor using the formula reported by Shityakov and colleagues,[58] which was applied as follows

$$K_i = e^{\Delta G \times 1000/R \times T \times 1{,}000{,}000}$$

where ΔG is the Vina score obtained from the docking software, R is the gas constant with a value of 1.98 cal·(mol·K) − 1, and T is the room temperature with a value of 25 °C. Thus, the calculated concentrations are given in Table 2.

Healthy Volunteers. Blood samples were taken from seven healthy subjects aged 25−35 years, 3 of whom were males and 4 of whom were females. None of them was taking medication. This study was approved by the National Commission for Scientific Research of the Social Security Institute of Mexico, IMSS (project number: R-2018-785-072). All participants signed their written informed consent.

Cell Culture. A total of 200 μL of blood taken from healthy volunteers was stimulated with human recombinant hrIL-6 (100 ng/mL) (GE Healthcare Biosciences, Piscataway, NJ) and maintained at 37 °C, 95% humidity, and 5% CO2 for 30 min. The flavoxate (0.1536 μM), eltrombopag (0.2548 μM), pitavastatin calcium (0.5004 μM), empagliflozin (0.2548 μM), and tofacitinib citrate (1.2 nM) (Sigma-Aldrich code PZ0017, Saint Louis) were added to the blood before recombinant human interleukin-6 (rhIL-6). Once the erythrocytes were lysed, for the detection of intracellular antigens (pSTAT1 and pSTAT3), a labeling procedure was performed with the fixation−permeabilization buffers supplied by eBioscience. Permeabilized leukocytes were immunostained with the following mAbs: anti-pSTAT3-Alexa Fluor 647 (Miltenyi Biotech, Auburn, CA) and anti-pSTAT1-phycoerythrin (PE) (Miltenyi Biotech, Auburn, CA). Finally, the samples were acquired on BD FACSCanto II (BD Biosciences), and the percentage of positive cells was determined using FACSDiva software version 6 (BD Biosciences). The percentage values were used to calculate the changes in phosphorylation of STAT1 and STAT3 using the Δ change calculation method as follows:

For IL-6-stimulated lymphocytes

$$\Delta\text{pSTAT (1 or 3)} = (\%\text{pSTAT}^{+}_{\text{stimulated}}) - (\%\text{pSTAT}^{+}_{\text{unstimulated}})$$

For the drug effect on IL-6-stimulated lymphocytes

$$\Delta\text{pSTAT (1 or 3)} = (\%\text{pSTAT}^{+}_{\text{drug+stimulated}}) - (\%\text{pSTAT}^{+}_{\text{stimulated}})$$

Statistical Analysis. Statistical analysis was performed using the GraphPad Prism 5.0 software (San Diego, CA). Data distribution was determined using the Kolmogorov−Smirnov test. Differences in the changes of phosphorylation of STAT1/3 were determined by the Mann−Whitney *U* test. Data were presented as mean ± SD, with $^*p < 0.05$ considered significant. The *p*-values are represented in horizontal lines; the asterisk indicates statistically significant differences between the studied groups.

https://doi.org/10.1021/acsomega.5c06639
ACS Omega 2025, 10, 51297−51308

■ ASSOCIATED CONTENT

Supporting Information

The Supporting Information is available free of charge at https://pubs.acs.org/doi/10.1021/acsomega.5c06639.

Raw docking scores (*), *z*-score normalization (**), and *z*-score consensus results (Table S1); comparison of root mean square deviation (RMSD) for apo JAK2 protein and protein−ligand complex during 100 ns simulation. The color lines indicate the apo form of JAK2 (black) and the ligand−protein complex during the simulation for baricitinib (BAR, green), dezocine (DEZ, blue), flavoxate (FLA, yellow), pitavastatin (PIT, brown), and empaglifozin (EMP, gray) (Figure S1); comparison of root mean square deviation (RMSD) for the protein−ligand complex during 200 ns independent simulation in triplicate. The different color lines indicate the number of independent molecular dynamics for baricitinib (BAR), eltrombopag (ELT), pitavastatin (PIT), empaglifozin (EMP), and flavoxate (FLA) (Figure S2); selected snapshots extracted from molecular dynamics at 40, 80, 120, 160, and 200 ns for (A) flavoxate (FLA), (B) pitavastatin (PIT), (C) empaglifozin (EMP), (D) baricitinib (BAR), and (E) eltrombopag (ELT). Red arcs indicate hydrophobic interactions; green dashed lines indicate hydrophilic interactions with the distance in Å; red circles indicate shared amino acid interactions among binding poses (Figure S3) (PDF)

■ AUTHOR INFORMATION

Corresponding Author

Edgar E. Lara-Ramírez − *Laboratorio de Biotecnología Farmacéutica, Centro de Biotecnología Genómica, Instituto Politécnico Nacional, Reynosa, Tamaulipas 88710, México;* orcid.org/0000-0001-7112-3233; Email: elarar@ipn.mx

Authors

Mariana H. García-Hernández − *Unidad de Investigación Biomédica de Zacatecas, Instituto Mexicano del Seguro Social (IMSS), Zacatecas 98000, México*

Elena Jaime-Sánchez − *Laboratorio de Biotecnología Farmacéutica, Centro de Biotecnología Genómica, Instituto Politécnico Nacional, Reynosa, Tamaulipas 88710, México*

Abraham Cardenas-Juarez − *Unidad de Investigación Biomédica de Zacatecas, Instituto Mexicano del Seguro Social (IMSS), Zacatecas 98000, México*

Carmen J. Serrano − *Unidad de Investigación Biomédica de Zacatecas, Instituto Mexicano del Seguro Social (IMSS), Zacatecas 98000, México*

Lenci K. Vázquez-Jiménez − *Laboratorio de Biotecnología Farmacéutica, Centro de Biotecnología Genómica, Instituto Politécnico Nacional, Reynosa, Tamaulipas 88710, México*

Gildardo Rivera − *Laboratorio de Biotecnología Farmacéutica, Centro de Biotecnología Genómica, Instituto Politécnico Nacional, Reynosa, Tamaulipas 88710, México;* orcid.org/0000-0001-9842-4167

Juan E. López-Ramos − *Unidad Profesional Interdisciplinaria de Ingeniería, Campus Zacatecas, Instituto Politécnico Nacional, Zacatecas 98160, México*

Complete contact information is available at: https://pubs.acs.org/10.1021/acsomega.5c06639

Author Contributions

M.H.G.-H.: conceptualization, data curation, formal analysis, methodology, supervision, and writing of the original draft. E.J.-S.: data curation, formal analysis, methodology, and writing, reviewing, and editing. A.C.-J.: formal analysis and writing, reviewing, and editing. C.J.S.: writing, reviewing, and editing. L.K.V.-J.: writing, reviewing, and editing. G.R.: writing, reviewing, and editing. J.E.L.-R.: writing, reviewing, and editing. E.E.L.-R.: conceptualization, data curation, formal analysis, methodology, supervision, and writing of the original draft. All authors have given approval to the final version of the manuscript.

Funding

This research was supported by "Secretaría de Investigación y Posgrado, IPN" grant numbers 20241055, 20243965 and 20254748.

Notes

The authors declare no competing financial interest.

■ ACKNOWLEDGMENTS

E.J.-S. and L.K.V.-J. acknowledge the postdoctoral SECIHTI scholarships CVU 705863 and CVU 707836, respectively.

■ REFERENCES

(1) Hu, X.; Li, J.; Fu, M.; Zhao, X.; Wang, W. The JAK/STAT Signaling Pathway: From Bench to Clinic. *Signal Transduction Targeted Ther.* **2021**, *6* (1), No. 402.

(2) Xue, C.; Yao, Q.; Gu, X.; Shi, Q.; Yuan, X.; Chu, Q.; Bao, Z.; Lu, J.; Li, L. Evolving Cognition of the JAK-STAT Signaling Pathway: Autoimmune Disorders and Cancer. *Signal Transduction Targeted Ther.* **2023**, *8* (1), No. 204.

(3) Shawky, A. M.; Almalki, F. A.; Abdalla, A. N.; Abdelazeem, A. H.; Gouda, A. M. A Comprehensive Overview of Globally Approved JAK Inhibitors. *Pharmaceutics* **2022**, *14* (5), No. 1001.

(4) Deisseroth, A.; Kaminskas, E.; Grillo, J.; Chen, W.; Saber, H.; Lu, H. L.; Rothmann, M. D.; Brar, S.; Wang, J.; Garnett, C.; Bullock, J.; Burke, L. B.; Rahman, A.; Sridhara, R.; Farrell, A.; Pazdur, R. U.S. Food and Drug Administration Approval: Ruxolitinib for the Treatment of Patients with Intermediate and High-Risk Myelofibrosis. *Clin. Cancer Res.* **2012**, *18* (12), 3212−3217.

(5) Raedler, L. A. Jakafi (Ruxolitinib): First FDA-Approved Medication for the Treatment of Patients with Polycythemia Vera. *Am. Health Drug Benefits* **2015**, *8*, 75−79.

(6) Rakieh, C.; Conaghan, P. G. Tofacitinib for Treatment of Rheumatoid Arthritis. *Adv. Ther.* **2013**, *30* (8), 713−726.

(7) Padda, I. S.; Bhatt, R.; Parmar, M. Tofacitinib, [Updated 2023 July 3]. In StatPearls [Internet]; Treasure Island (FL): StatPearls Publishing, Jan, 2025. https://www.ncbi.nlm.nih.gov/books/NBK572148/.

(8) Markham, A. Baricitinib: First Global Approval. *Drugs* **2017**, *77* (6), 697−704.

(9) Kincaid, C. M.; Arnold, J. D.; Mesinkovska, N. A. Baricitinib as the First Systemic Treatment for Severe Alopecia Areata. *Expert Rev. Clin. Immunol.* **2023**, *19* (6), 565−573.

(10) Rubin, R. Baricitinib Is First Approved COVID-19 Immunomodulatory Treatment. *JAMA* **2022**, *327* (23), 2281.

(11) Sriram, K.; Benkovic, S. A.; Hebert, M. A.; Miller, D. B.; O'Callaghan, J. P. Induction of Gp130-Related Cytokines and Activation of JAK2/STAT3 Pathway in Astrocytes Precedes up-Regulation of Glial Fibrillary Acidic Protein in the 1-Methyl-4-Phenyl-1,2,3,6-Tetrahydropyridine Model of Neurodegeneration: Key Signaling Pathway for Astrogliosis in Vivo? *J. Biol. Chem.* **2004**, *279* (19), 19936−19947.

(12) Ross, J. A.; Nagy, Z. S.; Cheng, H.; Stepkowski, S. M.; Kirken, R. A. Regulation of T Cell Homeostasis by JAKs and STATs. *Arch. Immunol. Ther. Exp.* **2007**, *55* (4), 231−245.

(13) Wei, X.-H.; Liu, Y.-Y. Potential Applications of JAK Inhibitors, Clinically Approved Drugs against Autoimmune Diseases, in Cancer Therapy. *Front. Pharmacol.* **2024**, *14*, No. 1326281.
(14) Hodge, J. A.; Kawabata, T. T.; Krishnaswami, S.; Clark, J. D.; Telliez, J.-B.; Dowty, M. E.; Menon, S.; Lamba, M.; Zwillich, S. The Mechanism of Action of Tofacitinib - an Oral Janus Kinase Inhibitor for the Treatment of Rheumatoid Arthritis. *Clin. Exp. Rheumatol.* **2016**, *34* (2), 318−328.
(15) Koes, D. R.; Baumgartner, M. P.; Camacho, C. J. Lessons Learned in Empirical Scoring with Smina from the CSAR 2011 Benchmarking Exercise. *J. Chem. Inf. Model.* **2013**, *53* (8), 1893−1904.
(16) Davis, R. R.; Li, B.; Yun, S. Y.; Chan, A.; Nareddy, P.; Gunawan, S.; Ayaz, M.; Lawrence, H. R.; Reuther, G. W.; Lawrence, N. J.; Schönbrunn, E. Structural Insights into JAK2 Inhibition by Ruxolitinib, Fedratinib, and Derivatives Thereof. *J. Med. Chem.* **2021**, *64* (4), 2228−2241.
(17) Hart, A. C.; Schroeder, G. M.; Wan, H.; Grebinski, J.; Inghrim, J.; Kempson, J.; Guo, J.; Pitts, W. J.; Tokarski, J. S.; Sack, J. S.; Khan, J. A.; Lippy, J.; Lorenzi, M. V.; You, D.; McDevitt, T.; Vuppugalla, R.; Zhang, Y.; Lombardo, L. J.; Trainor, G. L.; Purandare, A. V. Structure-Based Design of Selective Janus Kinase 2 Imidazo[4,5-d]Pyrrolo[2,3-b]Pyridine Inhibitors. *ACS Med. Chem. Lett.* **2015**, *6* (8), 845−849.
(18) Baber, J. C.; Shirley, W. A.; Gao, Y.; Feher, M. The Use of Consensus Scoring in Ligand-Based Virtual Screening. *J. Chem. Inf. Model.* **2006**, *46* (1), 277−288.
(19) Quiroga, R.; Villarreal, M. A. Vinardo: A Scoring Function Based on Autodock Vina Improves Scoring, Docking, and Virtual Screening. *PLoS One* **2016**, *11* (5), No. e0155183.
(20) Masters, L.; Eagon, S.; Heying, M. Evaluation of Consensus Scoring Methods for AutoDock Vina, Smina and Idock. *J. Mol. Graphics Modell.* **2020**, *96*, No. 107532.
(21) Zhou, T.; Georgeon, S.; Moser, R.; Moore, D. J.; Caflisch, A.; Hantschel, O. Specificity and Mechanism-of-Action of the JAK2 Tyrosine Kinase Inhibitors Ruxolitinib and SAR302503 (TG101348). *Leukemia* **2014**, *28* (2), 404−407.
(22) Suzuki, J.-i.; Koga, N.; Kosuge, H.; Ogawa, M.; Haraguchi, G.; Maejima, Y.; Saiki, H.; Isobe, M. Pitavastatin Suppresses Acute and Chronic Rejection in Murine Cardiac Allografts. *Transplantation* **2007**, *83* (8), 1093−1097.
(23) Kwak, B.; Mulhaupt, F.; Myit, S.; Mach, F. Statins as a Newly Recognized Type of Immunomodulator. *Nat. Med.* **2000**, *6* (12), 1399−1402.
(24) Romano, M.; Diomede, L.; Sironi, M.; Massimiliano, L.; Sottocorno, M.; Polentarutti, N.; Guglielmotti, A.; Albani, D.; Bruno, A.; Fruscella, P.; Salmona, M.; Vecchi, A.; Pinza, M.; Mantovani, A. Inhibition of Monocyte Chemotactic Protein-1 Synthesis by Statins. *Lab. Invest.* **2000**, *80* (7), 1095−1100.
(25) Weitz-Schmidt, G.; Welzenbach, K.; Brinkmann, V.; Kamata, T.; Kallen, J.; Bruns, C.; Cottens, S.; Takada, Y.; Hommel, U. Statins Selectively Inhibit Leukocyte Function Antigen-1 by Binding to a Novel Regulatory Integrin Site. *Nat. Med.* **2001**, *7* (6), 687−692.
(26) Nagashima, T.; Okazaki, H.; Yudoh, K.; Matsuno, H.; Minota, S. Apoptosis of Rheumatoid Synovial Cells by Statins through the Blocking of Protein Geranylgeranylation: A Potential Therapeutic Approach to Rheumatoid Arthritis. *Arthritis Rheum.* **2006**, *54* (2), 579−586.
(27) Erickson-Miller, C. L.; DeLorme, E.; Tian, S.-S.; Hopson, C. B.; Stark, K.; Giampa, L.; Valoret, E. I.; Duffy, K. J.; Luengo, J. L.; Rosen, J.; Miller, S. G.; Dillon, S. B.; Lamb, P. Discovery and Characterization of a Selective, Nonpeptidyl Thrombopoietin Receptor Agonist. *Exp. Hematol.* **2005**, *33* (1), 85−93.
(28) Erickson-Miller, C. L.; Delorme, E.; Tian, S.-S.; Hopson, C. B.; Landis, A. J.; Valoret, E. I.; Sellers, T. S.; Rosen, J.; Miller, S. G.; Luengo, J. I.; Duffy, K. J.; Jenkins, J. M. Preclinical Activity of Eltrombopag (SB-497115), an Oral, Nonpeptide Thrombopoietin Receptor Agonist. *Stem Cells* **2009**, *27* (2), 424−430.
(29) Rollinger-Holzinger, I.; Griesser, U.; Pollak, V.; Zwierzina, H. Expression and regulation of the thrombopoietin receptor variants MPLP and MPLK in PBMC. *Cytokine* **1998**, *10* (10), 795−802.
(30) Pandiyan, P.; Yang, X.-P.; Saravanamuthu, S. S.; Zheng, L.; Ishihara, S.; O'Shea, J. J.; Lenardo, M. J. The Role of IL-15 in Activating STAT5 and Fine-Tuning IL-17A Production in CD4 T Lymphocytes. *J. Immunol.* **2012**, *189* (9), 4237−4246.
(31) Cao, L.; Ma, X.; Zhang, J.; Yang, M.; He, Z.; Yang, C.; Li, S.; Rong, P.; Wang, W. CD27-Expressing Xenoantigen-Expanded Human Regulatory T Cells Are Efficient in Suppressing Xenogeneic Immune Response. *Cell Transplant.* **2023**, *32*, No. 09636897221149444.
(32) Sheng, W.; Yu, J.; Zhang, H.; Zhang, J. Empagliflozin Attenuates Inflammation Levels in Autoimmune Myocarditis through the STAT3 Pathway and Macrophage Phenotype Transformation. *Mol. Immunol.* **2024**, *167*, 43−52.
(33) Liu, W.; You, D.; Lin, J.; Zou, H.; Zhang, L.; Luo, S.; Yuan, Y.; Wang, Z.; Qi, J.; Wang, W.; Ye, X.; Yang, X.; Deng, Y.; Teng, F.; Zheng, X.; Lin, Y.; Huang, Z.; Huang, Y.; Yang, Z.; Zhou, X.; Zhang, Y.; Chen, R.; Xu, L.; Li, J.; Yang, W.; Zhang, H. SGLT2 Inhibitor Promotes Ketogenesis to Improve MASH by Suppressing CD8+ T Cell Activation. *Cell Metab.* **2024**, *36* (10), 2245−2261.E6.
(34) Semo, D.; Obergassel, J.; Dorenkamp, M.; Hemling, P.; Strutz, J.; Hiden, U.; Müller, N.; Müller, U. A.; Zulfikar, S. A.; Godfrey, R.; Waltenberger, J. The Sodium-Glucose Co-Transporter 2 (SGLT2) Inhibitor Empagliflozin Reverses Hyperglycemia-Induced Monocyte and Endothelial Dysfunction Primarily through Glucose Transport-Independent but Redox-Dependent Mechanisms. *J. Clin. Med.* **2023**, *12* (4), No. 1356.
(35) Liu, W.; You, D.; Lin, J.; et al. SGLT2 Inhibitor Promotes Ketogenesis to Improve MASH by Suppressing CD8+ T Cell Activation. *Cell Metab.* **2024**, *36* (10), 2245−2261.E6.
(36) Yu, Q.; Zeng, K.-W.; Ma, X.-L.; Jiang, Y.; Tu, P.-F.; Wang, X.-M. Ginsenoside Rk1 Suppresses Pro-Inflammatory Responses in Lipopolysaccharide-Stimulated RAW264.7 Cells by Inhibiting the Jak2/Stat3 Pathway. *Chin. J. Nat. Med.* **2017**, *15* (10), 751−757.
(37) Makaro, A.; Świerczyński, M.; Pokora, K.; Sarniak, B.; Kordek, R.; Fichna, J.; Salaga, M. Empagliflozin Attenuates Intestinal Inflammation through Suppression of Nitric Oxide Synthesis and Myeloperoxidase Activity in in Vitro and in Vivo Models of Colitis. *Inflammopharmacology* **2024**, *32* (1), 377−392.
(38) Lee, N.; Heo, Y. J.; Choi, S.-E.; Jeon, J. Y.; Han, S. J.; Kim, D. J.; Kang, Y.; Lee, K. W.; Kim, H. J. Anti-Inflammatory Effects of Empagliflozin and Gemigliptin on LPS-Stimulated Macrophage via the IKK/NF-κB, MKK7/JNK, and JAK2/STAT1 Signalling Pathways. *J. Immunol. Res.* **2021**, *2021*, No. 9944880.
(39) Barton, K.; Muthusamy, N.; Chanyangam, M.; Fischer, C.; Clendenin, C.; Leiden, J. M. Defective Thymocyte Proliferation and IL-2 Production in Transgenic Mice Expressing a Dominant-Negative Form of CREB. *Nature* **1996**, *379* (6560), 81−85.
(40) Bodor, J.; Feigenbaum, L.; Bodorova, J.; Bare, C.; Reitz, M. S.; Gress, R. E. Suppression of T-Cell Responsiveness by Inducible cAMP Early Repressor (ICER). *J. Leukocyte Biol.* **2001**, *69* (6), 1053−1059.
(41) Conti, M.; Setnikar, I. Flavoxate, a Potent Phosphodiesterase Inhibitor. *Arch. Int. Pharmacodyn. Ther.* **1975**, *213* (2), 186−189.
(42) Vaeth, M.; Gogishvili, T.; Bopp, T.; Klein, M.; Berberich-Siebelt, F.; Gattenloehner, S.; Avots, A.; Sparwasser, T.; Grebe, N.; Schmitt, E.; Hünig, T.; Serfling, E.; Bodor, J. Regulatory T Cells Facilitate the Nuclear Accumulation of Inducible cAMP Early Repressor (ICER) and Suppress Nuclear Factor of Activated T Cell C1 (NFATc1). *Proc. Natl. Acad. Sci. U.S.A.* **2011**, *108* (6), 2480−2485.
(43) Bodor, J.; Bopp, T.; Vaeth, M.; Klein, M.; Serfling, E.; Hünig, T.; Becker, C.; Schild, H.; Schmitt, E. Cyclic AMP Underpins Suppression by Regulatory T Cells. *Eur. J. Immunol.* **2012**, *42* (6), 1375−1384.
(44) Bopp, T.; Dehzad, N.; Reuter, S.; Klein, M.; Ullrich, N.; Stassen, M.; Schild, H.; Buhl, R.; Schmitt, E.; Taube, C. Inhibition of

https://doi.org/10.1021/acsomega.5c06639
ACS Omega 2025, 10, 51297−51308

cAMP Degradation Improves Regulatory T Cell-Mediated Suppression. *J. Immunol.* **2009**, *182* (7), 4017−4024.
(45) Forster, M.; Chaikuad, A.; Bauer, S. M.; Holstein, J.; Robers, M. B.; Corona, C. R.; Gehringer, M.; Pfaffenrot, E.; Ghoreschi, K.; Knapp, S.; Laufer, S. A. Selective JAK3 Inhibitors with a Covalent Reversible Binding Mode Targeting a New Induced Fit Binding Pocket. *Cell Chem. Biol.* **2016**, *23* (11), 1335−1340.
(46) Parmentier, J. M.; Voss, J.; Graff, C.; Schwartz, A.; Argiriadi, M.; Friedman, M.; Camp, H. S.; Padley, R. J.; George, J. S.; Hyland, D.; Rosebraugh, M.; Wishart, N.; Olson, L.; Long, A. J. In Vitro and in Vivo Characterization of the JAK1 Selectivity of Upadacitinib (ABT-494). *BMC Rheumatol.* **2018**, *2*, No. 23.
(47) O'Shea, J. J.; Gadina, M. Selective Janus Kinase Inhibitors Come of Age. *Nat. Rev. Rheumatol.* **2019**, *15* (2), 74−75.
(48) Palve, V.; Liao, Y.; Rix, L. L. R.; Rix, U. Turning Liabilities into Opportunities: Off-Target Based Drug Repurposing in Cancer. *Semin. Cancer Biol.* **2021**, *68*, 209−229.
(49) Pettersen, E. F.; Goddard, T. D.; Huang, C. C.; Couch, G. S.; Greenblatt, D. M.; Meng, E. C.; Ferrin, T. E. UCSF Chimera—A Visualization System for Exploratory Research and Analysis. *J. Comput. Chem.* **2004**, *25* (13), 1605−1612.
(50) Morris, G. M.; Huey, R.; Lindstrom, W.; Sanner, M. F.; Belew, R. K.; Goodsell, D. S.; Olson, A. J. AutoDock4 and AutoDockTools4: Automated Docking with Selective Receptor Flexibility. *J. Comput. Chem.* **2009**, *30* (16), 2785−2791.
(51) Bell, E. W.; Zhang, Y. DockRMSD: An Open-Source Tool for Atom Mapping and RMSD Calculation of Symmetric Molecules through Graph Isomorphism. *J. Cheminf.* **2019**, *11* (1), No. 40.
(52) Irwin, J. J.; Tang, K. G.; Young, J.; Dandarchuluun, C.; Wong, B. R.; Khurelbaatar, M.; Moroz, Y. S.; Mayfield, J.; Sayle, R. A. ZINC20—A Free Ultralarge-Scale Chemical Database for Ligand Discovery. *J. Chem. Inf. Model.* **2020**, *60* (12), 6065−6073.
(53) O'Boyle, N. M.; Banck, M.; James, C. A.; Morley, C.; Vandermeersch, T.; Hutchison, G. R. Open Babel: An Open Chemical Toolbox. *J. Cheminf.* **2011**, *3* (1), No. 33.
(54) Liu, Y.; Yang, X.; Gan, J.; Chen, S.; Xiao, Z.-X.; Cao, Y. CB-Dock2: Improved Protein−Ligand Blind Docking by Integrating Cavity Detection, Docking and Homologous Template Fitting. *Nucleic Acids Res.* **2022**, *50* (W1), W159−W164.
(55) Laskowski, R. A.; Swindells, M. B. LigPlot+: Multiple Ligand−Protein Interaction Diagrams for Drug Discovery. *J. Chem. Inf. Model.* **2011**, *51* (10), 2778−2786.
(56) Abraham, M. J.; Murtola, T.; Schulz, R.; Páll, S.; Smith, J. C.; Hess, B.; Lindahl, E. GROMACS: High Performance Molecular Simulations through Multi-Level Parallelism from Laptops to Supercomputers. *SoftwareX* **2015**, *1*−*2*, 19−25.
(57) Humphrey, W.; Dalke, A.; Schulten, K. VMD: Visual Molecular Dynamics. *J. Mol. Graphics* **1996**, *14* (1), 33−38.
(58) Shityakov, S.; Broscheit, J.; Förster, C. α-Cyclodextrin Dimer Complexes of Dopamine and Levodopa Derivatives to Assess Drug Delivery to the Central Nervous System: ADME and Molecular Docking Studies. *Int. J. Nanomed.* **2012**, *7*, 3211.

https://doi.org/10.1021/acsomega.5c06639
ACS Omega 2025, 10, 51297−51308